Mon. Not. R. astr. Soc. (1987) **226**, 747–768 and *Microfiche* MN 226/1

CCD surface photometry of elliptical galaxies – I. Observations, reduction and results

Robert I. Jedrzejewski *Institute of Astronomy, Madingley Road, Cambridge CB3 0HA and Mount Wilson and Las Campanas Observatories, 813 Santa Barbara Street, Pasadena, CA 91101, USA*

Accepted 1987 January 29. Received 1987 January 26; in original form 1986 October 21

Summary. A programme of CCD surface photometry of elliptical galaxies is described. A sample of 49 nearby early-type galaxies has been observed in the B and R passbands, and the isophotes fitted by ellipses. The cos (4θ) component of the isophotes has also been measured to investigate the degree to which the isophotes may be boxy or contain an edge-on disc component. Comparison with other observers shows that the surface brightness profiles and geometrical profiles are accurate to a few per cent when sky subtraction and seeing effects are not important. A future paper will use these data to investigate some important aspects of elliptical galaxy structure and dynamics.

1 Background

Our understanding of elliptical galaxies has experienced a profound change in the past few years. Prior to 1975, they were considered to be very simple objects, consisting of an ensemble of stars arranged in a shape that revealed the angular momentum of the system – the most rapidly rotating galaxies being the most flattened. The work of Liller (1960, 1966) went almost unnoticed in this respect, as in the observation of ellipticity changes and isophote twisting more complex behaviour was indicated. The revolution started in 1975, when Bertola & Capaccioli measured the rotation curve for NGC 4697, and found that the rotation speed was much lower than the previously derived value of the velocity dispersion (Bertola & Capaccioli 1975). Subsequent work by Illingworth (1977), Schechter & Gunn (1979), Peterson (1978) and Davies (1981) confirmed this type of behaviour for more galaxies, and around the same time Binney (1976, 1978) explained how ellipticals could be flattened and not rotating significantly – the shape is supported by an excess of random kinetic energy in the equatorial plane compared to the perpendicular direction. Recently, Davies *et al.* (1983) have shown that fainter elliptical galaxies do not share this property – rotation is sufficient to support the (presumed oblate) shapes of the galaxies and no anisotropy of the random velocity field is required. While kinematic observations have been made extensively for a large number of elliptical galaxies, the photometric observations have, to a certain extent, fallen behind and of the 50 galaxies in Davies *et al.* (their table 3), less than half have had accurate surface photometry performed on them.

The introduction of CCD's as astronomical detectors has led to considerable improvements in photometry. These detectors have (almost) ideal characteristics for astronomical imaging, and with the advance of technology the situation can only improve. Since it is relatively simple to acquire almost 'perfect' data (limited only by the effects of seeing and sky brightness), the need is for methods of data reduction that make most use of the accuracy of the data.

There are several properties of elliptical galaxies that are particularly amenable to investigation using CCD detectors. Since the noise can be very low, it is possible to investigate the shapes of isophotes in more detail than can be accomplished with photographic work. Are they always perfectly elliptical, or is it possible to detect distortions due to, for example, faint edge-on discs, dust absorption or even weak spiral structure? Are there objects analogous to the 'box-shaped' bulges? The wide dynamic range allows the investigation of the core properties, and in particular whether Schweizer's (1979) suggestion that most elliptical galaxies have apparent core sizes that are purely an artefact of 'seeing' is correct. The radius–luminosity relation is also measurable, and one might hope that the photometric accuracy of CCD's might offset the weakness of a small field of view. And finally, a search for colour gradients can be made in the inner regions where the uncertainty in the night sky brightness is not important.

In this paper, a programme of CCD surface photometry of elliptical galaxies is described, and the methods of reduction and results are presented in some detail. A future paper will describe the analysis of the reduced data, and the application of these data to some of the topics mentioned above. The selection of objects is described in Section 2, the observations in Section 3, the data reduction methods in Section 4, and the results in Section 5. Section 6 includes an investigation into the accuracy of the results, and comparisons are made with previously published work. Section 7 sums up.

2 Choice of galaxies

The main criterion for selection of programme objects was that kinematic data be available for them; either already published rotation curves and velocity dispersion profiles, or else collected and unreduced spectra from ongoing projects at Cambridge. A special effort was made to observe the low-luminosity ellipticals studied by Davies *et al.* (1983). Some additional qualities were sought: the objects should be photometrically 'normal', be classified as elliptical or perhaps S0 in the major catalogues, and there should be some overlap with previous investigations in order to check the accuracy of the results obtained in this work. The objects should cover a wide range of intrinsic luminosities, should populate the spread of ellipticities evenly, and come from a wide variety of environments (cluster, field, group). A small number of objects with photometric peculiarities that were known at the time of observation were also included; these were M87 (jet), M84 (dust lane), NGC 2865 (shell) and NGC 3923 (shell). The programme objects actually observed are listed in Table 1.

Of the 49 programme galaxies, all but two (IC 2597 and A1515−23) are classified in the *Second Reference Catalogue of Bright Galaxies* (de Vaucouleurs, de Vaucouleurs & Corwin 1976, hereafter RC2). Forty-one of these 47 are classified as ellipticals, two (NGC 4486 and 4696) are called 'cD' galaxies, and the other four are classed as S0 (NGC 3308, 3311, 4476 and IC 4329). In the *Revised Shapley–Ames Catalogue* (Sandage & Tammann 1981, hereafter RSA), four galaxies are absent; the two missing from RC2, plus NGC 3260 and 3308. The classification of many galaxies in the RSA differs from those in the RC2, partly because of the superior plate material used in classifying galaxies in the former catalogue, and partly because the investigators have slightly different criteria for judging an object to be an S0 galaxy. In particular, two galaxies are

Table 1. Programme objects.

Galaxy	Type		B_T <RC2>	Group	V_{group}	$-M_B$
NGC 1549	E2		10.57	HG3,DV16	810	20.48
NGC 2865	E4		11.85	-	2443	21.59
NGC 3091	E3		12.04	HG37	3556	22.22
NGC 3250	E3		11.44	(HG18)	2968	22.43
NGC 3258	E1		12.25	HG18	2968	21.62
NGC 3260	E2	*	13.0	(HG18)	2968	20.87
NGC 3268	E2		12.31	HG18	2968	21.56
NGC 3308	SB0(2)	*	12.80	(A1060)	3500	21.31
NGC 3309	E1		12.46	(A1060)	3500	21.65
NGC 3311	S0(0)	*	12.25	(A1060)	3500	21.86
NGC 3377	E6		10.85	HG56,GH68,DV11	1205	21.06
NGC 3379	E0		10.00	HG56,GH68,DV11	1205	21.91
NGC 3557	E3		10.88	-	2707	22.79
NGC 3605	E5		12.76	HG56,GH77	1205	19.15
NGC 3608	E1		11.70	HG56,GH77,DV49	1205	20.21
NGC 3818	E5		12.45	DV23	1583	20.05
NGC 3904	E2		11.59	HG28,DV44	1823	21.22
NGC 3923	E4/$S0_1$		10.74	HG28,DV44	1823	22.07
NGC 4374	E1		10.11	HG41,GH106,DV19	1100	21.60
NGC 4387	E5	*	12.75	GH106	1100	18.96
NGC 4458	E0	*	12.70	GH106	1100	19.01
NGC 4473	E5		10.81	HG41,GH106	1100	20.90
NGC 4476	E5pec(dust)		12.78	GH106	1100	18.93
NGC 4478	E2		11.92	HG41,GH106	1100	19.79
NGC 4486	E0		9.35	HG41,GH106,DV19	1100	22.36
NGC 4489	E1	*	12.51	HG41,GH106	1100	19.20
NGC 4551	E3	*	12.65	GH106	1100	19.06
NGC 4696	(E3)		11.25	HG14	3256	22.82
NGC 4697	E6		9.96	HG41,DV20	1100	21.75
NGC 4709	E1	*	12.50	(HG14)	3256	21.57
NGC 4767	S0/a		12.16	HG14	3256	21.91
NGC 4976	$S0_1(4)$		10.46	-	1133	21.32
NGC 5638	E1		11.90	HG49,GH145	1883	20.98
NGC 5813	E1		11.30	HG50,GH150,DV50	1973	21.68
NGC 5831	E4		12.10	HG50,GH150	1973	20.88
NGC 5845	E3	*	12.80	GH150	1973	20.18
NGC 5898	$S0_{2/3}(0)$		12.09	-	2300	21.22
NGC 5903	E3/$S0_1(3)$		11.97	-	2300	21.34
NGC 6868	E3/$S0_{2/3}(3)$		11.40	HG9,DV52	2766	22.31
NGC 6876	E3		12.12	DV38	3803	22.29
NGC 6909	E5		12.35	-	2610	21.24
NGC 7029	$S0_1(5)$		12.29	-	2779	21.43
NGC 7144	E0		11.27	HG7,DV45	1706	21.40
NGC 7145	E0		11.73	HG7	1706	20.94
IC 2597	S0(2)	Δ	12.5	(A1060)	3500	21.11
IC 4296	E0		11.15	HG22	3673	23.18
IC 4329	$S0_1(5)$		12.06	-	4243	22.58
IC 4889	$S0_{1/2}(5)$		11.75	-	2418	21.67
A1515-23	E6	Δ	14.07	-	2300	19.24

Classification from RSA, except * (RC2) and Δ (ESO)

classified as being intermediate to late S0 galaxies, and hence containing dust. These are NGC 5898 and 6868. NGC 4476 is classified as E5pec(dust). Of the 45 galaxies in the RSA, 29 are E, seven are 'early-type' (the classification goes no further for these fainter objects), three are E/S0, five are S0, and NGC 4767 is classed as S0/a.

The magnitudes in Table 1 are on the B_T scale of the RC2. For the galaxies without an RC2 magnitude, those of the RSA were used, converted to the RC2 system using the best-fit straight

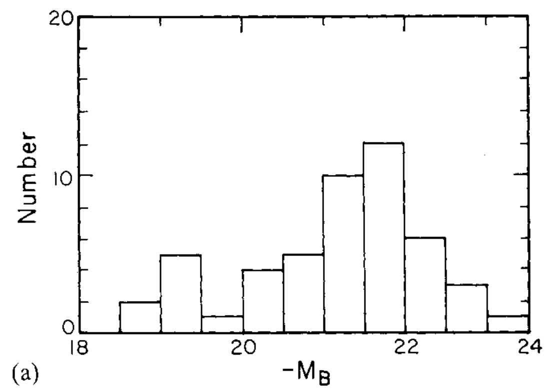

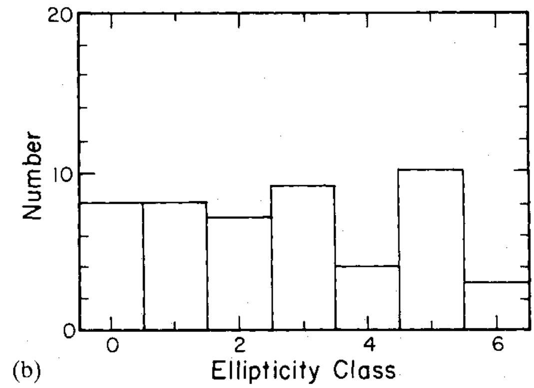

Figure 1. Histograms of (a) absolute magnitudes and (b) ellipticity classes of the programme sample.

line for the galaxies that have magnitudes in both catalogues. The relation is:

$$B_T(\mathrm{RC2})=0.9784\,B_T(\mathrm{RSA})-0.0176,$$

with a dispersion of 0.13 mag. For NGC 3260, the unpublished photometry of Burstein *et al.* was used, while for IC 2597 that of Smyth & Stobie (1980) was adopted. Group assignment was from Huchra & Geller (1982, HG), Geller & Huchra (1983, GH), de Vaucouleurs (1975, DV) and Abell (1958, A, redshift from Sandage 1975). For galaxies with no group assignment in these catalogues, the individual galaxy redshift was used. The greatest discrepancy between catalogue redshifts arose for the galaxies NGC 3377 and 3379, where there was nearly a factor of 2 disagreement between the redshifts of the group assignments of HG and DV. The work of HG was adopted in this case. The redshift of the Virgo cluster was taken to be 1100 km s^{-1}, and absolute magnitudes were calculated using H_0=50 km s^{-1} Mpc^{-1}, with no correction for virgocentric infall. Since the most distant galaxy is at z=0.014, K-corrections were not applied [K_B<0.1 (Pence 1976)].

Histograms of the distribution of ellipticities and absolute magnitude are plotted in Fig. 1, and it can be seen that the programme galaxies cover a fairly wide range in absolute magnitude (~4–5 mag), and populate the distribution of observed ellipticities evenly. While the sample is by no means complete, it is believed to be reasonably typical of the set of elliptical galaxies.

3 Observations

The observations were made using the Royal Greenwich Observatory CCD camera (RGO CCD) at the prime focus of the Anglo–Australian Telescope on 1982 April 21–22 by the author and Roger Davies. Details of this device can be found in Jorden, Thorne & van Breda (1982). Frames were taken using B and R filters, made up of components detailed in Table 2. The most important parameters describing the performance of the telescope/CCD combination are given in Table 3.

The weather was clear throughout the two nights, and dark until the Moon rose at 1.30 and 2.30 am. We attempted to adjust exposure times to make use of the widest possible dynamic range, by having the central regions of the target galaxy just within the linearity limit. By inspecting the counts in the centres of galaxies in a first exposure online, a second exposure could be taken to make the number of counts in the centre of the galaxy ~6000. Typical exposures times were 1 min–100 s in R and 3–5 min in B. Offset sky frames were taken in the cases where the

Table 2. Details of the filters.

B	2 mm GG385+1 mm BG12+1 mm BG18+2 mm KG3
R	2 mm RG610+2 mm BG20+2 mm KG3

Table 3. CCD/telescope parameters.

CCD chip: RCA 53612 thinned
Format: 320×512
Pixel size: 30 μm
Pixel size at prime focus of AAT: 0.49 arcsec
Frame size at prime focus of AAT: 2.6×4.2 arcmin
Readout noise: ~73 electrons rms
System gain: 0.067 ADU/e^-=15 e^-/ADU
Linearity limit: ~110 000 e^-=7000 ADU
Dark current: ~0.04 e^- pixel^{-1} s^{-1}=136 e^- pixel^{-1} hr^{-1}
Cosmic ray sensitivity: ~3–5 min^{-1}
Cosmetic details: very good, one bad column, No. 142
Operating temperature: 150 K

galaxy image was so large as to fill the field, but for smaller galaxies this was not thought necessary. Frames of standard fields in ω Centauri and E-regions were also taken to provide some means of photometric calibration. The chip was orientated with its long axis roughly north–south.

To map the flat-field response, exposures of a matt screen inside the dome illuminated by an incandescent lamp were taken, and also exposures of the twilight sky. Zero-duration exposures were recorded to determine the electronic offset applied to the counts; these are called bias frames. Dark exposures of 1000 and 4000 s were also obtained. In all, over 400 frames were taken, including 49 galaxies, in two nights.

4 Data reduction

4.1 PRELIMINARY REDUCTIONS

The bias level was removed from the data by subtracting pixel-by-pixel a high signal-to-noise average of several zero-length exposures. Since the camera electronics does not overscan the CCD, a local measure of the bias level was not available. It was found that comparison of successive bias frames indicates stability to about +/−1 ADU (1 ADU=1 Analogue-to-Digital Unit=15 electrons) over short time-scales, but only to about +/−4 ADUs over longer periods of time (~1 day). The bias frames had considerable structure that was fortunately accurately repeatable over the whole run, hence the need for pixel-by-pixel subtraction. Since the surface brightness measurements involve the subtraction of the night sky contribution, in general the uncertainty in bias level manifests itself as an uncertain sky brightness.

The *R*-frames suffered from fringeing due to the thinness and transparency at these wavelengths and the presence of strong night-sky emission lines. However, the fringe pattern is relatively stable, so can be removed by subtracting the correct multiple of the fringe pattern. A fringe frame was kindly provided by J. V. Wall of the Royal Greenwich Observatory, and by subtracting multiples of this pattern interactively using a colour graphics display it was possible to remove all visible traces of the fringe pattern. Because the amplitude of the fringe pattern is only 3–5 per cent of the mean sky level, it was found that to reduce the amplitude to $\leqq$1 per cent was perfectly satisfactory, as it was then well below the readout noise level.

The dark counts are very small for typical exposures taken here, merely adding 1 or 2 counts to each of the pixels, except in one corner where there is a region of enhanced dark current. This was treated as an 'interfering star' in subsequent analysis and removed, and the rest of the dark counts assumed to be the same for all the pixels.

To remove cosmic rays, which appear as single- or double-pixel events of high charge, and 'hot' and 'cold' pixels, a routine was written to find pixels of more than four standard deviations from the local mean, and to replace them with zeros (or 'don't know' values).

The next step in the preparation is to detect and remove interfering stars and other cosmetic defects missed by the previous step. In many other studies, this has been dealt with by replacing interfering images by the local mean, but this can be criticized in that increased weight is given to areas near to interfering stars. As well as including pixels near stars in any isophote fitting algorithm (and these are quite likely to be slightly high with respect to the intrinsic galaxy intensity), these pixels enter into the interpolated intensities in the substituted area. Thus, possible discrepant pixels are given greater weight in any subsequent analysis. In the analysis in this work, interfering stars are replaced by zero, a 'don't know' value, and then given zero weight in the ellipse-fitting procedure.

The last step is to inspect the centre of the galaxy image for small (1–2 pixel) defects and evidence of bad columns. Column 231 occasionally appeared very noisy, and if this interfered with the galaxy image, it was set to zero.

Finally, a word about the display of CCD frames of bright elliptical galaxies on a graphics monitor. The intensity contrast between the bright central regions of ellipticals and the low surface brightness outer parts is very difficult to portray using a linear relation between the CCD pixel value and the TV intensity (or colour, if a 'false colour' image is displayed). It has been found by the author and many other investigators that a better method is to display the picture with a logarithmic transformation, with an offset subtracted. In other words, instead of displaying the scaled pixel value, it is better to display $k \log(I - \text{offset})$. The offset should be chosen so that areas of 'blank sky' are several tens of counts above the offset level, and the constant k chosen to make the dynamic range of the CCD fit snugly into the number of significant bits used in the display device. A look-up table that cycles through light and dark (or through the colour spectrum) several (2–5) times then provides a 'pseudo-contour' display that allows inspection of detail at all intensity levels.

4.2 ISOPHOTE FITTING

A CCD frame obtained for this study consists of 320×512 pixels which, in good seeing conditions, are all virtually independent. When chip defects, interfering stars, cosmic rays, etc. have been removed, approximately 100 000 pixels still remain. It is thus rather wasteful to analyse the galaxy image along a limited number of directions, for example, the major and minor axes only, as the rest of the image is then completely redundant. There is much more information to be had, especially if the noise in the data is small, by a more thorough investigation of the galaxy light distribution.

Many of the algorithms used for isophotometry extract an intensity level from the galaxy frame, and then fit an ellipse to all the points with that intensity level to determine the X and Y centre, ellipticity, position angle and semi-major axis length. It is always assumed that the isophotes are representable by ellipses, but there have been very few studies that measure any departure from pure ellipse shape. Carter (1977) worked out the coordinates of points on an isophote and then made a coordinate rotation and scale change to transform these coordinates to those on a unit circle. He then Fourier-analysed the distance of his contour points R as a function of azimuthal angle, ϕ, to determine the quantities

$$A_n = \frac{1}{\pi} \int R(\phi) \sin(n\phi)\, d\phi,$$

$$B_n = \frac{1}{\pi} \int R(\phi) \cos(n\phi)\, d\phi.$$

The terms A_1, A_2, B_1 and B_2 indicate errors in the fitting procedure, which will be small if the fit has been carried out correctly. The terms A_3 and B_3 give 'egg-shaped' or 'heart-shaped' isophotes, but the most interesting is B_4. If this is negative, then the isophote will appear 'boxy', while if positive, the isophote has pointed ends, much like an edge-on disc galaxy would produce (e.g. NGC 3115). Now, boxy isophotes are observed in some edge-on spiral galaxies, for example NGC 128 and 4565; this appears to be associated with a cylindrical rotation velocity field (Kormendy & Illingworth 1982). Quantitative measures of the strength of these features have not been made, and such behaviour has not been observed in an elliptical galaxy (but see Lauer 1985b). Similarly, pointed isophotes will be present if the galaxy contains a nearly edge-on disc. Carter's results, using photographic data, were too noisy to allow any firm statements to be made about whether any of his detections of non-zero B_4 were secure.

A method was therefore sought which uses all of the data for a galaxy image, and calculates the run of ellipse centre $X0$ and $Y0$, ellipticity ε, position angle, ϕ, and the 'non-ellipse' coefficients A_3, B_3, A_4 and B_4. Such an algorithm has been developed at Cambridge by M. Cawson (now Steward Observatory), and, after some testing, a variant of his procedure was adopted. The method is similar to that described in Kent (1983) in his examination of the centre of M31.

For a given semi-major axis length, an initial guess at the ellipse parameters $X0$, $Y0$, ε and ϕ is made, and the intensity in the galaxy image around this ellipse is sampled at equal intervals in the eccentric anomaly E. If the sampling ellipse is a good description of an isophote, then the intensity will be the same value at all sampling points within the noise. However, if the sampling ellipse has one or more of its parameters wrong, then the resulting intensity function will have low-order harmonics superposed. The amplitude of the harmonics gives information about which ellipse parameters are wrong, and by how much.

The intensity measurements around the trial ellipse are fitted by weighted least-squares to:

$$I=I_0+A_1\sin(E)+B_1\cos(E)+A_2\sin(2E)+B_2\cos(2E). \tag{1}$$

If an interpolated point had been set to a 'don't know' value, the weight assigned was zero, otherwise it was 1. The interpolation process will be described in more detail later.

From the amplitudes of the coefficients A_1, A_2, B_1 and B_2, correction factors to each of the sampling ellipse parameters can be calculated. For small errors in the ellipse parameters:

$$\Delta \text{ major axis position}=\frac{-B_1}{I'},$$

$$\Delta \text{ minor axis position}=\frac{-A_1(1-\varepsilon)}{I'},$$

$$\Delta \text{ ellipticity}=\frac{-2B_2(1-\varepsilon)}{a_0 I'},$$

$$\Delta \text{ position angle}=\frac{2A_2(1-\varepsilon)}{a_0 I'\{(1-\varepsilon)^2-1\}},$$

where I' is the derivative of the intensity along the major axis direction evaluated at a semi-major axis length of a_0.

The ellipse parameter corresponding to the harmonic with the largest amplitude is then changed by the amount given by the above equations, which should reduce the amplitude of the harmonic to zero, and the galaxy is sampled using the corrected parameters iteratively until a sufficiently good fit to I=constant is obtained. The ellipse parameters are then the best that can be fitted to an isophote at that semi-major axis length. In addition, the intensity measures around the isophote have been averaged azimuthally, and this increases the signal-to-noise ratio by effectively using all of the pixel information.

A minimum of eight iterations is performed, and the criterion for a fit is that the largest harmonic amplitude be less than 4 per cent of the rms residual of the intensity distribution from the functional fit of equation (1). When a fit is found, the third and fourth harmonics for the resulting intensity distribution are measured by a least-squares fit to

$$I = I_0 + A_n \sin(nE) + B_n \cos(nE)$$

where $n=3$ or 4.

Clearly, making A_1, A_2, B_1 and B_2 zero does not constrain the amplitudes of the third and fourth harmonics, due to the fact that the orders are all orthogonal. To interpret the amplitudes obtained, they are transformed from intensity coefficients to coefficients describing deviations from a unit circle as in Carter (1977), by dividing by the local slope of the intensity profile and by the semi-major axis length.

The ellipse parameters for that semi-major axis length are then output to file, the semi-major axis length increased by 10 per cent, and a new iteration commenced using the best-fit parameters from the previous isophote. If a satisfactory fit is not obtained after 20 iterations, the parameters which gave the smallest amplitude for the largest coefficient are output to file. The slope of the intensity profile is found by sampling the intensity on ellipses with the same parameters as the guess ellipse, but with semi-major axis lengths of 1.05 and 0.95 times the sampling axis length. Dividing the difference in intensity by the difference in radii gives the slope. If the sampling ellipse is not a very good approximation to an isophote, then the slope found this way will be slightly wrong, but this is a second-order effect and the iterative process converges rapidly.

When the outer parts of the frame are reached, some of the ellipse lies outside the frame. However, it is still possible to attempt to fit the harmonic function to the intensity distribution and determine the ellipse parameters even though there is not full phase coverage around the sampling ellipse. Also, the slope of the galaxy profile becomes small and very difficult to measure accurately. This would make the ellipse parameter corrections large and uncertain, as they all contain a 1/slope term. To prevent this, if the modulus of the galaxy slope becomes less than 0.5 times the rms residual, the ellipse parameters are thereafter kept constant at the last successful values. In practice, for a large galaxy, the ellipse parameters could be determined for all but the outermost few radii. If over half of the sampled points either have zero weight or are outside the frame, iterations are ceased and fitting restarts in the central regions. The ratio between successive radii is inverted, and ellipse fitting carries on from 10 pixels to the centre of the galaxy. The process is stopped at 1 pixel.

4.3 INTERPOLATION

For semi-major axis lengths of less than 20 pixels, a bilinear interpolation scheme is used to estimate the intensity of the galaxy at a point intermediate between pixels. This uses the nearest four pixels to the interpolation point, and is equivalent to placing a square 'pixel' on the galaxy image and sampling the intensity by adding the contributions from the four pixels that fall within this square. The interpolant is thus similar in operation to one of the CCD pixels.

This is clearly not accurate in regions where the slope of the galaxy brightness profile is changing rapidly, or where the curvature of the isophotes is large. It also has the physically unrealistic properties of:

(i) Discontinuities in the slope of the interpolated intensity.

(ii) The integrated sum of the interpolated intensity over a pixel is in general *not* equal to the pixel value. An ideal interpolator would fulfil this criterion.

The scheme is easy to use, however fast, and its characteristics have been extensively tested. The number of interpolation points is chosen to make the distance along the elliptical arc between consecutive interpolation points equal to 1 pixel – this is achieved by making the increment in E between sampling points equal to $1/a$, where a is the semi-major axis length.

For semi-major axis lengths of more than 20 pixels, a different routine was used which performs spatial averaging (to improve the signal-to-noise ratio for a given interpolated intensity) while still retaining the elliptical symmetry of the spatial bin. An elliptical annulus of width 10 per cent of the semi-major axis length is divided into 64 sectors equally spaced in E, and the mean pixel value calculated in these sectors. A method was found that takes into account pixels that lie partially within a sector. If any of the pixels had been set to zero (i.e. were zero-weight pixels), then the sector for that azimuthal angle is itself given zero weight. It was found that this method was not significantly slower than the less complicated approach of taking only pixels that are more than half inside the sector. It is necessary to perform this spatial averaging, otherwise the large amount of noise makes the detection of small harmonics very difficult.

The X and Y centre parameters are a good diagnostic for anything interfering with the image that had not been detected in the star deletion process. If there is a region of very diffuse emission on one side of the frame only, then this will show up as a shift in the centres of the outer isophotes with respect to the inner ones. The effect of a linear graduation over the frame affects only the X and Y centre parameters, and thus a sky gradient would not affect the ellipticity and position angle (to first order). However, measurement of averages of rows and columns for flat-fielded sky frames showed that any gradients were small enough to be inconsequential.

For each galaxy image, at radii spaced by 10 per cent, the 18 parameters in Table 4 were measured and recorded.

Table 4. Isophote fit parameters.

1	Mean intensity	10	A_1
2	B_3	11	B_2
3	Slope	12	A_2
4	Semi-major axis length	13	Ellipticity $(1-b/a)$
5	rms residual of intensity	14	Position angle
6	B_4	15	X centre $X0$
7	Number of iterations	16	Y centre $Y0$
8	Number of points used in fit	17	A_3
9	B_1	18	$A4$

4.4 TESTING THE ALGORITHMS

Because it is very difficult to determine the accuracy of the measurements of intensity, ellipticity, position angle and higher harmonics, it was decided to construct artificial 'frames' of simulated data with known geometrical and photometric parameters, and then to degrade them to make them resemble closely the real CCD data. Then any systematic effects produced, for example by the interpolators used, can be detected and allowance made for them. The regions where the results can be believed, and where the answers start to break down due to sampling the same pixels in the central regions and noise in the outer parts, can be identified.

One notable feature found was that at small radii, the ellipticity is consistently underestimated if the galaxy is flattened. This is because the bilinear interpolator introduces a $\cos(2\theta)$ harmonic of its own into the interpolated intensity. The interpolator tries to approximate the curved sections of an ellipse by straight lines, and so it 'cuts the corners'. This effect is most serious at the ends of the major axis, and least at the minor axis ends, so this appears as a $\cos(2\theta)$ term. Many different interpolators were tried in an attempt to remove this effect, but none were successful. It was thus decided to leave it in, and note its effects. Since the discrepancy only arises if the ellipticity is >0.2 at radii of <5 pixels, and since seeing usually makes the images round in the central regions anyway, this was not considered a problem. In other respects, the programme does very well, introducing no systematic errors into the position angle or the B_4 term. The rms residuals from the expected results for the model galaxies give an accuracy for intensity measurements of ±0.02 mag, for ellipticity, ±0.02 for $a>5$ pixels, and for position angle, ±2 degrees, for ellipticities >0.2. The rms deviation of the B_4 term about zero is 0.001 for bright galaxies, and 0.005 for faint galaxies. These figures refer to intensities and noise levels comparable to those of galaxies of average brightness observed in this study. Clearly, very large and bright galaxies, such as M87 and NGC 3379, will measure better than these errors, while smaller galaxies like NGC 5845 and 5638 will be measured less accurately.

4.5 DETERMINATION OF SKY LEVEL

To transform the intensities on to an absolute scale, the sky value and photometric offset constant for each frame must be known:

$$\mu(a)=C-2.5\log_{10}[I(a)-\mathrm{sky}]$$

where $\mu(a)$ is the surface brightness of the isophote of semi-major axis length a and $I(a)$ is the measured intensity of this isophote. Note that the offset constant C, as well as containing information about the exposure time, camera sensitivity in counts photon^{-1} and extinction, also includes a component due to the fact that μ is normally expressed in mag arcsec^{-2}, while I is the intensity measured per pixel. Clearly C is the surface brightness that is obtained when the isophote intensity is 1 count above the sky level.

It has already been mentioned that the determination of the sky level in CCD observations is difficult. For the big, bright galaxies such as NGC 4486, 4696, 5813, 1549 etc., we obtained a sky frame in each colour of an area ~25 arcmin from the galaxy. To determine how useful the sky frames are, it is necessary to find out how much the sky level drifts between exposures, and how linear the response of the astronomical system (atmosphere+telescope+camera) is.

The order in which the frames were taken was R_g, R_g, R_s, B_s, B_g, B_g, where the subscript g refers to a galaxy observation and s to a sky frame. The offset sky exposures are generally of shorter length than the galaxy exposures, as it was considered wasteful to spend any more time than necessary to obtain a statistical estimate accurate to a few tenths of a per cent for the whole frame. Since these frames are almost completely readout-noise dominated, the 'error on the mean' from the $N=320\times512$ estimates of the sky value should be

$$\frac{\sigma_{\mathrm{pix}}}{\sqrt{N}}=\frac{\sim5}{\sqrt{320\times512}}=\sim0.02.$$

Hence, to obtain a 'signal to noise' of <0.1 per cent, the sky level need only be ~20 counts. This is achieved in ~20 s in R and ~40 s in B. To allow some leeway (as not all pixels are uncontaminated, and the bias frame must be subtracted), sky exposures were generally 40 s in R and 100 s in B. The anticipated statistical accuracy is <1 per cent. However, the bias level instability of ~1–2 counts adds on a few per cent to the sky level uncertainty, so the adopted figure is ±5 per cent.

Since the surface brightness profile must be the same in both galaxy frames of a given colour (apart from an offset due to the different values of C), the sky values in the two frames can be adjusted until the difference profile $\mu_1-\mu_2$ is flat against log (r). The behaviour of the difference

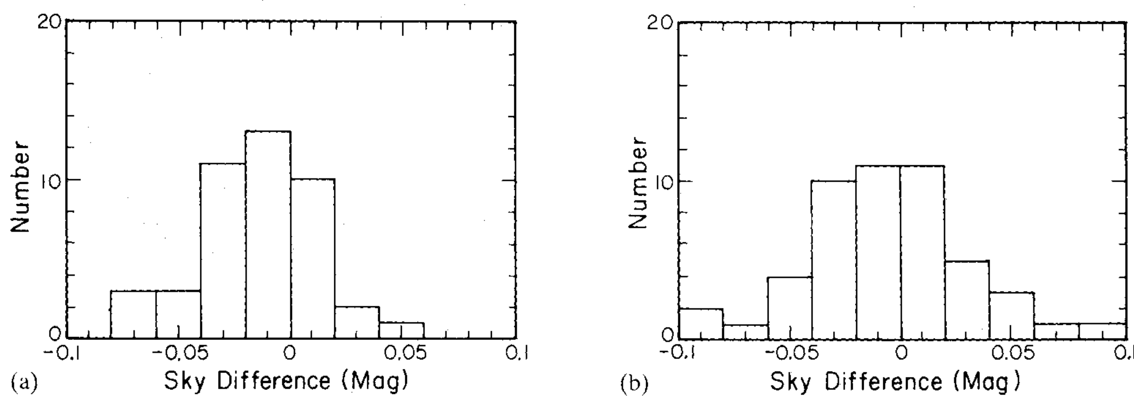

Figure 2. Histograms of sky brightness differences between successive CCD frames: (a) B filter, (b) R filter.

profile at large radii is very sensitive to the change in sky brightness between the two observations, and almost completely insensitive to the absolute 'accuracy' of the sky determinations. At small radii, any differences are due to a change in the seeing between the two frames, any non-linearities being much below 1 per cent in magnitude. A histogram of the differences in sky surface brightnesses between two frames in each colour is presented in Fig. 2. In B, 2/3 of the data points are in the interval $(-0.04, +0.02)$, while in R, 2/3 of the differences are in the range $(-0.05, +0.03)$. Thus we may take the rms sky change between consecutive frames as 0.03 mag in B and 0.04 mag in R, which is similar to the previously quoted value of a few per cent. Several pairs of frames showed quite large sky differences and do not appear on the histograms; these are mainly due to the Moon rising or else astronomical twilight approaching. Other pairs had no such explanation, and the reason for their anomalously large differences is unknown – possibly related to the bias level instability mentioned in Section 4.1. Clearly, the histograms in Fig. 2 include the contribution from this effect.

For the smaller galaxies, the edges of the frames were considered to be sufficiently free from contamination by the galaxy that a good estimate of the sky value could be determined by working out the mean intensity value there. This certainly gives an upper limit to the sky value. By taking the lowest measured corner value (the four corners were measured for each frame), it is believed that a good estimate of the sky brightness is obtained, to better than 1 per cent. This corresponds to a surface brightness 5 mag below sky, or ~ 27 mag arcsec^{-2} in B.

The random noise in the profiles is completely swamped at large radii by the uncertainty that incorrect sky subtraction introduces, and this must be seen as the major weakness of this study. For some objects, the sky level could not be reliably established as the offset sky frames gave results that appeared to indicate the presence of enormous colour gradients which are clearly not present in the data.

4.6 PHOTOMETRIC OFFSET CONSTANTS

Determination of the photometric constant for each frame involves the use of published aperture photometry. If the magnitude of a galaxy within a circular aperture of radius r is M, the following relation must apply:

$$M(r) = C - 2.5 \log_{10}\{I(r) - \pi r^2 S\}$$

where $I(r)$ is the total intensity (galaxy+sky+faint stars) within the radius r and S is the sky intensity per pixel. Applying the same equation to different apertures gives several estimates of the photometric constant C.

Table 5. Aperture photometry sources.

de Vaucouleurs & de Vaucouleurs	1972	B	DV2
Sandage	1973	B, R	S73
Sandage	1975	B, R	S75
de Vaucouleurs, de Vaucouleurs & Corwin	1978	B	DVC
Persson Frogel & Aaronson	1979	B, R	P79
Wegner	1979	B	W79
Michard	1982	B	M82
Sadler	1984	B	S84
Burstein *et al.*	unpubl.	B	B85

Rather than search for every possible aperture measurement for these objects, it was decided to select a few relatively recent and (hopefully) reliable works that include a large fraction of the galaxies studied here. The sources used are given in Table 5.

The observations in this study can thus be considered to be normalized to a photometric system that is a composite of these works. The most notable omission from this list is the work of Sandage & Visvanathan (1978). This was because their measurements are in the *ubVr* system, and results in the *BR* system were required. While they give equations for the transformation from their system to the *UBVR* system, the discrepancy between the magnitudes derived using the transformation equation for stars and the equation for galaxies was, at a few per cent, considered slightly too large. Of course it is realized that most other works involve (unspecified) transformations from their magnitude system to the *UBVR* scale, and these almost certainly introduce at least as much uncertainty into the results.

Since each aperture gives one measurement of the photometric constant, a plot of the scatter of these estimates with magnitude can pinpoint suspect measurements (that deviate by more than ~0.1 mag from the rest), and can allow an estimate of how well determined the value of C is. Occasionally the measurements split into two groups, differing by ~0.1 mag, from different observers: these were discarded. Some measurements were clearly of the wrong galaxy; the measurements of NGC 3258 in W79 are really NGC 3257, and similarly Sandage's (1975) measurements of IC 4329 refer to IC 4327.

Most of the edited measurements were either for very small apertures (where mis-centering and seeing effects are the major source of error), or for very large apertures (where the sky brightness dominates). Clearly, unless the photometer chops between object and sky at rates of ~1 Hz, the aperture photometry measurements will suffer from variations in the sky brightness, just as the CCD frames do.

The aperture photometry measurements for the well-studied galaxies were used to calculate the extinction and zero-point constant in each colour for each night, and then all of the observations were placed on to a uniform scale formed from the best-fit coefficients. Rms residuals of measured photometric constants from the assumed relations were 0.03 mag in B and 0.04 mag in R.

4.7 CHECKS OF CAMERA LINEARITY AND FLAT-FIELDING

By comparing two exposures of the same galaxy in the same colour but with different exposure times, the linearity of the camera can be demonstrated. Since the CCD does not suffer from coincidence-type losses of photon-counting detectors [e.g. IPCS (Boksenberg), 2d-Frutti (Shectman), PCA (Stapinski)], it is only necessary to show that if twice as many photons fall on a pixel, the number of counts produced is doubled. This demonstrates linearity between these two intensity values. For a whole profile, each isophote must be the same factor in one frame relative to the other, so the plot of magnitude difference should be flat against $\log(r)$. In all ~100 cases, *no* systematic deviations of >1 per cent were found that could not be accounted for by seeing changes or sky brightness differences. The linearity of the camera is therefore demonstrated to better than 1 per cent.

At low light levels, some brands of CCD suffer from non-linearities due to poor charge-transfer on the chip. The sky level in these observations was nearly always greater than 500 electrons pixel^{-1}, well above the level at which TI CCDs suffer problems. The deduced sky surface brightnesses for long and short exposures of the same galaxy agree to a few per cent, as demonstrated in Fig. 2, which implies that non-linearities are less than a few per cent even at the lowest charge levels encountered here.

For some objects, the first exposure of the galaxy showed that the object was not ideally placed in the frame – sometimes appearing to one edge and at other times so that the centre of the galaxy was very close to the bad column. The second exposure was offset to improve the positioning. This affords an opportunity to test the flat-fielding; the galaxy parameters should be independent of the position of the galaxy on the chip. In each case where the telescope was moved between successive observations, the results are relatively free from systematic differences.

4.8 PLATE-SCALE AND CHIP ORIENTATION

A check was made on the pixel scale for the CCD and the true orientation of the chip with respect to the sky by measuring the positions of stars on SERC-J sky survey transparencies for some of the fields. The solution for the stars on the corresponding CCD frames relative to stars with known positions on the Sky Survey gave the plate-scale as 0.4915 ± 0.0003 arcsec pixel^{-1} for three B-frames and 0.4918 ± 0.003 arcsec pixel^{-1} for four R-frames. Comparison of the positions of stars on B- and R-frames showed that any scale differences amount to less than 0.1 arcsec over the whole chip, and can thus be ignored. The orientation of the chip's longer axis was found to be at 1°.5 from north–south, and the position angles given in the figures and tables have been corrected for this.

5 Results

Tables of surface brightness, ellipticity, position angle and cos (4θ) component are presented for each of the 49 galaxies in the Appendix, on *Microfiche* MN 226/1. However, since NGC 3379 and 4486 are often observed as surface photometry standards, the results for these two galaxies are provided here (Table 6). The geometry profiles for a few of the most interesting objects will be provided in a future paper. Since the cos (4θ) profiles are a relatively new feature to elliptical galaxy surface photometry, galaxies with the most significant profiles are shown.

The B surface brightness profiles are presented in Fig. 3. The X-coordinate is r_*, the equivalent radius of the best-fitting ellipse. This is defined as the geometric mean of the semi-major and semi-minor axes, or $r_*=a\sqrt{(1-\varepsilon)}$, where a is the semi-major axis length. This has the effect of reducing all profiles to 'equivalent circular' profiles. The profiles are offset by 2 mag arcsec^{-2} from each other.

The profiles are similar in general shape to each other, but in detail they differ markedly. Some galaxies have power-law profiles outside seeing-dominated cores (e.g. NGC 3557, 3608, 5903), others have very 'bumpy' profiles (e.g. NGC 2865, 3308, 4489), while others have gently curving profiles (e.g. NGC 4387, 3605, 4551). Note also the wide difference in surface brightness between some galaxies – for example, NGC 7144 and 7145 have very similar profiles, but NGC 3311 has a much more diffuse core than NGC 3557; NGC 4767 and 4976 have similar profiles shapes but the latter galaxy is about 1 mag arcsec^{-2} brighter everywhere. Clearly, it is not possible to fit these observations by a single model curve (for example, the $r^{1/4}$ law), and nor would any fitting function with a small number of free parameters fit the profile of, among others, NGC 4489.

Table 6. (a) Surface photometry of NGC 3379.

Semi-Major Axis Length (Arcsec)	Surface Brightness B	R	Ellipticity 1-b/a	Position Angle N thru E	Cos(4θ) Component X100
0.547	17.162	15.191			
0.662	17.172	15.207			
0.801	17.187	15.230			
0.969	17.210	15.260			
1.173	17.243	15.303			
1.419	17.288	15.362			
1.717	17.352	15.440			
2.078	17.438	15.544	0.035	73.0	-0.1
2.514	17.550	15.673	0.042	74.4	0.1
3.043	17.693	15.834	0.047	75.6	0.0
3.681	17.873	16.024	0.052	73.6	0.0
4.455	18.086	16.250	0.059	75.0	0.1
5.390	18.337	16.502	0.061	73.8	0.0
6.522	18.613	16.781	0.063	73.6	0.0
7.891	18.904	17.069	0.068	73.7	-0.1
8.681	19.052	17.214	0.072	73.2	0.0
9.549	19.201	17.363	0.075	73.5	0.0
10.504	19.358	17.517	0.077	72.6	-0.1
11.554	19.520	17.678	0.078	72.5	0.0
12.709	19.685	17.842	0.080	72.0	0.0
13.980	19.858	18.013	0.084	72.3	0.0
15.378	20.039	18.192	0.084	71.6	0.0
16.916	20.218	18.375	0.089	71.3	0.0
18.608	20.396	18.555	0.093	71.0	0.1
20.469	20.567	18.727	0.098	71.0	0.0
22.515	20.727	18.984	0.103	70.4	-0.1
24.767	20.875	19.039	0.112	70.0	0.0
27.244	21.010	19.180	0.122	69.2	0.0
29.968	21.137	19.316	0.129	69.0	-0.1
32.965	21.267	19.453	0.134	68.6	0.1
36.261	21.407	19.596	0.130	67.2	0.0
39.887	21.548	19.743	0.133	67.2	0.0
43.876	21.715	19.909	0.125	66.2	0.1
48.264	21.880	20.092	0.125	68.4	-0.1
53.090	22.065	20.287	0.127	69.5	0.0
58.399	22.269	20.495	0.125	68.9	0.0
64.239	22.459	20.705	0.134	71.0	-0.1
70.663	22.672	20.924	0.140	71.1	0.0
77.729	22.866	21.142	0.147	71.9	-0.1
85.502	23.063	21.366	0.156	72.4	0.0
94.052	23.306	21.669	0.149	73.2	0.0
103.458	23.530	22.010	0.153	73.2	0.2

The cos (4θ) component plots are presented in Fig. 4. Most galaxies have isophotes that are very well fit by ellipses, in particular NGC 3379, which deviates from pure ellipse shape by less than 0.2 per cent at each measured radius. Some galaxies, particularly NGC 3818, 4697 and 7029, have strongly positive terms over part of the measured range, implying the presence of an edge-on disc component. Other objects have negative coefficients, which means that the isophotes are 'boxy', notably NGC4387, 4478 and 6909. NGC 1549 changes from boxy interior to 30 arcsec to 'pointed' outside this, and in fact a small bar-like perturbation in the other parts is visible in the processed CCD frame. All reduced frames are plotted for each galaxy (usually two R and two B frames), showing the internal consistency and relative insensitivity of this parameter to colour.

6 Comparison with other work

The sample includes several objects in common with recent published surface photometry, and allows a check on the results obtained here. Not every previous observation is compared, only the

Table 6. (b) Surface photometry of NGC 4486.

Semi-Major Axis Length (Arcsec)	Surface Brightness B	R	Ellipticity 1-b/a	Position Angle N thru E	Cos(4θ) Component X100
0.547	17.827	15.953			
0.662	17.859	16.005			
0.801	17.910	16.070			
0.969	17.982	16.147			
1.173	18.076	16.236			
1.419	18.177	16.327			
1.717	18.269	16.412			
2.078	18.338	16.480			
2.514	18.397	16.548			
3.043	18.462	16.615			
3.681	18.555	16.694			
4.455	18.555	16.774			
5.390	18.759	16.878	0.015	15.6	-0.1
6.522	18.889	17.006	0.023	18.3	0.3
7.891	19.049	17.163	0.020	12.9	0.4
8.681	19.140	17.255	0.022	7.8	0.4
9.549	19.239	17.352	0.023	6.2	0.2
10.504	19.344	17.455	0.023	-2.0	0.0
11.554	19.453	17.562	0.029	-4.0	-0.1
12.709	19.570	17.678	0.029	-1.3	0.1
13.980	19.691	17.678	0.031	-2.9	0.1
15.378	19.817	17.924	0.031	-5.3	0.0
16.916	19.943	18.051	0.035	-6.7	0.0
18.608	20.076	18.183	0.037	-11.6	0.1
20.469	20.213	18.320	0.041	-12.5	0.0
22.515	20.353	18.461	0.041	-14.7	0.0
24.767	20.489	18.602	0.048	-17.6	-0.3
27.244	20.636	18.749	0.052	-16.8	-0.1
29.968	20.786	18.895	0.054	-17.7	0.1
32.965	20.932	19.044	0.055	-19.9	-0.1
36.261	21.086	19.194	0.059	-20.2	0.0
39.887	21.230	19.194	0.065	-19.0	-0.1
43.876	21.379	19.499	0.073	-20.5	0.0
48.264	21.534	19.655	0.074	-19.9	0.0
53.090	21.682	19.801	0.079	-21.4	-0.1
58.399	21.840	19.963	0.087	-22.1	0.0
64.239	21.997	20.119	0.091	-24.7	-0.1
70.663	22.157	20.119	0.094	-23.5	-0.1
77.729	22.316	20.440	0.096	-25.7	0.0
85.502	22.478	20.440	0.105	-25.8	0.2

most recent and well known. These are all observations of NGC 3379 or 4486. The comparison works are listed in Table 7.

There are five different types of profile; (i) major axis, (ii) equivalent radius, (iii) constant position angle, (iv) azimuthally averaged and (v) 45° to the major axis. To convert my work on to these radial scales, the following transformations were applied:

$$r_{\rm ma}=a_{rj};$$

$$r_{\rm eq}=a_{rj}\sqrt{(1-\varepsilon)};$$

$$r_{\phi}=\frac{a_{rj}(1-\varepsilon)}{\sqrt{1-\varepsilon(2-\varepsilon)\cos^2\phi}};$$

$$r_{\rm azim}=a_{rj};\qquad I_r=I_a+\frac{\varepsilon I'a}{2};\qquad I'=\frac{dI}{da};$$

$$r_{45}=\frac{a_{rj}(1-\varepsilon)\sqrt{2}}{\sqrt{1+(1-\varepsilon)^2}}.$$

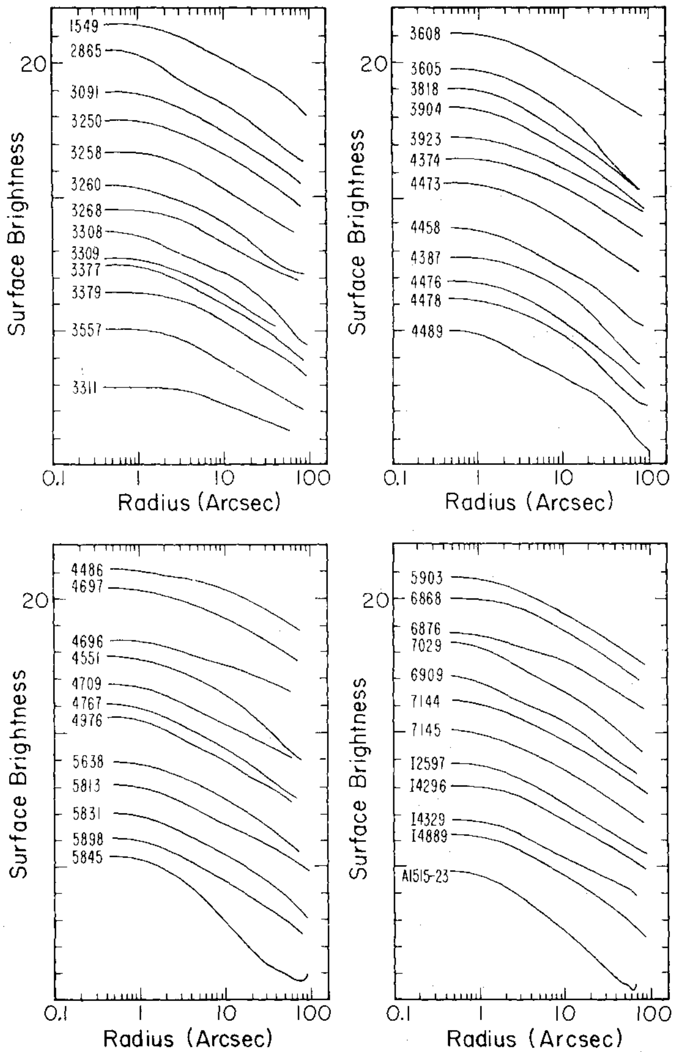

Figure 3. Profiles of surface brightness for the 49 programme galaxies. The ordinate is r_*, the equivalent radius of the best-fitting isophote, defined as $r_* = \sqrt{(ab)}$, where a and b are the semi-major and semi-minor axis length, respectively. The abscissa is the B surface brightness in mag arcsec^{-1}. There is a 2 mag arcsec^{-2} offset between successive galaxies, and the vertical divisions are 2 mag arcsec^{-2}. The '20' at the top of each Y-axis gives the absolute scale for the uppermost galaxy in each panel.

Note that the transformation formula given in Kent (1984) is incorrect. The comparison with each source is discussed in turn.

(i) Kormendy (1977) derived photographic profiles for M87 and NGC 3379. While the profile for the latter galaxy agrees reasonably well (to ~0.1 mag) everywhere except the central regions (where the seeing in my frame is much worse), the M87 profile shows very poor agreement, with a systematic downward trend of 0.5 mag over the region of overlap (Figs 5a and 6a). A similar conclusion was reached by Boroson, Thompson & Shectman (1983).

(ii) The study of King (1978) was seen as an important advance in accurate surface photometry. The comparison for NGC 4486 is quite good, with differences less than 0.15 mag (Fig. 6a).

(iii) Young *et al.* (1978) were the first to apply the CCD to surface photometry. Outside the central parts, their B profile agrees with mine to ±0.02 mag (Fig. 6a) apart from a zero-point offset of ~0.1 mag that de Vaucouleurs & Nieto (1979) also comment upon. In R, there is a steady drift of ~0.04 mag outside 3 arcsec (Fig. 6a), in the opposite sense to that in Boroson *et al.* (1983).

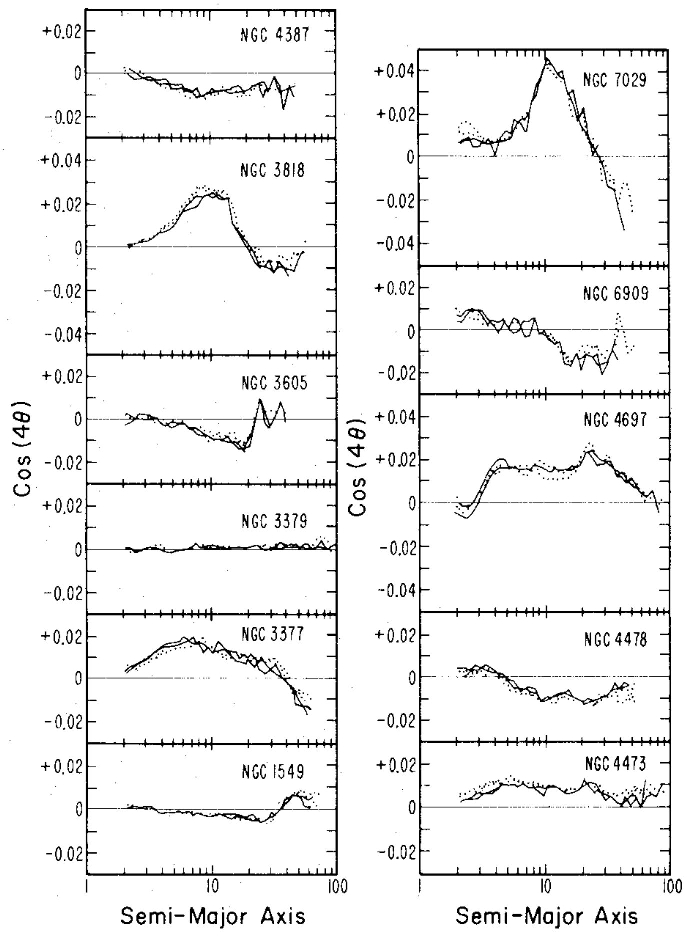

Figure 4. Profiles of cos (4θ) component for selected galaxies. This parameter measures deviations from perfect ellipse shape in the isophotes, such that if the term is positive, then the isophotes are 'pointed' compared to an ellipse, while if negative, then the isophote is 'boxy'. An amplitude of 1 per cent means that the isophote 'semi-major axis' is 1 per cent longer than that of the best-fitting ellipse. The solid lines are the B results, and the dotted lines are R.

Table 7. Sources of comparison of surface photometry.

Reference	Observations	Profile type
Kormendy (1977)	G	Const ϕ
King (1978)	B, ε	45 degrees
Young *et al.* (1978)	B, R	Azimuthally averaged
Burstein (1979)	B	Const ϕ
de Vaucouleurs & Capaccioli (1979)	B	Const ϕ
de Vaucouleurs & Nieto (1979)	B	Equivalent radius
Boroson *et al.* (1983)	B, R	Azimuthally averaged
Kent (1984)	r, ε, ϕ	Major axis
Davis *et al.* (1985)	B, R, ε, ϕ	Major axis
Lauer (1985a)	R, ε, ϕ	Major axis

(iv) Burstein (1979) observed NGC 3379 as a standard for his photographic study of S0 galaxies. Comparison of his B measures with mine show excellent agreement for $20 \leqq \mu_B \leqq 23$ mag per square arcsec, with an rms scatter of ~0.05 mag and no systematic trend. At higher intensity levels, there is a systematic change of 0.2 mag, in the sense of my measured brightness being higher (Fig. 5a). This may be due to much different seeing, or else to a calibration discrepancy at

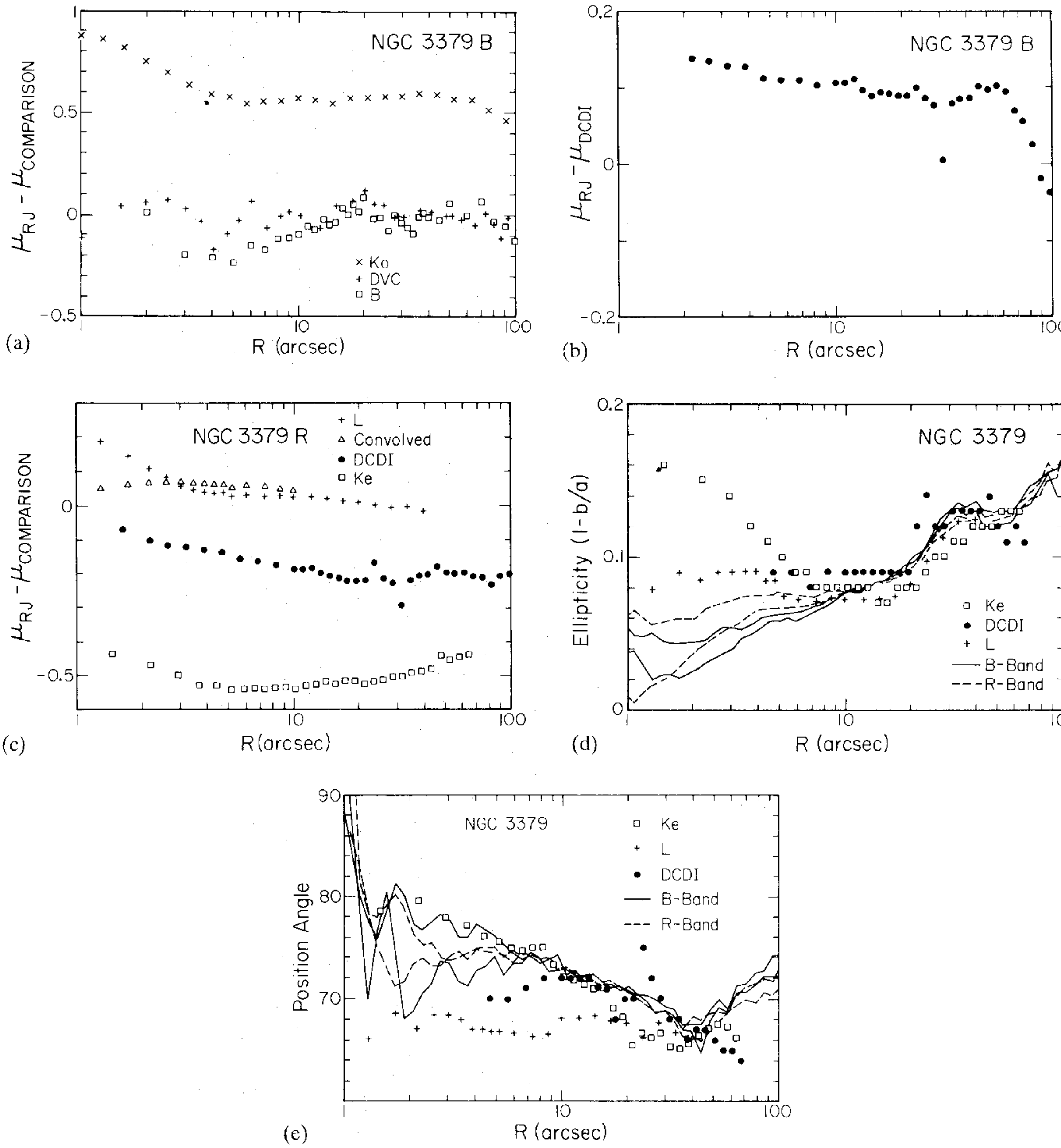

Figure 5. Comparison with surface brightness and geometry measurements of other investigators for NGC 3379. (a) Comparison of B surface brightness profile with photographic or photoelectric works: Burstein (B □), de Vaucouleurs & Capaccioli (DVC +) and Kormendy (Ko × – G band). (b) Comparison of B surface brightness profile with CCD work: Davis *et al.* (DCDI ●). (c) Comparison of R surface brightness profile with CCD works: Lauer (L +), convolved Lauer (△), Kent (Ke □ – r-band) and Davis *et al.* (DCDI ● – R_C-band). (d) Comparison of ellipticity profiles with Lauer (L +), Kent (Ke □) and Davis *et al.* (DCDI ●). The lines refer to the results obtained in this work – solid lines are B-band and dashed lines are R-band. (e) Comparison of position angle profiles, legend as in (d). Position angles are in degrees measured from north to east.

high surface brightness levels. The former explanation is unlikely, as the minimum at ~18 mag arcsec^{-2} is fully 5 arcsec from the galaxy centre.

(v) de Vaucouleurs & Capaccioli (1979) presented an exhaustive study of NGC 3379, with the view to establishing this galaxy as a photometric standard. They collected together all known sources of photometry and transformed them on to a uniform scale, rejecting the less precise

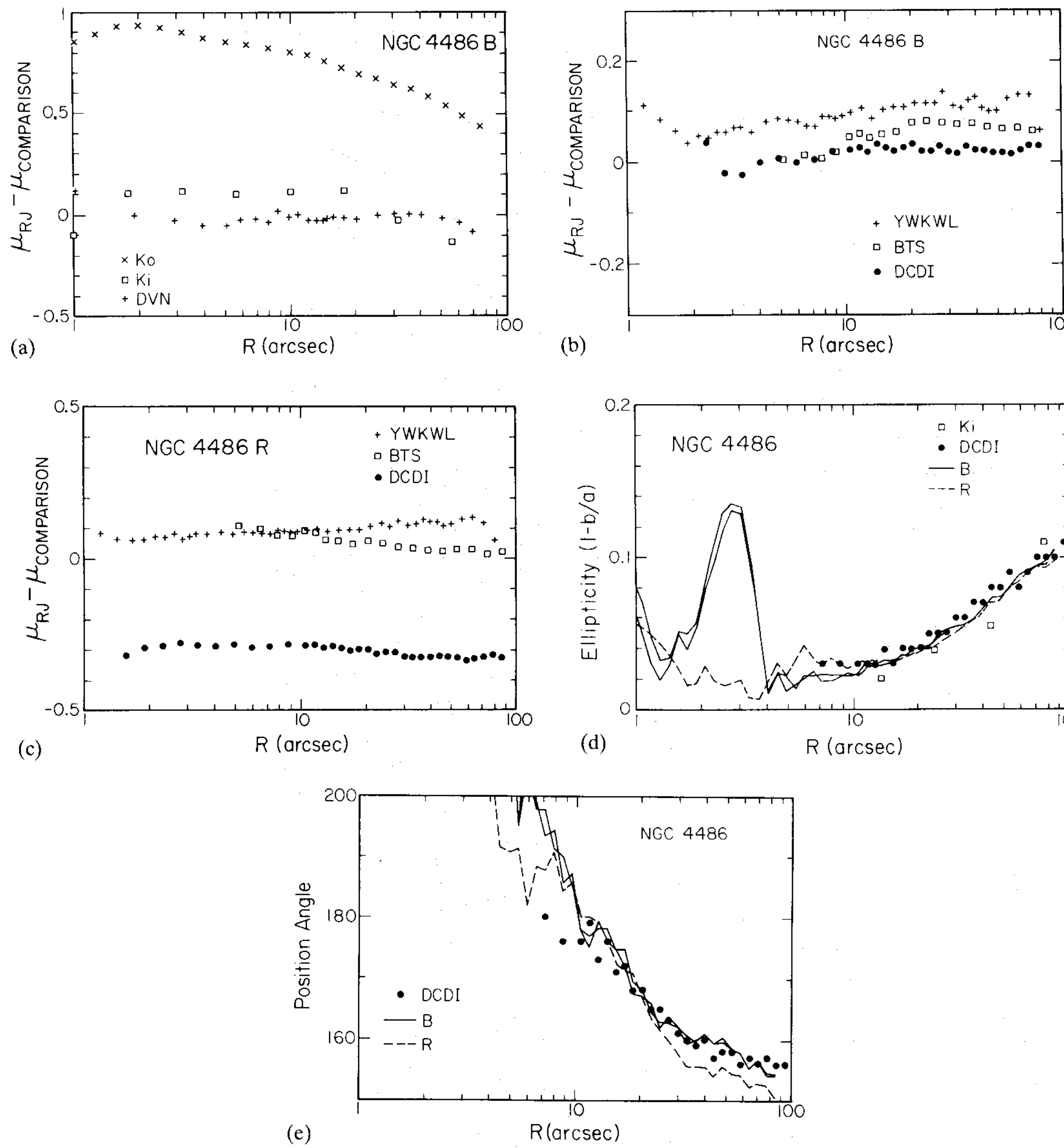

Figure 6. Comparison with surface brightness and geometry measurements of other investigators for NGC 4486. (a) Comparison of B surface brightness profile with photographic or photoelectric works: King (Ki □), de Vaucouleurs & Nieto (DVN +) and Kormendy (Ko × – G-band). (b) Comparison of B surface brightness profile with CCD work: Davis *et al.* (DCDI ●), Young *et al.* (YWKWL +) and Boroson *et al.* (BTS □). (c) Comparison of R surface brightness profile with CCD works: Young *et al.* (YWKWL +), Boroson *et al.* (BTS □) and Davis *et al.* (DCDI ● – R_C-band). (d) Comparison of ellipticity profiles with Davis *et al.* (DCDI ●) and King (Ki □). The lines refer to the results obtained in this work – solid lines are B-band and dashed lines are R-band. The peak in the B-band results at $r=3$ arcsec is due to contamination by M87's jet. (e) Comparison of position angle profiles, legend as in (d). Position angles are in degrees measured from north to east.

studies. The comparison of their profile with mine is very favourable; no systematic trends and a random component with rms ~0.05 mag (Fig. 5a). Despite this agreement, the profile deviates significantly at large radius (≧20 arcsec) from an $r^{1/4}$ law, which they find to be such a good fit.

(vi) de Vaucouleurs & Nieto (1979) presented a photographic and photoelectric profile of

M87. The comparison with this work is again very favourable, with much lower random errors than in DVC (~0.02 mag) and systematic excursions of +0.1 mag in the centre (seeing?) and −0.1 mag at the outside (sky?) (Fig. 6a).

(vii) Boroson *et al.* (1983) used a CCD in a drift-scan mode, which allows accurate flat-fielding and includes more uncontaminated sky. They obtained azimuthally averaged profiles for three galaxies, including M87. In both B and R, the random fluctuations are of order 0.01 mag, but both filters showed a systematic trend of nearly 0.1 mag over the region of overlap (Fig. 6b and c). The reason for this is not clear.

(viii) Kent (1984) uses the same technique for ellipse fitting (except that he keeps the centre fixed), so one might expect the results to be directly comparable. His r-band CCD profile shows systematic trends of $\geqq 0.1$ mag at the low and high brightness levels (Fig. 5c). One possible reason is the disagreement in ellipse parameters (Fig. 5a and b); his ellipticities are ~0.01 low for $1.2 \leqq \log(r) \leqq 1.6$, and position angle ~5 degrees removed from the profiles obtained here.

(ix) Lauer (1985a) and (x) Davis *et al.* (1985, hereafter DCDI) are the two most recent comparisons, so special attention is paid. Both investigators use an ellipse-fitting programme, but Lauer, like Kent, considers the ellipse centres to be fixed. The comparisons for NGC 3379 are shown in Fig.5(c–d). In B, the agreement with DCDI is reasonable (Fig. 5b), with a zero-point difference of 0.1 mag and a small trend at the high surface brightness end, which is probably due to seeing differences. There is a strong fall-off below 23 mag arcsec^{-2}, which cannot be removed by changing the adopted sky value without introducing a hump in the difference profile at a slightly higher surface brightness level. Noticeable also is the strongly deviant point at $B=21.2$, which is possibly an error in transcription of DCDI's table VIII. The zero-point difference arises because different aperture photometry measurements were used to tie in the photometry: DCDI used two apertures from Sandage & Visvanathan (1978), while I used 17 apertures from four different studies.

In R, there is a systematic trend of about 0.1 mag over the range of surface brightnesses from 16 to 22 mag arcsec^{-2} (Fig. 5c) which is probably not an effect of seeing as the FWHMs were similar for the two observations. The zero-point difference arises because the magnitudes of DCDI are reduced to the Cousins system, while those in this work are on the Johnson scale. The comparison with Lauer seems less favourable (Fig. 5c), showing a rise in the residuals of more than 0.2 mag at surface brightnesses above 16, but it should be remembered that the seeing was much better in Lauer's observations than in this work. To quantify this, Lauer's profile was convolved with a Gaussian point-spread function of width 0.97, which represents the square-root of the difference between the squares of the seeing widths. The resulting difference profile is shown in Fig. 5c, and it is seen that the large differences at the high surface brightness end are much reduced, although a trend of about 0.1 mag remains, similar in slope and magnitude to the comparison with DCDI and Boroson *et al.*

The comparison of the geometrical profiles is presented in some detail here, as the results of these three studies should be very similar to those in this work. The ellipticity profiles of Kent, DCDI and Lauer are plotted in Fig. 5(d), along with the ellipticity profiles of all four frames reduced here. The agreement is good over the whole radius range, apart from the high-resolution observations of Lauer in the central few arcseconds. Seeing is almost certainly the cause of this. Notice that the four profiles from this work diverge in the centre, again because the seeing changed between observations.

For the position angle plots, shown in Fig. 5(e), the agreement was less good. Lauer's data shows no evidence for an isophotal twist interior to $r=30$ arcsec, but all four frames reduced here and DCDI show a significant twist of about 7° between $r=6$ and $r=40$ arcsec. Outside this, however, the profiles here all reverse in direction, while those of DCDI continue to twist.

The comparison with DCDI for M87 is shown in Fig. 6(b). The *B* surface brightness profiles agree extremely well, with a zero-point difference of about 0.025 mag and a small trend of 0.05 mag at high surface brightness (<19). In *R*, there was again a downward trend in the difference profile, with magnitude of about 0.05 mag in 3 mag of surface brightness (Fig. 6c). Again, the zero-point difference is due to the difference between Cousins and Johnson *R*-bands. The ellipticity profiles show very good agreement (Fig. 6d), although the three profiles measured here agree with each other better than they agree with DCDI's values. The position angles also agree very well (Fig. 6e), and interestingly the blue position angle profiles here are different from those in the *R*-band for radii between 25 and 100 arcsec. M87 is the only galaxy in this study to show this property, and it is not clear what is the cause of the difference or whether it is real.

Overall, the comparisons with previous work strengthen the belief that the surface brightness profiles are accurate to ± 0.05 mag wherever sky uncertainties and seeing effects are not important. The most serious limitation is the sky level uncertainty, and, unfortunately, there is no way around this with the present data. A combination of photographic and CCD photometry would be a powerful method of obtaining very accurate surface brightness profiles even to very large radii.

7 Conclusions

This paper reports the CCD surface photometry of a sample of 49 early-type galaxies in the *B* and *R* passbands. The galaxy isophotes have been fitted by elliptical isophotes, and higher order harmonic terms have been measured to evaluate the importance of non-ellipticities in the isophotes. The data have been reduced to a uniform magnitude system, and shown to be of comparable precision to the best recent measurements. A future paper will analyse the data in more detail.

Acknowledgments

This work was done while a research student at the Institute of Astronomy, Cambridge. Special thanks go to my supervisors, Roger Davies and George Efstathiou for their help and guidance throughout the course of this work. I have also greatly benefited from discussions with Mike Cawson, Donald Lynden-Bell, Martin Rees and Mike Irwin. The Panel for Allocation of Telescope Time is thanked for two productive nights of AAT time. Financial support was through a SERC studentship, and in the latter stages of this work came from an Isaac Newton Studentship and the DHSS.

References

Abell, G. O., 1958. *Astrophys. J. Suppl. Ser.*, **3,** 211.
Bertola, F. & Capaccioli, M., 1975. *Astrophys. J.*, **200,** 439.
Binney, J., 1976. *Mon. Not. R. astr. Soc.*, **177,** 19.
Binney, J., 1978. *Mon. Not. R. astr. Soc.*, **183,** 501.
Boroson, T. A., Thompson, I. B. & Shectman, S. A., 1983. *Astr. J.*, **88,** 1707.
Burstein, D., 1979. *Astrophys. J. Suppl. Ser.*, **41,** 435.
Carter, D., 1977. *PhD thesis,* University of Cambridge.
Davies, R. L., 1981. *Mon. Not. R. astr. Soc.*, **194,** 879.
Davies, R. L., Efstathiou, G. P., Fall, S. M., Illingworth, G. D. & Schechter, P. L., 1983. *Astrophys. J.*, **266,** 41.
Davis, L. E., Cawson, M., Davies, R. L. & Illingworth, G., 1985. *Astr. J.*, **90,** 169.
de Vaucouleurs, G., 1975. In: *Stars and Stellar Systems, Vol. 9, Galaxies and the Universe,* eds Sandage, A., Sandage, M. & Kristian, J., University of Chicago Press.
de Vaucouleurs, G. & Capaccioli, M., 1979. *Astrophys. J. Suppl. Ser.*, **40,** 699.
de Vaucouleurs, G. & de Vaucouleurs, A., 1972. *Mem. R. astr. Soc.*, **77,** 1.

de Vaucouleurs, G. & Nieto, J.-L., 1979. *Astrophys. J.*, **230**, 697.
de Vaucouleurs, G., de Vaucouleurs, A. & Corwin, H. R., 1976. *Some Reference Catalogue of Bright Galaxies*, University of Texas Press, Austin.
de Vaucouleurs, G., de Vaucouleurs, A. & Corwin, H. G., 1978. *Astr. J.*, **83**, 1331.
Geller, M. J. & Huchra, J. P., 1983. *Astrophys. J. Suppl. Ser.*, **52**, 61.
Huchra, J. P. & Geller, M. J., 1982. *Astrophys. J.*, **257**, 423.
Illingworth, G. D., 1977. *Astrophys. J.*, **218**, L43.
Jorden, P. R., Thorne, D. J. & van Breda, I. G., 1982. *Instrumentation in Astronomy, IV, Proc. SPIE Conference*, Tucson, Arizona.
Kent, S. M., 1983. *Astrophys. J.*, **266**, 562.
Kent, S. M., 1984. *Astrophys. J. Suppl. Ser.*, **56**, 105.
King, I. R., 1978. *Astrophys. J.*, **222**, 1.
Kormendy, J., 1977. *Astrophys. J.*, **214**, 359.
Kormendy, J. & Illingworth, G., 1982. *Astrophys. J.*, **256**, 460.
Lauer, T. R., 1985a. *Astrophys. J. Suppl. Ser.*, **57**, 473.
Lauer, T. R., 1985b. *Mon. Not. R. astr. Soc.*, **216**, 429.
Liller, M. H., 1960. *Astrophys. J.*, **132**, 306.
Liller, M. H., 1966. *Astrophys. J.*, **146**, 28.
Michard, R., 1982. *Astr. Astrophys. Suppl. Ser.*, **49**, 591.
Pence, W., 1976. *Astrophys. J.*, **203**, 39.
Persson, S. E., Frogel, J. A. & Aaronson, M., 1979. *Astrophys. J. Suppl. Ser.*, **39**, 61.
Peterson, C. J., 1978. *Astrophys. J.*, **222**, 84.
Sadler, E. M., 1984. *Astr. J.*, **89**, 34.
Sandage, A., 1973. *Astrophys. J.*, **183**, 711.
Sandage, A., 1975. *Astrophys. J.*, **202**, 563.
Sandage, A. & Tammann, G. A., 1981. *A Revised Shapley–Ames Catalogue of Bright Galaxies*, Carnegie Institute of Washington, Washington.
Sandage, A. & Visvanathan, N., 1978. *Astrophys. J.*, **223**, 707.
Schechter, P. L. & Gunn, J. E., 1979. *Astrophys. J.*, **229**, 472.
Schweizer, F., 1979. *Astrophys. J.*, **233**, 23.
Smyth, R. J. & Stobie, R. S., 1980. *Mon. Not. R. astr. Soc.*, **190**, 631.
Wegner, G., 1979. *Astrophys. Space Sci.*, **60**, 15.
Young, P. J., Westphal, J. A., Kristian, J., Wilson, P. & Landauer, F. P., 1978. *Astrophys. J.*, **221**, 721.

Monthly Notices of the ROYAL ASTRONOMICAL SOCIETY

VOL. 226, NO. 3, 1987

CCD surface photometry of elliptical galaxies - I. Observations, reduction and results

Robert I. Jedrezejewski

Published for
the Royal Astronomical Society
by
Blackwell Scientific Publications Ltd
Osney Mead
Oxford
OX2 0EL

The microfiches are 105 × 148mm archivally permanent silver halide film produced to internationally accepted standards in the NMA 98-image format

Microfiches produced by Micromedia, Bicester, Oxon

Table A1: Surface Photometry of NGC 1549

Seeing σ = 1.2 arcsec (R) and 1.2 arcsec (B)

Semi-Major Axis Length (Arcsec)	Surface Brightness		Ellipticity 1-b/a		Position Angle N thru E		Cos(4θ) Component X100	
	B	R	B	R	B	R	B	R
0.547	17.175	15.405						
0.662	17.192	15.424						
0.801	17.218	15.450						
0.969	17.253	15.487						
1.173	17.302	15.541						
1.419	17.371	15.615						
1.717	17.464	15.712						
2.078	17.590	15.838	0.124	0.107	97.8	98.0	0.0	0.2
2.514	17.753	15.997	0.124	0.115	98.8	99.1	0.1	0.1
3.043	17.947	16.192	0.132	0.119	98.9	100.0	0.1	0.0
3.681	18.178	16.415	0.136	0.127	99.1	100.9	-0.1	0.0
4.455	18.438	16.668	0.141	0.133	100.5	101.2	-0.2	0.0
5.390	18.717	16.938	0.148	0.140	101.8	101.6	-0.1	-0.2
6.522	19.007	17.226	0.152	0.143	103.2	103.6	-0.2	-0.2
7.891	19.294	17.512	0.157	0.144	104.5	105.2	-0.2	-0.2
8.681	19.435	17.648	0.157	0.148	105.7	105.9	-0.4	-0.3
9.549	19.576	17.784	0.155	0.150	106.1	107.1	-0.4	-0.3
10.504	19.711	17.917	0.156	0.152	107.6	108.3	-0.4	-0.3
11.554	19.846	18.056	0.156	0.149	108.4	108.8	-0.2	-0.3
12.709	19.985	18.194	0.153	0.148	110.0	109.7	-0.3	-0.3
13.980	20.129	18.336	0.147	0.143	111.1	110.1	-0.4	-0.3
15.378	20.282	18.489	0.140	0.137	112.6	111.6	-0.3	-0.4
16.916	20.440	18.643	0.133	0.133	114.1	113.2	-0.4	-0.6
18.608	20.592	18.796	0.132	0.128	116.2	115.1	-0.5	-0.5
20.469	20.740	18.945	0.132	0.129	118.8	118.7	-0.4	-0.4
22.515	20.879	19.087	0.137	0.131	120.7	120.2	-0.5	-0.5
24.767	21.020	19.230	0.136	0.131	123.3	122.8	-0.6	-0.6
27.244	21.156	19.369	0.141	0.131	124.0	124.5	-0.5	-0.7
29.968	21.302	19.511	0.136	0.126	127.4	126.7	-0.3	-0.7
32.965	21.444	19.659	0.135	0.128	128.8	129.9	-0.2	-0.1
36.261	21.595	19.807	0.133	0.127	131.8	132.6	0.1	0.1
39.887	21.744	19.961	0.135	0.125	134.3	135.0	0.4	0.4
43.876	21.905	20.121	0.129	0.120	136.4	136.8	0.6	0.6
48.264	22.077	20.287	0.123	0.117	136.9	138.4	0.6	0.7
53.090	22.263	20.474	0.117	0.113	136.9	137.2	0.5	0.7
58.399	22.472	20.686	0.111	0.102	135.5	134.6	0.2	0.4
64.239	22.699	20.913	0.106	0.092	135.7	135.0	0.3	0.6
70.663	22.945	21.132		0.092		132.8		0.3
77.729	23.195	21.367		0.071		140.8		0.6
85.502	23.444	21.588						
94.052	23.692	21.769						
103.458	23.920							

Table A2: Surface Photometry of NGC 2865

Seeing σ = 0.65 arcsec (R) and 0.85 arcsec (B)

Semi-Major Axis Length (Arcsec)	Surface Brightness		Ellipticity 1-b/a		Position Angle N thru E		Cos(4θ) Component X100	
	B	R	B	R	B	R	B	R
0.547	17.080	15.365						
0.662	17.143	15.428						
0.801	17.230	15.528						
0.969	17.348	15.674						
1.173	17.512	15.874						
1.419	17.737	16.124						
1.717	18.018	16.417						
2.078	18.360	16.742	0.070	0.098	159.8	165.2	-0.1	0.2
2.514	18.722	17.076	0.083	0.105	163.1	166.0	-0.2	0.1
3.043	19.079	17.391	0.092	0.109	164.7	166.3	-0.3	0.1
3.681	19.401	17.669	0.104	0.122	165.5	165.4	-0.2	-0.1
4.455	19.686	17.921	0.130	0.150	163.9	163.3	-0.1	0.1
5.390	19.962	18.176	0.154	0.175	162.4	161.1	-0.1	-0.1
6.522	20.231	18.433	0.193	0.202	160.4	160.6	0.0	0.1
7.891	20.513	18.696	0.219	0.235	159.7	159.6	-0.2	0.1
8.681	20.652	18.837	0.235	0.244	159.6	158.9	0.0	0.1
9.549	20.797	18.984	0.247	0.250	159.2	158.9	-0.2	-0.3
10.504	20.937	19.126	0.255	0.256	159.4	158.8	-0.1	-0.2
11.554	21.072	19.259	0.265	0.265	158.3	158.1	-0.3	-0.1
12.709	21.207	19.394	0.278	0.273	158.2	157.6	0.3	-0.3
13.980	21.355	19.533	0.273	0.280	157.9	157.5	0.2	0.2
15.378	21.499	19.691	0.285	0.278	156.9	157.0	-0.1	-0.1
16.916	21.682	19.861	0.276	0.275	156.6	156.5	-0.3	-0.2
18.608	21.865	20.051	0.279	0.267	156.7	156.9	0.1	0.2
20.469	22.053	20.256	0.269	0.260	156.0	157.0	-0.4	0.2
22.515	22.261	20.453	0.259	0.254	156.2	156.3	0.1	0.2
24.767	22.461	20.664	0.256	0.251	155.9	155.9	0.8	0.7
27.244	22.665	20.883	0.252	0.245	155.8	155.4	0.8	0.8
29.968	22.908	21.131	0.227	0.217	155.5	154.3	0.8	1.0
32.965	23.120	21.355	0.225	0.208	155.6	153.7	1.5	1.1
36.261	23.306	21.559	0.219	0.216	153.8	153.2	0.5	1.0
39.887	23.513	21.804	0.218	0.208	150.9	150.4	0.5	0.3
43.876	23.755	22.052	0.187	0.202	148.1	148.5	-0.3	-0.5
48.264	23.938	22.271		0.227		149.5		0.2
53.090	24.098	22.480						
58.399	24.263	22.659						
64.239	24.449	22.882						
70.663	24.653	23.134						
77.729	24.874	23.462						
85.502	25.083	23.715						
94.052	25.288	24.016						
103.458	25.385	24.102						

Table A3: Surface Photometry of NGC 3091

Seeing σ = 0.8 arcsec (R) and 1.0 arcsec (B)

Semi-Major Axis Length (Arcsec)	Surface Brightness		Ellipticity 1-b/a		Position Angle N thru E		Cos(4θ) Component X100	
	B	R	B	R	B	R	B	R
0.547	18.242	16.272						
0.662	18.265	16.299						
0.801	18.299	16.339						
0.969	18.347	16.393						
1.173	18.413	16.466						
1.419	18.501	16.565						
1.717	18.616	16.687						
2.078	18.762	16.842	0.138	0.141	142.9	145.0	-0.1	-0.2
2.514	18.941	17.027	0.146	0.155	144.4	146.2	-0.2	-0.1
3.043	19.156	17.242	0.159	0.170	145.3	146.4	-0.2	-0.1
3.681	19.401	17.486	0.173	0.182	146.6	146.6	-0.2	-0.4
4.455	19.675	17.754	0.183	0.192	146.7	147.2	-0.4	-0.6
5.390	19.970	18.044	0.194	0.202	147.4	147.3	-0.4	-0.5
6.522	20.276	18.348	0.204	0.205	147.9	147.5	-0.7	-0.6
7.891	20.572	18.637	0.216	0.218	147.6	148.2	-0.6	-0.7
8.681	20.710	18.773	0.226	0.228	148.2	148.1	-0.6	-0.4
9.549	20.846	18.909	0.236	0.232	147.1	147.6	-0.4	-0.5
10.504	20.982	19.044	0.242	0.241	147.9	147.8	-0.6	-0.6
11.554	21.127	19.187	0.247	0.241	147.3	147.9	-0.7	-0.7
12.709	21.279	19.340	0.244	0.243	147.6	147.9	-0.7	-0.6
13.980	21.440	19.496	0.245	0.239	146.8	147.6	-0.6	-0.6
15.378	21.598	19.655	0.247	0.241	147.0	147.5	-0.5	-0.5
16.916	21.770	19.832	0.246	0.237	146.7	147.5	-0.5	-0.6
18.608	21.942	19.998	0.245	0.241	146.7	146.5	-0.4	-0.4
20.469	22.112	20.169	0.243	0.238	146.8	146.4	-0.2	-0.3
22.515	22.267	20.330	0.255	0.248	147.2	147.1	0.1	-0.1
24.767	22.431	20.486	0.263	0.257	147.2	147.0	-0.4	-0.7
27.244	22.576	20.632	0.279	0.274	146.2	146.3	0.0	0.1
29.968	22.719	20.784	0.294	0.285	145.9	145.5	-0.1	-0.3
32.965	22.861	20.931	0.305	0.297	146.3	145.9	0.2	0.3
36.261	23.004	21.085	0.316	0.304	145.7	145.1	-0.3	0.0
39.887	23.158	21.235	0.326	0.318	145.4	144.5	0.0	0.0
43.876	23.315	21.409	0.329	0.320	145.2	144.2	0.1	-0.1
48.264	23.478	21.574	0.336	0.327	144.7	143.5	0.2	0.4
53.090	23.613	21.745	0.354	0.340	143.9	144.2	0.3	0.7
58.399	23.817	21.950	0.347		143.3		-0.2	
64.239	24.025	22.144						
70.663	24.223	22.397						
77.729	24.408	22.589						
85.502	24.640	22.787						
94.052	24.882							
103.458	25.127							

1987MNRAS.226..747J

Table A4: Surface Photometry of NGC 3250

Seeing σ = 0.7 arcsec (R) and 0.85 arcsec (B)

Semi-Major Axis Length (Arcsec)	Surface Brightness		Ellipticity 1-b/a		Position Angle N thru E		Cos(4θ) Component X100	
	B	R	B	R	B	R	B	R
0.547	18.289	16.231						
0.662	18.310	16.255						
0.801	18.342	16.291						
0.969	18.385	16.339						
1.173	18.444	16.405						
1.419	18.519	16.493						
1.717	18.618	16.603						
2.078	18.743	16.732	0.160	0.170	137.3	137.9	0.0	0.1
2.514	18.892	16.884	0.170	0.183	137.2	137.8	0.0	0.1
3.043	19.058	17.057	0.188	0.196	137.2	138.0	0.1	-0.2
3.681	19.255	17.249	0.198	0.210	137.6	137.2	-0.2	-0.2
4.455	19.467	17.470	0.212	0.216	137.7	137.8	-0.3	-0.3
5.390	19.707	17.704	0.221	0.228	137.4	137.8	-0.4	-0.5
6.522	19.967	17.964	0.229	0.233	137.4	137.9	-0.4	-0.5
7.891	20.241	18.231	0.240	0.245	137.2	137.3	-0.4	-0.5
8.681	20.378	18.369	0.247	0.247	137.0	137.1	-0.3	-0.4
9.549	20.518	18.504	0.255	0.257	137.5	137.2	-0.3	-0.4
10.504	20.659	18.645	0.263	0.263	137.2	137.5	-0.4	-0.3
11.554	20.804	18.789	0.269	0.268	137.3	137.1	-0.3	-0.6
12.709	20.955	18.942	0.272	0.267	137.4	137.5	-0.3	-0.4
13.980	21.120	19.105	0.270	0.265	137.3	137.4	-0.4	-0.6
15.378	21.292	19.273	0.267	0.263	137.2	137.7	-0.1	-0.4
16.916	21.469	19.451	0.266	0.261	137.2	137.8	0.1	-0.3
18.608	21.641	19.627	0.270	0.260	137.0	137.7	-0.2	-0.2
20.469	21.825	19.814	0.264	0.255	137.1	137.4	-0.1	-0.4
22.515	22.004	19.993	0.268	0.259	136.8	136.9	0.0	0.0
24.767	22.176	20.172	0.267	0.261	136.0	136.3	0.0	-0.1
27.244	22.339	20.338	0.276	0.268	136.2	136.2	-0.2	0.0
29.968	22.508	20.514	0.282	0.269	135.9	136.2	-0.1	-0.2
32.965	22.682	20.698	0.282	0.268	136.8	136.7	-0.1	0.1
36.261	22.868	20.887	0.275	0.262	136.2	136.1	-0.4	-0.2
39.887	23.063	21.100	0.262	0.252	135.9	135.8	-0.2	-0.2
43.876	23.261	21.317	0.254	0.240	136.4	135.9	0.3	0.1
48.264	23.483	21.553	0.239	0.225	137.0	136.9	0.7	0.7
53.090	23.688	21.767	0.228	0.225	137.2	136.9	1.1	0.8
58.399	23.890	21.992	0.223	0.211	137.8	137.3	0.9	1.0
64.239	24.093	22.213	0.201	0.195	133.3	134.4	0.4	1.0
70.663	24.270	22.431		0.165		128.8		0.6
77.729	24.449	22.654						
85.502		22.756						

Table A5: Surface Photometry of NGC 3258

Seeing σ = 0.65 arcsec (R) and 0.95 arcsec (B)

Semi-Major Axis Length (Arcsec)	Surface Brightness		Ellipticity 1-b/a		Position Angle N thru E		Cos(4θ) Component X100	
	B	R	B	R	B	R	B	R
0.547	18.643	16.571						
0.662	18.657	16.588						
0.801	18.678	16.612						
0.969	18.706	16.648						
1.173	18.747	16.696						
1.419	18.805	16.766						
1.717	18.886	16.864						
2.078	18.997	16.993	0.147	0.159	76.6	76.6	0.0	0.0
2.514	19.145	17.160	0.149	0.166	76.4	76.5	0.1	0.1
3.043	19.337	17.368	0.152	0.166	76.0	76.4	0.0	0.1
3.681	19.571	17.611	0.150	0.164	76.8	76.4	0.0	0.0
4.455	19.837	17.880	0.152	0.164	76.3	76.3	-0.1	0.0
5.390	20.134	18.175	0.150	0.159	75.3	75.5	-0.1	0.0
6.522	20.453	18.489	0.146	0.152	75.2	75.3	-0.1	-0.1
7.891	20.784	18.812	0.141	0.143	75.1	75.5	-0.1	0.1
8.681	20.956	18.978	0.134	0.137	75.3	75.9	-0.1	0.0
9.549	21.125	19.144	0.131	0.130	75.3	75.9	0.2	0.0
10.504	21.293	19.303	0.124	0.124	75.8	77.9	0.0	-0.4
11.554	21.457	19.460	0.121	0.120	77.4	79.7	0.1	-0.5
12.709	21.621	19.621	0.115	0.115	78.0	77.9	0.1	-0.1
13.980	21.789	19.778	0.107	0.112	77.1	76.6	-0.1	0.0
15.378	21.956	19.939	0.102	0.104	75.3	75.3	0.1	0.0
16.916	22.124	20.104	0.095	0.094	74.1	74.0	0.0	0.0
18.608	22.305	20.277	0.087	0.085	73.5	72.5	0.1	0.1
20.469	22.491	20.454	0.081	0.078	73.3	70.3	0.5	0.1
22.515	22.683	20.636	0.076	0.073	68.2	69.3	-0.1	-0.1
24.767	22.884	20.820	0.073	0.069	67.3	66.0	0.4	0.1
27.244	23.061	20.988	0.075	0.070	67.0	66.7	0.5	0.2
29.968	23.236	21.147	0.079	0.069	65.1	64.5	0.5	0.7
32.965	23.380	21.293	0.102	0.079	62.6	63.0	0.2	0.4
36.261	23.539	21.443	0.110	0.074	60.7	65.4	0.2	0.7
39.887	23.684	21.573	0.116	0.085	57.1	60.6	0.2	-0.2
43.876	23.830	21.681	0.121	0.105	58.3	62.4	0.3	-0.1
48.264	23.968	21.796	0.138	0.131	57.2	58.9	0.1	0.2
53.090	24.124	21.913	0.127	0.124	56.5	58.8	-0.2	0.1
58.399	24.297	22.023	0.124	0.160	52.8	59.3	-0.2	0.1
64.239	24.446		0.122		50.2		0.1	
70.663	24.626							

Table A6: Surface Photometry of NGC 3260

Seeing σ = 0.7 arcsec (R) and 0.9 arcsec (B)

Semi-Major Axis Length (Arcsec)	Surface Brightness		Ellipticity 1-b/a		Position Angle N thru E		Cos(4θ) Component X100	
	B	R	B	R	B	R	B	R
0.547	19.113	17.000						
0.662	19.153	17.052						
0.801	19.213	17.123						
0.969	19.294	17.220						
1.173	19.401	17.346						
1.419	19.537	17.500						
1.717	19.704	17.679						
2.078	19.892	17.880	0.114	0.121	4.2	6.5	0.5	-0.7
2.514	20.086	18.079	0.129	0.148	5.4	5.5	0.8	-0.7
3.043	20.266	18.267	0.144	0.171	8.2	6.8	0.7	-0.7
3.681	20.413	18.441	0.172	0.196	14.4	6.3	1.5	-0.7
4.455	20.575	18.619	0.191	0.226	9.4	4.3	0.1	-0.9
5.390	20.738	18.816	0.238	0.257	5.8	3.8	0.1	-0.8
6.522	20.957	19.043	0.263	0.279	5.5	3.9	0.2	-0.9
7.891	21.236	19.322	0.272	0.288	3.3	3.2	0.9	-1.3
8.681	21.398	19.481	0.271	0.288	2.8	2.2	1.1	-1.5
9.549	21.568	19.665	0.271	0.276	2.4	2.0	1.4	-1.1
10.504	21.752	19.842	0.262	0.269	1.9	2.0	1.7	-1.2
11.554	21.927	20.022	0.265	0.264	2.1	1.6	1.6	-1.5
12.709	22.104	20.209	0.266	0.258	1.8	1.9	1.9	-1.5
13.980	22.309	20.388	0.259	0.258	2.1	1.6	1.6	-1.2
15.378	22.491	20.539	0.263	0.273	2.5	2.6	1.6	-1.7
16.916	22.664	20.693	0.275	0.291	2.7	3.2	1.8	-1.7
18.608	22.855	20.873	0.283	0.297	4.1	3.4	2.0	-1.6
20.469	23.048	21.053	0.290	0.301	4.5	3.9	1.3	-1.4
22.515	23.233	21.255	0.297	0.301	5.5	4.6	1.9	-1.4
24.767	23.396	21.408	0.312	0.322	7.0	5.8	2.2	-1.4
27.244	23.627	21.612	0.297	0.311	7.7	7.8	1.8	-0.8
29.968	23.909	21.852	0.259	0.292	11.2	9.7	1.4	-0.9
32.965	24.152	22.111	0.245	0.262	15.3	11.4	0.7	0.2
36.261	24.405	22.367	0.225	0.238	19.9	16.0	0.5	0.2
39.887	24.643							
43.876	24.863							
48.264	25.029							
53.090	25.203							
58.399	25.340							
64.239	25.475							
70.663	25.542							
77.729	25.686							
85.502	25.822							
94.052	25.942							
103.458	25.962							

Table A7: Surface Photometry of NGC 3268

Seeing σ = 0.7 arcsec (R) and 0.85 arcsec (B)

Semi-Major Axis Length (Arcsec)	Surface Brightness		Ellipticity 1-b/a		Position Angle N thru E		Cos(4θ) Component X100	
	B	R	B	R	B	R	B	R
0.547	18.977	16.782						
0.662	18.994	16.801						
0.801	19.017	16.829						
0.969	19.046	16.871						
1.173	19.091	16.928						
1.419	19.153	17.000						
1.717	19.230	17.095						
2.078	19.324	17.209	0.107	0.107	76.3	69.7	0.2	-0.2
2.514	19.441	17.352	0.114	0.118	73.2	69.7	0.1	-0.1
3.043	19.593	17.534	0.126	0.134	70.1	69.4	0.1	0.2
3.681	19.794	17.759	0.142	0.151	69.9	68.9	0.3	0.2
4.455	20.045	18.032	0.153	0.158	68.6	68.7	0.2	0.2
5.390	20.334	18.331	0.160	0.162	69.2	68.5	0.3	0.1
6.522	20.629	18.634	0.169	0.169	68.3	68.1	0.1	0.1
7.891	20.931	18.932	0.176	0.178	67.9	68.3	0.3	0.3
8.681	21.075	19.081	0.181	0.180	68.3	68.0	0.3	0.2
9.549	21.223	19.229	0.185	0.184	68.1	68.1	0.1	0.1
10.504	21.374	19.377	0.185	0.186	68.0	68.1	0.2	0.2
11.554	21.524	19.529	0.188	0.185	68.0	68.1	0.2	0.3
12.709	21.676	19.683	0.189	0.186	67.9	67.4	0.2	0.2
13.980	21.825	19.833	0.192	0.187	68.2	66.8	0.1	0.1
15.378	21.963	19.973	0.200	0.195	67.8	67.5	-0.3	-0.2
16.916	22.107	20.117	0.203	0.199	66.6	66.5	-0.5	-0.3
18.608	22.267	20.279	0.197	0.193	66.6	65.7	-0.1	-0.1
20.469	22.404	20.426	0.204	0.197	67.3	67.2	0.0	-0.1
22.515	22.537	20.565	0.209	0.201	67.3	67.5	-0.2	-0.2
24.767	22.667	20.707	0.215	0.203	67.1	66.9	0.3	0.1
27.244	22.821	20.862	0.210	0.199	67.1	67.1	-0.1	-0.3
29.968	22.964	21.014	0.211	0.199	67.3	68.2	0.1	0.0
32.965	23.100	21.174	0.209	0.191	66.1	66.5	0.0	0.2
36.261	23.237	21.323	0.211	0.192	64.9	66.3	0.2	-0.2
39.887	23.369	21.466	0.215	0.194	64.9	65.9	0.1	0.1
43.876	23.484	21.597	0.224	0.200	66.0	66.5	0.6	0.2
48.264	23.593	21.712	0.229	0.215	67.4	67.5	-0.3	-0.3
53.090	23.708	21.841	0.236	0.218	69.0	67.5	-0.3	0.0
58.399	23.829	21.977	0.236	0.223	68.5	66.5	-0.3	0.2
64.239	23.946	22.094	0.243	0.241	66.6	66.6	0.4	0.9
70.663	24.087	22.218	0.223	0.251	66.0	68.4	-1.1	0.5
77.729	24.196	22.344		0.262		67.3		0.2
85.502	24.296							

Table A8: Surface Photometry of NGC 3308

Seeing σ = 0.6 arcsec (R) and 0.75 arcsec (B)

Semi-Major Axis Length (Arcsec)	Surface Brightness		Ellipticity 1-b/a		Position Angle N thru E		Cos(4θ) Component X100	
	B	R	B	R	B	R	B	R
0.547	18.620	16.594						
0.662	18.688	16.673						
0.801	18.772	16.779						
0.969	18.888	16.916						
1.173	19.045	17.091						
1.419	19.232	17.297						
1.717	19.452	17.528						
2.078	19.688	17.768	0.054	0.060	47.6	36.4	-0.1	0.0
2.514	19.929	18.004	0.061	0.068	42.6	37.4	-0.3	-0.3
3.043	20.163	18.233	0.073	0.077	38.9	34.2	-0.3	-0.1
3.681	20.403	18.469	0.074	0.077	35.8	34.5	-0.4	-0.6
4.455	20.656	18.713	0.072	0.070	34.3	33.1	-0.4	-0.5
5.390	20.912	18.967	0.070	0.069	33.1	33.9	-0.6	-0.5
6.522	21.165	19.211	0.068	0.063	32.0	30.1	-0.4	-0.2
7.891	21.399	19.438	0.069	0.067	27.8	26.5	-0.2	-0.1
8.681	21.507	19.538	0.073	0.081	27.4	30.5	-0.3	-0.2
9.549	21.608	19.649	0.087	0.077	29.4	27.1	-0.2	0.1
10.504	21.713	19.744	0.095	0.097	29.6	29.2	-0.2	0.2
11.554	21.810	19.843	0.113	0.113	31.1	31.0	0.1	0.1
12.709	21.922	19.942	0.131	0.133	31.4	31.3	0.0	0.2
13.980	22.037	20.058	0.152	0.157	31.5	32.3	0.2	0.1
15.378	22.170	20.195	0.171	0.173	31.8	32.1	0.4	0.5
16.916	22.343	20.358	0.182	0.181	32.7	33.3	0.7	0.9
18.608	22.534	20.534	0.187	0.193	33.3	32.7	1.0	1.0
20.469	22.726	20.732	0.199	0.196	33.4	33.0	1.3	1.2
22.515	22.914	20.921	0.214	0.210	33.0	33.5	1.8	1.6
24.767	23.085	21.089	0.238	0.230	32.6	32.8	2.2	1.8
27.244	23.231	21.229	0.267	0.258	32.3	33.4	2.5	2.3
29.968	23.391	21.393	0.282	0.271	32.6	32.9	2.3	2.0
32.965	23.595	21.591	0.278	0.273	33.9	33.0	1.2	1.8
36.261	23.829	21.811	0.268	0.262	35.1	34.5	0.2	0.5
39.887	24.063	22.033	0.268	0.265	34.2	33.9	0.5	0.5
43.876	24.311	22.277	0.265	0.251	33.2	31.9	0.5	0.1
48.264	24.561	22.512	0.265	0.239	33.0	32.4	0.6	0.7
53.090	24.875	22.726	0.220		30.3		-0.3	
58.399	25.225	22.963	0.188		27.3		-1.0	
64.239	25.590	23.251						
70.663	25.956	23.467						
77.729	26.340	23.705						
85.502	26.641	23.883						
94.052	26.962	24.041						
103.458	27.091	24.057						
113.803	27.272							

Table A9: Surface Photometry of NGC 3309

Seeing σ = 0.6 arcsec (R) and 0.7 arcsec (B)

Semi-Major Axis Length (Arcsec)	Surface Brightness		Ellipticity 1-b/a		Position Angle N thru E		Cos(4θ) Component X100	
	B	R	B	R	B	R	B	R
0.547	18.578	16.558						
0.662	18.608	16.591						
0.801	18.648	16.638						
0.969	18.700	16.701						
1.173	18.772	16.785						
1.419	18.870	16.893						
1.717	18.995	17.028						
2.078	19.148	17.190	0.134	0.137	50.3	50.8	-0.2	0.0
2.514	19.330	17.378	0.143	0.144	49.9	49.3	-0.3	-0.4
3.043	19.538	17.589	0.151	0.153	49.6	48.2	-0.3	-0.4
3.681	19.780	17.828	0.152	0.155	49.0	48.3	-0.5	-0.5
4.455	20.045	18.092	0.149	0.151	48.3	48.2	-0.3	-0.6
5.390	20.326	18.372	0.149	0.149	47.6	48.3	-0.3	-0.5
6.522	20.607	18.649	0.150	0.152	47.1	47.1	-0.3	-0.4
7.891	20.891	18.927	0.155	0.154	47.0	45.9	-0.4	-0.4
8.681	21.042	19.076	0.152	0.151	46.2	46.7	-0.1	-0.3
9.549	21.195	19.228	0.149	0.149	45.9	45.9	-0.2	-0.1
10.504	21.352	19.385	0.150	0.147	45.6	45.8	-0.1	-0.1
11.554	21.522	19.549	0.143	0.143	45.3	45.8	-0.1	-0.1
12.709	21.695	19.724	0.138	0.135	45.3	44.6	-0.2	-0.2
13.980	21.870	19.896	0.133	0.128	44.1	44.7	0.1	0.0
15.378	22.048	20.073	0.132	0.125	44.3	44.6	-0.1	-0.3
16.916	22.208	20.231	0.138	0.131	45.4	45.7	-0.2	-0.2
18.608	22.368	20.391	0.145	0.132	44.6	45.0	-0.3	-0.1
20.469	22.526	20.550	0.148	0.130	47.0	47.1	-0.6	-0.4
22.515	22.693	20.730	0.142	0.115	49.2	50.8	-0.4	-0.2
24.767	22.873	20.903	0.127	0.108	51.2	55.9	-0.7	-0.2
27.244	23.066	21.096	0.119	0.101	52.0	52.3	-0.1	0.1
29.968	23.240	21.266	0.096	0.077	56.6	65.7	0.4	0.1
32.965	23.398	21.378	0.095	0.102	66.3	85.2	0.6	0.1
36.261	23.546	21.577	0.094	0.093	79.9	85.2	0.2	0.1
39.887	23.731	21.764	0.083	0.092	82.2	85.5	-0.1	0.0
43.876	23.929	21.976	0.080	0.097	83.3	84.9	0.2	0.5
48.264		22.219						
53.090		22.447						
58.399		22.543						

Table A10: Surface Photometry of NGC 3311

Seeing σ = 0.6 arcsec (R) and 0.8 arcsec (B)

Semi-Major Axis Length (Arcsec)	Surface Brightness		Ellipticity 1-b/a		Position Angle N thru E		Cos(4θ) Component X100	
	B	R	B	R	B	R	B	R
0.547	20.294	18.385						
0.662	20.336	18.385						
0.801	20.344	18.385						
0.969	20.366	18.397						
1.173	20.359	18.384						
1.419	20.354	18.388						
1.717	20.359	18.399						
2.078	20.352	18.404	0.325	0.361	66.5	97.9	2.4	-12.5
2.514	20.347	18.414	0.782	0.289	66.5	67.7	2.4	0.7
3.043	20.442	18.478	0.265	0.212	61.1	54.6	1.5	0.9
3.681	20.538	18.573	0.206	0.193	53.2	50.3	1.4	0.8
4.455	20.679	18.710	0.170	0.164	49.4	49.1	1.0	0.8
5.390	20.845	18.875	0.162	0.160	47.4	47.8	0.6	0.9
6.522	21.033	19.060	0.164	0.165	45.4	46.8	0.6	0.6
7.891	21.236	19.265	0.167	0.166	42.9	44.8	0.4	0.5
8.681	21.350	19.375	0.162	0.165	43.8	44.1	0.1	0.3
9.549	21.462	19.490	0.158	0.158	42.6	42.2	-0.1	0.1
10.504	21.581	19.606	0.149	0.149	40.8	41.1	-0.2	-0.3
11.554	21.695	19.721	0.144	0.143	39.5	39.6	-0.3	-0.1
12.709	21.807	19.836	0.145	0.136	36.3	37.8	-0.3	-0.3
13.980	21.926	19.955	0.132	0.122	37.1	36.9	-0.1	-0.2
15.378	22.047	20.073	0.123	0.116	33.7	33.6	0.0	0.0
16.916	22.157	20.184	0.111	0.109	34.3	34.9	0.3	0.2
18.608	22.279	20.299	0.088	0.095	34.0	32.6	0.4	0.4
20.469	22.394	20.419	0.067	0.069	30.6	31.5	1.0	0.8
22.515	22.486	20.521	0.068	0.067	37.2	34.1	0.3	0.7
24.767	22.587	20.626	0.067	0.066	44.5	37.6	0.1	0.5
27.244	22.706	20.738	0.058	0.061	40.8	37.8	0.2	0.5
29.968	22.822	20.852	0.043	0.046	39.7	38.8	0.2	0.2
32.965	22.919	20.958	0.055	0.048	39.7	47.9	-0.3	0.1
36.261	23.018	21.068	0.056	0.050	46.4	44.2	-0.3	0.0
39.887	23.117	21.172	0.054	0.048	49.1	51.5	-0.5	-0.9
43.876	23.229	21.298	0.033	0.013				
48.264		21.416		0.010				
53.090	23.477	21.548	0.012	0.016				
58.399	23.600	21.686	0.033	0.026				

Table A11: Surface Photometry of NGC 3377

Seeing σ = 1.15 arcsec (R) and 1.3 arcsec (B)

Semi-Major Axis Length (Arcsec)	Surface Brightness		Ellipticity 1-b/a		Position Angle N thru E		Cos(4θ) Component X100	
	B	R	B	R	B	R	B	R
0.547	17.143	15.369						
0.662	17.167	15.390						
0.801	17.198	15.425						
0.969	17.248	15.475						
1.173	17.319	15.549						
1.419	17.416	15.655						
1.717	17.545	15.792						
2.078	17.710	15.964	0.198	0.201	42.8	40.7	0.3	0.4
2.514	17.908	16.161	0.219	0.226	42.7	40.5	0.7	0.6
3.043	18.134	16.381	0.246	0.257	42.1	40.7	0.9	0.9
3.681	18.376	16.618	0.280	0.290	41.6	40.8	1.3	1.2
4.455	18.629	16.864	0.317	0.326	41.4	40.9	1.5	1.5
5.390	18.894	17.123	0.351	0.357	41.2	41.1	1.6	1.7
6.522	19.162	17.389	0.380	0.384	41.4	41.2	1.8	1.7
7.891	19.435	17.662	0.405	0.406	41.1	41.2	1.6	1.6
8.681	19.569	17.800	0.416	0.416	41.3	41.2	1.4	1.7
9.549	19.706	17.937	0.425	0.425	41.0	41.1	1.4	1.5
10.504	19.832	18.076	0.438	0.433	40.7	40.9	1.2	1.3
11.554	19.974	18.216	0.444	0.440	40.5	40.8	1.5	1.2
12.709	20.105	18.353	0.452	0.446	40.2	40.9	1.4	1.0
13.980	20.234	18.490	0.462	0.452	40.2	40.8	1.2	1.0
15.378	20.367	18.622	0.468	0.460	40.6	40.9	1.1	0.9
16.916	20.497	18.755	0.47[illegible]	0.467	40.4	41.0	0.8	1.0
18.608	20.626	18.888	0.485	0.474	40.7	41.0	0.9	1.0
20.469	20.757	19.025	0.491	0.480	40.6	41.0	1.0	0.8
22.515	20.894	19.164	0.497	0.486	41.1	41.4	0.8	0.8
24.767	21.037	19.310	0.501	0.488	41.2	41.3	0.7	0.8
27.244	21.193	19.468	0.501	0.489	41.3	41.4	0.4	0.8
29.968	21.356	19.637	0.500	0.489	41.4	41.1	0.4	0.9
32.965	21.537	19.814	0.496	0.486	41.2	40.9	0.4	0.8
36.261	21.721	20.002	0.491	0.481	41.5	41.2	0.1	0.5
39.887	21.923	20.213	0.483	0.472	41.3	41.2	-0.2	0.2
43.876	22.139	20.442	0.469	0.456	41.3	41.4	-0.4	-0.4
48.264	22.352	20.658	0.457	0.447	41.1	41.0	-1.1	-0.4
53.090	22.590	20.899	0.441	0.430	40.9	41.1	-1.3	-0.8
58.399	22.837	21.120	0.421	0.420	41.4	41.4	-1.5	-1.0
64.239	23.067	21.353	0.397	0.396	41.3	41.4	-1.6	-1.1
70.663	23.263	21.570		0.382		41.9		-1.5
77.729	23.464	21.781						
85.502	23.660	21.995						
94.052	23.866	22.212						
103.458	24.095	22.446						
113.803	24.317	22.694						

Table A12: Surface Photometry of NGC 3379

Seeing σ = 1.15 arcsec (R) and 1.45 arcsec (B)

Semi-Major Axis Length (Arcsec)	Surface Brightness		Ellipticity 1-b/a		Position Angle N thru E		Cos(4θ) Component X100	
	B	R	B	R	B	R	B	R
0.547	17.162	15.191						
0.662	17.172	15.207						
0.801	17.187	15.230						
0.969	17.210	15.260						
1.173	17.243	15.303						
1.419	17.288	15.362						
1.717	17.352	15.440						
2.078	17.438	15.544	0.035	0.050	73.0	74.8	0.1	0.0
2.514	17.550	15.673	0.042	0.058	74.4	74.3	-0.1	-0.1
3.043	17.693	15.834	0.047	0.063	75.6	73.9	0.1	0.0
3.681	17.873	16.024	0.052	0.069	73.6	74.1	0.1	0.1
4.455	18.086	16.250	0.059	0.070	75.0	74.7	-0.1	0.0
5.390	18.337	16.502	0.061	0.071	73.8	74.2	0.0	0.0
6.522	18.613	16.781	0.063	0.071	73.6	74.2	0.0	0.1
7.891	18.904	17.069	0.068	0.073	73.7	73.5	0.2	0.1
8.681	19.052	17.214	0.072	0.076	73.2	74.2	0.1	0.2
9.549	19.201	17.363	0.075	0.078	73.5	72.9	0.1	0.1
10.504	19.358	17.517	0.077	0.079	72.6	72.8	0.1	0.1
11.554	19.520	17.678	0.078	0.078	72.5	72.3	0.1	0.1
12.709	19.685	17.842	0.080	0.082	72.0	71.9	0.1	0.1
13.980	19.858	18.013	0.084	0.083	72.3	71.8	0.0	0.1
15.378	20.039	18.192	0.084	0.084	71.6	71.4	0.1	0.1
16.916	20.218	18.375	0.089	0.086	71.3	71.4	0.0	0.1
18.608	20.396	18.555	0.093	0.090	71.0	71.2	0.0	0.0
20.469	20.567	18.727	0.098	0.094	71.0	70.7	0.1	0.1
22.515	20.727	18.889	0.103	0.099	70.4	70.0	0.1	0.2
24.767	20.875	19.039	0.112	0.109	70.0	69.9	0.1	0.2
27.244	21.010	19.180	0.122	0.115	69.2	69.4	0.0	0.2
29.968	21.137	19.316	0.129	0.120	69.0	69.2	-0.1	0.0
32.965	21.267	19.453	0.134	0.124	68.6	68.2	0.2	0.1
36.261	21.407	19.596	0.130	0.125	67.2	66.6	0.2	0.3
39.887	21.548	19.743	0.133	0.127	67.2	67.5	0.1	0.1
43.876	21.715	19.909	0.125	0.123	66.2	66.9	0.2	0.2
48.264	21.880	20.092	0.125	0.126	68.4	68.3	0.2	0.1
53.090	22.065	20.287	0.127	0.127	69.5	68.3	0.1	0.1
58.399	22.269	20.495	0.125	0.128	68.9	68.7	0.3	0.2
64.239	22.459	20.705	0.134	0.134	71.0	69.9	0.1	0.1
70.663	22.672	20.924	0.140	0.139	71.1	70.5	0.1	0.2
77.729	22.866	21.142	0.147	0.144	71.9	70.5	0.3	0.4
85.502	23.063	21.366	0.156	0.156	72.4	71.3	0.0	0.2
94.052	23.306	21.669	0.149	0.152	73.2	70.9	0.1	-0.1
103.458	23.530	21.900	0.166	0.169	74.2	72.6	0.2	0.1

Table A13: Surface Photometry of NGC 3557

Seeing σ = 0.75 arcsec (R) and 0.9 arcsec (B)

Semi-Major Axis Length (Arcsec)	Surface Brightness		Ellipticity 1-b/a		Position Angle N thru E		Cos(4θ) Component X100	
	B	R	B	R	B	R	B	R
0.547	17.957	15.907						
0.662	17.968	15.918						
0.801	17.982	15.934						
0.969	18.001	15.959						
1.173	18.031	15.994						
1.419	18.077	16.048						
1.717	18.143	16.127						
2.078	18.241	16.241	0.192	0.191	36.9	34.9	0.0	0.1
2.514	18.379	16.393	0.191	0.193	36.5	34.4	0.0	0.1
3.043	18.559	16.582	0.189	0.193	35.6	33.9	0.0	0.0
3.681	18.778	16.804	0.190	0.197	35.3	34.1	0.0	0.1
4.455	19.023	17.049	0.198	0.204	34.8	33.9	0.0	-0.1
5.390	19.288	17.317	0.207	0.211	34.5	34.0	0.1	0.0
6.522	19.581	17.605	0.213	0.217	33.9	33.5	-0.1	0.0
7.891	19.889	17.910	0.219	0.220	33.9	33.4	0.0	0.0
8.681	20.044	18.064	0.222	0.223	34.2	33.6	-0.1	-0.1
9.549	20.200	18.221	0.227	0.224	33.7	33.3	0.1	-0.2
10.504	20.356	18.372	0.228	0.227	33.6	33.2	-0.1	-0.2
11.554	20.513	18.527	0.231	0.228	33.4	33.4	-0.1	-0.1
12.709	20.663	18.677	0.236	0.232	33.6	33.4	0.0	0.0
13.980	20.813	18.829	0.240	0.235	33.4	33.1	0.0	-0.1
15.378	20.966	18.979	0.242	0.237	33.1	33.2	-0.1	0.0
16.916	21.116	19.131	0.246	0.239	32.7	33.0	-0.1	-0.2
18.608	21.265	19.285	0.249	0.240	32.5	32.4	-0.1	0.0
20.469	21.414	19.434	0.253	0.243	32.4	32.6	0.0	-0.1
22.515	21.574	19.591	0.252	0.243	32.3	32.6	0.2	0.1
24.767	21.730	19.745	0.251	0.245	32.6	32.2	-0.2	0.0
27.244	21.883	19.904	0.253	0.245	32.7	31.8	-0.4	-0.2
29.968	22.048	20.064	0.254	0.246	31.6	31.7	-0.2	-0.2
32.965	22.197	20.219	0.258	0.250	32.4	32.1	-0.4	-0.1
36.261	22.343	20.372	0.264	0.253	32.1	31.8	0.0	0.0
39.887	22.490	20.527	0.268	0.254	32.8	32.5	0.1	-0.1
43.876	22.635	20.680	0.267	0.256	32.5	32.4	-0.2	0.1
48.264	22.789	20.837	0.268	0.255	32.9	32.8	0.0	0.2
53.090	22.965	21.009	0.249	0.245	33.5	33.0	-0.2	0.2
58.399	23.144	21.191	0.233	0.229	34.0	33.4	-0.1	0.2
64.239	23.341	21.380	0.216	0.219	33.5	33.3	0.0	0.1
70.663	23.532	21.583	0.200	0.200	35.1	34.8	0.2	0.2
77.729	23.701	21.756	0.191	0.197	37.5	37.4	0.4	0.3
85.502	23.878		0.183		38.8		0.4	
94.052	24.021							

Table A14: Surface Photometry of NGC 3605

Seeing σ = 1.15 arcsec (R) and 1.3 arcsec (B)

Semi-Major Axis Length (Arcsec)	Surface Brightness B	Surface Brightness R	Ellipticity 1-b/a B	Ellipticity 1-b/a R	Position Angle N thru E B	Position Angle N thru E R	Cos(4θ) Component X100 B	Cos(4θ) Component X100 R
0.547	18.685	16.912						
0.662	18.706	16.932						
0.801	18.735	16.963						
0.969	18.775	17.006						
1.173	18.831	17.072						
1.419	18.909	17.159						
1.717	19.013	17.279						
2.078	19.153	17.431	0.147	0.160	14.9	14.5	0.0	0.0
2.514	19.332	17.620	0.157	0.164	16.0	15.7	0.0	0.1
3.043	19.546	17.846	0.172	0.180	16.7	15.9	0.1	0.1
3.681	19.791	18.104	0.191	0.202	17.6	16.4	0.0	-0.1
4.455	20.052	18.361	0.217	0.225	18.4	18.1	-0.3	-0.1
5.390	20.321	18.630	0.250	0.253	18.7	18.8	-0.2	-0.3
6.522	20.603	18.905	0.281	0.284	19.0	18.9	-0.4	-0.3
7.891	20.900	19.196	0.309	0.310	19.0	18.9	-0.6	-0.5
8.681	21.045	19.346	0.324	0.322	19.4	18.9	-0.7	-0.6
9.549	21.201	19.501	0.339	0.335	19.1	19.1	-0.8	-0.8
10.504	21.360	19.658	0.351	0.347	18.9	19.0	-1.0	-0.9
11.554	21.530	19.817	0.361	0.361	18.9	19.0	-1.0	-0.7
12.709	21.702	19.989	0.372	0.371	18.8	19.1	-1.0	-0.9
13.980	21.871	20.160	0.386	0.381	18.3	18.7	-0.9	-0.9
15.378	22.061	20.351	0.396	0.389	18.4	18.5	-1.1	-0.8
16.916	22.266	20.559	0.403	0.394	18.1	18.5	-1.3	-1.1
18.608	22.504	20.790	0.404	0.395	17.8	18.2	-1.4	-1.2
20.469	22.760	21.049	0.403	0.392	17.9	18.3	-1.0	-0.7
22.515	23.006	21.292	0.410	0.399	18.2	18.7	-0.2	0.1
24.767	23.244	21.537	0.423	0.408	18.9	19.1	0.8	0.9
27.244	23.574	21.864	0.418	0.400	19.0	19.4	-0.1	0.2
29.968	23.984	22.267	0.395	0.370	19.5	19.8	-0.4	0.2
32.965	24.377	22.664	0.372	0.342	18.2	20.0	0.0	0.1
36.261	24.742	23.024	0.355	0.325	18.0	18.9	0.8	0.6
39.887	24.917	23.264	0.379	0.332	19.3	19.5	0.1	0.2
43.876	25.196	23.560	0.393	0.351	21.6	19.2	0.1	0.2
48.264	25.538	23.792	0.395	0.364	17.6	24.0	0.1	0.2
53.090	25.817	24.326	0.360		21.4		0.1	
58.399	25.955	24.603	0.389		21.4		0.1	
64.239	26.382	24.997						
70.663	26.551	25.189						
77.729	26.623	25.511						
85.502	27.118	25.196						
94.052		25.881						

Table A15: Surface Photometry of NGC 3608

Seeing σ = 1.1 arcsec (R) and 1.4 arcsec (B)

Semi-Major Axis Length (Arcsec)	Surface Brightness		Ellipticity 1-b/a		Position Angle N thru E		Cos(4θ) Component X100	
	B	R	B	R	B	R	B	R
0.547	17.998	15.958						
0.662	18.016	15.983						
0.801	18.043	16.022						
0.969	18.084	16.076						
1.173	18.140	16.152						
1.419	18.216	16.254						
1.717	18.316	16.389						
2.078	18.453	16.560	0.045	0.104	85.4	89.0	0.0	-0.1
2.514	18.623	16.766	0.055	0.107	80.8	86.9	0.1	0.1
3.043	18.822	16.997	0.071	0.117	77.9	84.6	0.0	0.0
3.681	19.054	17.248	0.087	0.127	80.2	83.2	0.1	0.0
4.455	19.309	17.506	0.104	0.142	78.8	81.8	-0.1	0.0
5.390	19.571	17.772	0.125	0.156	79.0	81.0	0.1	-0.1
6.522	19.850	18.053	0.142	0.164	78.9	80.6	-0.1	-0.1
7.891	20.140	18.341	0.155	0.171	79.5	80.5	-0.2	-0.1
8.681	20.291	18.489	0.159	0.172	79.7	80.6	-0.4	-0.2
9.549	20.434	18.633	0.166	0.175	79.8	80.3	-0.1	-0.3
10.504	20.588	18.779	0.168	0.180	79.6	80.4	-0.1	-0.2
11.554	20.738	18.930	0.174	0.181	79.7	79.9	-0.2	-0.2
12.709	20.885	19.076	0.182	0.186	80.0	80.3	-0.1	0.1
13.980	21.044	19.229	0.181	0.187	79.9	80.0	0.0	0.0
15.378	21.196	19.381	0.187	0.191	79.8	79.9	-0.2	-0.1
16.916	21.347	19.532	0.193	0.193	79.4	79.9	-0.3	-0.3
18.608	21.495	19.677	0.199	0.198	79.8	79.6	-0.2	-0.2
20.469	21.636	19.817	0.209	0.208	79.8	79.5	-0.4	-0.2
22.515	21.767	19.948	0.221	0.218	79.9	79.8	-0.3	-0.1
24.767	21.900	20.081	0.233	0.228	80.0	79.8	-0.3	-0.2
27.244	22.042	20.222	0.238	0.232	79.7	79.5	-0.3	0.0
29.968	22.167	20.356	0.250	0.239	79.6	79.2	0.0	-0.1
32.965	22.316	20.504	0.248	0.238	79.4	79.5	-0.3	-0.3
36.261	22.474	20.660	0.241	0.233	79.7	79.6	-0.4	-0.3
39.887	22.647	20.819	0.232	0.226	80.5	80.5	-0.2	-0.4
43.876	22.818	20.982	0.228	0.222	79.9	80.4	-0.4	-0.5
48.264	22.999	21.162	0.216	0.212	80.4	80.7	-0.8	-0.5
53.090	23.170	21.324	0.214	0.214	81.0	81.4	-0.4	-0.4
58.399	23.336	21.492	0.213	0.207	81.9	82.4	0.1	-0.1
64.239	23.493	21.613	0.217	0.223	83.5	84.9	-0.1	-0.4
70.663	23.661	21.766	0.215	0.223	82.8	84.9	-0.2	-0.4
77.729	23.805	21.905	0.216	0.224	83.9	84.9	-0.2	-0.4
85.502	23.944	22.030	0.218	0.226	82.0	83.3	-2.3	-0.4
94.052	24.052	22.149	0.223	0.226	84.0	79.8	-1.3	0.6

Table A16: Surface Photometry of NGC 3818

Seeing σ = 0.95 arcsec (R) and 1.15 arcsec (B)

Semi-Major Axis Length (Arcsec)	Surface Brightness		Ellipticity 1-b/a		Position Angle N thru E		Cos(4θ) Component X100	
	B	R	B	R	B	R	B	R
0.547	18.179	16.064						
0.662	18.208	16.102						
0.801	18.246	16.159						
0.969	18.294	16.237						
1.173	18.365	16.342						
1.419	18.463	16.482						
1.717	18.589	16.659						
2.078	18.758	16.874	0.106	0.115	95.4	97.9	0.1	0.0
2.514	18.967	17.120	0.116	0.133	96.1	97.7	0.0	0.2
3.043	19.210	17.391	0.135	0.155	96.8	97.6	0.2	0.3
3.681	19.483	17.682	0.158	0.180	96.9	97.5	0.5	0.5
4.455	19.778	17.973	0.188	0.214	97.2	97.5	0.7	0.9
5.390	20.090	18.270	0.218	0.251	97.8	97.8	1.1	1.4
6.522	20.371	18.560	0.267	0.292	97.5	97.6	1.8	2.0
7.891	20.678	18.857	0.307	0.332	98.0	97.8	2.1	2.6
8.681	20.834	19.010	0.327	0.349	97.9	98.0	2.2	2.8
9.549	20.984	19.162	0.346	0.366	98.5	97.8	2.4	2.6
10.504	21.138	19.317	0.363	0.380	98.3	98.0	2.4	2.5
11.554	21.296	19.478	0.378	0.390	98.4	98.4	2.3	2.5
12.709	21.453	19.635	0.390	0.398	98.6	98.4	2.2	2.6
13.980	21.614	19.799	0.398	0.405	98.7	98.5	2.3	2.4
15.378	21.791	19.973	0.397	0.401	98.6	99.0	1.1	1.7
16.916	21.972	20.162	0.394	0.393	98.7	98.8	0.7	0.8
18.608	22.152	20.338	0.389	0.386	98.6	98.7	0.3	0.5
20.469	22.332	20.532	0.382	0.374	98.9	99.0	0.0	0.0
22.515	22.510	20.713	0.378	0.366	99.2	99.6	-0.4	-0.2
24.767	22.707	20.891	0.371	0.363	98.8	99.1	-0.9	-0.3
27.244	22.891	21.088	0.362	0.352	99.1	99.1	-1.0	-1.0
29.968	23.081	21.281	0.357	0.345	99.0	99.4	-0.8	-0.6
32.965	23.268	21.480	0.351	0.335	99.4	99.5	-1.3	-0.7
36.261	23.445	21.665	0.355	0.337	99.6	99.8	-0.9	-0.5
39.887	23.641	21.856	0.348	0.333	99.5	100.0	-1.1	-0.8
43.876	23.866	22.087	0.336	0.319	99.9	100.3	-1.3	-0.7
48.264	24.066	22.270	0.341	0.331	100.4	100.4	-1.2	-0.5
53.090	24.267	22.506	0.353	0.327	100.4	100.3	-0.3	-0.4
58.399	24.475	22.713	0.346	0.333	100.1	100.9	-0.3	0.3
64.239	24.713	22.918						
70.663	24.906	23.145						
77.729	25.155	23.355						
85.502	25.350	23.558						
94.052	25.628	23.780						
103.458	25.790	23.911						

Table A17: Surface Photometry of NGC 3904

Seeing σ = 0.55 arcsec (R) and 0.8 arcsec (B)

Semi-Major Axis Length (Arcsec)	Surface Brightness		Ellipticity 1-b/a		Position Angle N thru E		Cos(4θ) Component X100	
	B	R	B	R	B	R	B	R
0.547	17.492	15.360						
0.662	17.530	15.416						
0.801	17.586	15.497						
0.969	17.663	15.605						
1.173	17.764	15.749						
1.419	17.895	15.922						
1.717	18.058	16.119						
2.078	18.248	16.332	0.099	0.153	21.1	18.7	-0.1	0.1
2.514	18.461	16.557	0.115	0.162	19.6	18.3	0.0	0.2
3.043	18.681	16.782	0.136	0.173	19.5	17.6	0.2	0.3
3.681	18.914	17.017	0.153	0.184	18.3	17.5	0.4	0.4
4.455	19.160	17.263	0.170	0.192	17.8	17.3	0.3	0.4
5.390	19.420	17.530	0.179	0.194	17.2	16.8	0.3	0.3
6.522	19.688	17.795	0.193	0.203	16.6	16.7	0.3	0.3
7.891	19.961	18.064	0.211	0.218	16.7	16.6	0.2	0.1
8.681	20.101	18.201	0.221	0.228	16.8	16.7	0.0	0.0
9.549	20.247	18.344	0.232	0.235	16.8	17.1	-0.2	-0.3
10.504	20.398	18.489	0.236	0.243	17.3	17.0	-0.2	-0.2
11.554	20.553	18.644	0.244	0.248	16.9	16.9	-0.2	-0.2
12.709	20.717	18.805	0.247	0.250	17.0	17.2	-0.3	-0.2
13.980	20.886	18.968	0.250	0.253	17.2	17.0	-0.2	-0.1
15.378	21.052	19.137	0.255	0.254	17.0	16.8	-0.1	-0.2
16.916	21.231	19.303	0.259	0.256	16.9	17.1	0.2	0.2
18.608	21.396	19.464	0.267	0.266	16.5	16.9	0.6	0.4
20.469	21.551	19.627	0.280	0.273	16.5	16.5	0.5	0.4
22.515	21.708	19.774	0.291	0.286	16.1	16.5	0.5	0.6
24.767	21.862	19.924	0.300	0.297	16.9	16.4	0.8	0.4
27.244	22.015	20.070	0.305	0.308	16.8	16.1	0.4	0.4
29.968	22.156	20.214	0.312	0.314	16.3	16.2	0.5	0.6
32.965	22.299	20.361	0.325	0.319	16.3	16.2	0.5	0.8
36.261	22.461	20.518	0.324	0.318	16.1	16.1	0.3	0.4
39.887	22.649	20.701	0.317	0.311	15.6	15.8	0.3	0.6
43.876	22.885	20.919	0.295	0.292	15.4	15.5	0.4	0.7
48.264	23.144	21.176	0.272	0.271	15.5	15.3	0.2	0.5
53.090	23.433	21.434	0.246	0.253	14.4	14.7	0.3	0.5
58.399	23.713	21.692	0.240	0.241	13.6	13.7	1.1	0.9
64.239	23.980	21.931	0.237	0.240	12.4	12.4	0.7	0.8
70.663	24.224	22.136		0.252		12.8		0.8
77.729	24.459	22.339		0.259		12.2		1.1
85.502	24.694	22.520		0.273		10.5		1.1
94.052	24.910	22.707						
103.458	25.121	22.854						

Table A18: Surface Photometry of NGC 3923

Seeing σ = 0.6 arcsec (R) and 0.8 arcsec (B)

Semi-Major Axis Length (Arcsec)	Surface Brightness		Ellipticity 1-b/a		Position Angle N thru E		Cos(4θ) Component X100	
	B	R	B	R	B	R	B	R
0.547	17.762	15.774						
0.662	17.780	15.796						
0.801	17.804	15.826						
0.969	17.841	15.867						
1.173	17.892	15.923						
1.419	17.960	15.998						
1.717	18.048	16.093						
2.078	18.158	16.205	0.122	0.118	52.6	49.3	-0.1	0.0
2.514	18.289	16.339	0.142	0.141	50.5	49.1	0.1	0.2
3.043	18.443	16.493	0.165	0.164	49.4	48.9	-0.1	-0.1
3.681	18.612	16.663	0.194	0.197	49.0	48.2	0.1	0.1
4.455	18.794	16.847	0.229	0.229	48.8	48.3	0.3	0.1
5.390	18.988	17.041	0.264	0.263	48.6	48.2	0.2	0.2
6.522	19.193	17.240	0.298	0.299	48.1	47.9	0.3	0.2
7.891	19.407	17.460	0.328	0.325	48.0	48.0	0.1	0.1
8.681	19.520	17.572	0.341	0.337	48.1	47.9	0.0	0.1
9.549	19.631	17.689	0.355	0.348	48.0	47.8	0.1	-0.2
10.504	19.747	17.801	0.366	0.360	48.1	47.8	-0.2	-0.2
11.554	19.865	17.918	0.376	0.370	48.0	47.8	-0.3	-0.2
12.709	19.980	18.036	0.386	0.378	48.1	47.7	-0.3	-0.3
13.980	20.098	18.152	0.394	0.387	47.9	47.9	-0.2	-0.3
15.378	20.222	18.280	0.398	0.388	48.0	47.9	-0.5	-0.6
16.916	20.352	18.410	0.399	0.390	48.1	48.0	-0.5	-0.4
18.608	20.505	18.563	0.391	0.380	48.0	47.8	-0.9	-0.6
20.469	20.665	18.725	0.382	0.369	47.9	47.8	-0.9	-0.7
22.515	20.813	18.875	0.381	0.370	47.8	47.9	-0.4	-0.3
24.767	20.956	19.020	0.383	0.372	48.0	47.8	-0.2	-0.2
27.244	21.108	19.170	0.381	0.371	47.8	47.6	-0.2	-0.1
29.968	21.280	19.349	0.370	0.357	47.7	47.7	-0.5	-0.6
32.965	21.452	19.525	0.359	0.345	47.9	47.6	-0.6	-0.3
36.261	21.599	19.683	0.360	0.346	48.0	47.6	-0.3	0.0
39.887	21.728	19.810	0.372	0.359	47.7	47.7	0.5	0.4
43.876	21.860	19.943	0.381	0.368	47.6	47.3	0.2	0.3
48.264	21.999	20.092	0.379	0.366	47.6	47.5	-0.4	-0.3
53.090	22.133	20.231	0.378	0.365	47.5	47.4	-0.1	0.1
58.399	22.265	20.373	0.374	0.361	47.2	47.2	0.0	0.2
64.239	22.432	20.531	0.355	0.347	47.0	47.1	0.0	-0.1
70.663	22.609	20.717	0.330	0.326	47.1	47.5	-0.2	-0.6
77.729	22.794	20.921	0.306	0.299	47.9	48.5	-0.7	-0.8
85.502	22.957	21.096	0.296	0.285	49.4	50.1	-0.9	-0.8
94.052	23.154	21.291	0.277	0.269	48.9	48.6	-0.8	-0.5
103.458	23.286	21.443	0.290		49.9		-0.9	

Table A19: Surface Photometry of NGC 4374

Seeing σ = 0.65 arcsec (R) and 1.0 arcsec (B)

Semi-Major Axis Length (Arcsec)	Surface Brightness		Ellipticity 1-b/a		Position Angle N thru E		Cos(4θ) Component X100	
	B	R	B	R	B	R	B	R
0.547	17.373	15.311						
0.662	17.384	15.326						
0.801	17.398	15.348						
0.969	17.419	15.378						
1.173	17.447	15.419						
1.419	17.484	15.478						
1.717	17.538	15.558						
2.078	17.614	15.659	0.228	0.166	141.0	137.1	-0.8	-0.5
2.514	17.712	15.779	0.235	0.170	142.9	141.4	-0.3	0.5
3.043	17.835	15.942	0.243	0.134	145.0	139.4	-0.4	1.5
3.681	17.998	16.118	0.236	0.150	144.7	132.9	-0.8	0.3
4.455	18.202	16.332	0.222	0.165	141.5	132.4	-1.0	0.0
5.390	18.434	16.558	0.210	0.177	137.3	129.2	-0.8	-0.1
6.522	18.685	16.804	0.205	0.183	134.6	127.5	-0.3	-0.6
7.891	18.952	17.067	0.200	0.186	133.4	127.5	0.0	-0.6
8.681	19.092	17.205	0.195	0.185	132.7	127.7	0.0	-0.6
9.549	19.239	17.349	0.184	0.180	131.0	127.6	-0.2	-0.7
10.504	19.387	17.496	0.174	0.174	128.7	127.2	-0.4	-0.5
11.554	19.542	17.651	0.165	0.166	127.9	126.7	-0.4	-0.5
12.709	19.700	17.807	0.160	0.160	127.4	126.6	-0.5	-0.5
13.980	19.859	17.967	0.157	0.154	127.2	126.8	-0.4	-0.4
15.378	20.018	18.123	0.153	0.152	127.5	126.8	-0.4	-0.4
16.916	20.173	18.276	0.151	0.149	127.7	127.2	-0.5	-0.6
18.608	20.331	18.432	0.146	0.144	127.9	127.6	-0.5	-0.4
20.469	20.480	18.582	0.146	0.143	128.1	127.3	-0.2	-0.4
22.515	20.624	18.729	0.147	0.140	127.4	127.4	-0.3	-0.2
24.767	20.775	18.874	0.139	0.139	126.5	126.9	-0.3	-0.3
27.244	20.929	19.031	0.134	0.131	126.9	127.3	-0.4	-0.4
29.968	21.093	19.193	0.124	0.120	125.6	126.1	-0.5	-0.5
32.965	21.254	19.358	0.117	0.114	125.5	126.4	-0.3	-0.4
36.261	21.416	19.517	0.113	0.111	125.1	126.2	-0.4	-0.3
39.887	21.578	19.682	0.110	0.107	126.0	127.1	-0.3	-0.2
43.876	21.749	19.856	0.104	0.101	125.0	126.5	-0.3	-0.2
48.264	21.929	20.028	0.098	0.096	126.3	126.7	-0.2	-0.2
53.090	22.111	20.212	0.093	0.091	125.9	126.4	-0.4	-0.3
58.399	22.303	20.400	0.083	0.083	127.4	126.8	-0.3	-0.3
64.239	22.501	20.590	0.075	0.076	126.0	126.3	-0.2	-0.4
70.663	22.694	20.772	0.067	0.070	127.0	126.9	-0.5	-0.5
77.729	22.881	20.954	0.066	0.063	128.6	125.4	-0.3	-0.3
85.502	23.084	21.140	0.056	0.058	128.8	124.9	-0.3	-0.4

1987MNRAS.226..747J

Table A20: Surface Photometry of NGC 4387

Seeing σ = 1.05 arcsec (R) and 1.2 arcsec (B)

Semi-Major Axis Length (Arcsec)	Surface Brightness		Ellipticity 1-b/a		Position Angle N thru E		Cos(4θ) Component X100	
	B	R	B	R	B	R	B	R
0.547	18.803	16.919						
0.662	18.820	16.941						
0.801	18.844	16.972						
0.969	18.878	17.014						
1.173	18.923	17.072						
1.419	18.987	17.149						
1.717	19.070	17.246						
2.078	19.174	17.366	0.134	0.142	141.7	143.3	0.1	0.1
2.514	19.303	17.507	0.149	0.161	141.8	143.2	-0.2	0.0
3.043	19.452	17.662	0.173	0.186	141.8	142.7	-0.3	-0.1
3.681	19.621	17.836	0.202	0.213	141.9	142.7	-0.3	-0.4
4.455	19.812	18.028	0.230	0.241	142.0	142.4	-0.4	-0.6
5.390	20.027	18.237	0.257	0.272	141.9	142.4	-0.7	-0.8
6.522	20.266	18.473	0.284	0.298	142.0	141.9	-0.8	-1.1
7.891	20.535	18.740	0.308	0.320	141.6	141.8	-0.9	-1.0
8.681	20.683	18.886	0.318	0.329	141.9	141.7	-1.1	-1.2
9.549	20.841	19.040	0.329	0.339	141.8	141.8	-1.0	-1.0
10.504	21.001	19.194	0.341	0.349	142.0	141.7	-0.8	-1.0
11.554	21.158	19.356	0.352	0.360	141.4	141.4	-0.9	-0.9
12.709	21.328	19.521	0.363	0.371	141.2	141.4	-0.8	-0.7
13.980	21.506	19.695	0.374	0.380	141.3	141.4	-0.8	-0.9
15.378	21.691	19.874	0.384	0.390	141.2	141.4	-0.8	-0.8
16.916	21.888	20.064	0.390	0.396	141.1	141.5	-0.8	-1.0
18.608	22.100	20.264	0.393	0.400	141.4	141.6	-0.9	-1.0
20.469	22.309	20.475	0.398	0.403	141.6	141.9	-0.8	-1.0
22.515	22.554	20.704	0.396	0.402	141.8	142.0	-0.8	-0.7
24.767	22.806	20.954	0.397	0.397	142.5	142.7	-0.5	-0.5
27.244	23.089	21.223	0.390	0.391	143.2	143.4	-0.7	-0.7
29.968	23.363	21.503	0.385	0.382	143.5	143.5	-0.7	-0.6
32.965	23.683	21.793	0.375	0.370	143.7	144.1	-0.2	-0.5
36.261	23.984	22.070	0.371	0.364	144.0	144.6	-0.7	-0.8
39.887	24.298	22.352	0.356	0.352	144.0	145.7	-1.3	-1.2
43.876	24.618	22.633	0.337	0.332	144.8	144.1	-0.6	-1.0
48.264	24.935	22.928	0.320	0.323	143.1	144.7	-0.9	-0.9
53.090	25.222	23.193						
58.399	25.508	23.465						
64.239	25.806	23.679						
70.663	26.074	23.993						
77.729	26.344	24.209						
85.502	26.641							
94.052	26.694							

Table A21 Surface Photometry of NGC 4458

Seeing σ = 1.0 arcsec (R) and 1.2 arcsec (B)

Semi-Major Axis Length (Arcsec)	Surface Brightness		Ellipticity 1-b/a		Position Angle N thru E		Cos(4θ) Component X100	
	B	R	B	R	B	R	B	R
0.547	18.523	16.599						
0.662	18.554	16.649						
0.801	18.602	16.717						
0.969	18.667	16.805						
1.173	18.755	16.926						
1.419	18.875	17.091						
1.717	19.037	17.286						
2.078	19.237	17.521	0.070	0.084	-4.9	5.3	0.0	0.2
2.514	19.471	17.780	0.077	0.090	-2.5	5.2	-0.1	0.1
3.043	19.726	18.038	0.085	0.105	-0.2	4.5	-0.1	0.3
3.681	19.995	18.296	0.099	0.117	1.7	3.3	0.0	0.4
4.455	20.260	18.557	0.112	0.123	1.9	3.9	0.2	0.4
5.390	20.534	18.825	0.114	0.121	3.6	5.0	-0.1	0.6
6.522	20.816	19.097	0.112	0.116	5.2	6.1	0.1	0.3
7.891	21.105	19.374	0.112	0.115	6.4	6.7	-0.3	0.4
8.681	21.253	19.517	0.106	0.112	6.8	7.3	-0.1	0.2
9.549	21.407	19.669	0.106	0.111	6.1	6.2	-0.2	0.1
10.504	21.557	19.816	0.112	0.111	5.7	6.3	0.1	0.3
11.554	21.714	19.969	0.110	0.108	5.3	5.7	0.1	0.5
12.709	21.864	20.117	0.110	0.110	4.9	4.8	0.0	0.6
13.980	22.016	20.259	0.116	0.116	6.2	4.7	-0.1	0.9
15.378	22.176	20.409	0.109	0.112	5.6	6.2	0.0	0.9
16.916	22.332	20.573	0.111	0.100	7.6	7.5	0.2	0.3
18.608	22.506	20.731	0.102	0.101	7.3	8.0	-0.1	0.0
20.469	22.676	20.900	0.100	0.097	7.4	5.8	0.1	0.3
22.515	22.869	21.081	0.095	0.090	7.4	6.4	0.0	0.2
24.767	23.066	21.265	0.083	0.082	6.6	6.6	-0.2	0.2
27.244	23.264	21.465	0.082	0.082	6.4	5.4	-0.2	0.0
29.968	23.488	21.667	0.073	0.080	6.7	6.2	0.2	0.3
32.965	23.723	21.871	0.067	0.072	9.5	6.1	-0.3	0.2
36.261	23.963	22.080	0.063	0.062	6.1	10.0	0.2	0.3
39.887	24.212	22.315	0.048	0.042	7.6	7.6	0.1	0.3
43.876	24.477	22.541	0.039	0.031	5.9	-0.7	0.1	0.5
48.264	24.751	22.767	0.015	0.017	0.3	-12.4	-0.4	-0.2
53.090	25.004	22.948	0.010	0.031	53.8	45.2	-0.2	-0.2
58.399	25.243							
64.239	25.465							
70.663	25.690							
77.729	25.801							
85.502	25.927							

1987MNRAS.226..747J

Table A22 Surface Photometry of NGC 4473

Seeing σ = 0.85 arcsec (R) and 1.05 arcsec (B)

Semi-Major Axis Length (Arcsec)	Surface Brightness		Ellipticity 1-b/a		Position Angle N thru E		Cos(4θ) Component X100	
	B	R	B	R	B	R	B	R
0.547	17.191	15.244						
0.662	17.205	15.263						
0.801	17.227	15.293						
0.969	17.258	15.333						
1.173	17.303	15.390						
1.419	17.365	15.468						
1.717	17.447	15.568						
2.078	17.553	15.691	0.290	0.311	96.4	94.2	0.3	0.5
2.514	17.688	15.842	0.304	0.325	95.9	94.0	0.4	0.6
3.043	17.853	16.018	0.317	0.342	95.2	93.9	0.6	0.9
3.681	18.048	16.222	0.330	0.356	94.8	93.9	0.6	1.1
4.455	18.271	16.454	0.345	0.368	94.4	93.8	1.0	1.1
5.390	18.523	16.711	0.356	0.375	94.4	93.8	1.0	1.3
6.522	18.800	16.994	0.365	0.378	93.9	93.6	1.0	1.1
7.891	19.107	17.304	0.368	0.377	93.9	93.5	0.9	1.1
8.681	19.267	17.461	0.370	0.379	93.8	93.5	0.8	1.0
9.549	19.429	17.620	0.372	0.381	93.8	93.5	0.7	0.9
10.504	19.593	17.787	0.377	0.382	93.7	93.5	0.9	1.0
11.554	19.763	17.955	0.380	0.383	93.5	93.5	0.9	1.0
12.709	19.933	18.126	0.384	0.385	93.6	93.6	0.8	0.8
13.980	20.108	18.300	0.387	0.387	93.6	93.5	0.7	0.7
15.378	20.286	18.473	0.391	0.390	93.6	93.6	0.6	0.8
16.916	20.456	18.645	0.398	0.396	93.5	93.4	0.7	0.8
18.608	20.632	18.818	0.404	0.400	93.4	93.3	0.8	0.8
20.469	20.795	18.982	0.414	0.409	93.3	93.3	1.1	1.0
22.515	20.963	19.148	0.422	0.416	93.3	93.2	1.0	1.1
24.767	21.123	19.309	0.432	0.424	93.2	93.1	0.9	0.9
27.244	21.292	19.477	0.438	0.430	93.2	93.3	0.7	0.9
29.968	21.456	19.640	0.445	0.436	93.3	93.2	0.4	0.7
32.965	21.625	19.804	0.451	0.442	93.2	93.1	0.5	0.6
36.261	21.794	19.970	0.456	0.445	92.9	93.1	0.3	0.5
39.887	21.961	20.146	0.458	0.446	92.6	92.9	0.1	0.5
43.876	22.127	20.323	0.461	0.444	92.6	92.9	0.4	0.7
48.264	22.299	20.496	0.463	0.445	92.7	92.9	0.3	0.6
53.090	22.484	20.669	0.461	0.445	92.8	93.2	0.4	0.8
58.399	22.674	20.863	0.457	0.439	92.8	93.2	-0.1	0.7
64.239	22.885	21.038	0.445	0.440	92.4	92.9	0.8	0.6
70.663	23.059	21.229	0.450	0.433	91.9	92.3	0.6	0.8
77.729	23.295	21.440	0.431	0.426	92.0	92.3	0.5	0.6
85.502	23.486	21.631	0.427	0.425	92.0	92.3	0.9	0.6
94.052	23.686	21.820		0.420		92.2		0.7
103.458	23.869	22.000						

Table A23: Surface Photometry of NGC 4476

Seeing σ = 0.65 arcsec (R) and 0.95 arcsec (B)

Semi-Major Axis Length (Arcsec)	Surface Brightness		Ellipticity 1-b/a		Position Angle N thru E		Cos(4θ) Component X100	
	B	R	B	R	B	R	B	R
0.547	18.581	16.749						
0.662	18.600	16.781						
0.801	18.624	16.821						
0.969	18.661	16.874						
1.173	18.713	16.942						
1.419	18.780	17.023						
1.717	18.870	17.114						
2.078	18.981	17.217	0.339	0.399	32.2	31.1	1.8	2.8
2.514	19.107	17.333	0.369	0.438	31.0	30.4	2.7	3.9
3.043	19.254	17.472	0.403	0.472	29.8	29.6	3.4	4.6
3.681	19.434	17.650	0.434	0.494	28.3	28.5	3.5	4.6
4.455	19.666	17.907	0.447	0.490	26.1	27.1	2.1	2.8
5.390	19.966	18.218	0.443	0.476	24.0	25.3	0.4	0.9
6.522	20.349	18.602	0.413	0.432	22.3	23.6	-0.4	0.3
7.891	20.706	18.935	0.362	0.395	21.9	24.3	0.6	0.5
8.681	20.866	19.110	0.355	0.390	23.6	25.2	0.1	0.1
9.549	21.034	19.308	0.355	0.379	24.5	25.3	-0.2	0.3
10.504	21.206	19.512	0.360	0.371	25.2	25.8	0.1	0.6
11.554	21.377	19.705	0.368	0.370	25.7	26.0	0.7	0.7
12.709	21.556	19.903	0.372	0.364	26.4	26.5	1.2	0.8
13.980	21.759	20.100	0.365	0.360	26.7	26.5	1.0	1.0
15.378	21.960	20.307	0.365	0.347	26.2	25.9	1.2	0.7
16.916	22.161	20.498	0.359	0.347	26.2	26.2	0.8	0.6
18.608	22.370	20.700	0.353	0.340	26.4	26.2	0.5	0.1
20.469	22.578	20.917	0.345	0.323	26.3	26.4	0.4	-0.1
22.515	22.782	21.106	0.341	0.327	26.6	26.3	0.4	0.4
24.767	22.978	21.315	0.334	0.321	27.0	26.3	0.4	0.2
27.244	23.185	21.512	0.330	0.316	27.1	26.6	0.0	-0.3
29.968	23.402	21.718	0.324	0.310	26.7	27.0	-0.7	-0.4
32.965	23.636	21.922	0.307	0.303	26.3	27.4	-0.7	-0.4
36.261	23.855	22.167	0.301	0.283	26.9	26.1	-1.6	-0.5
39.887	24.093	22.395	0.279	0.268	26.5	27.4	-1.0	-1.0
43.876	24.337	22.631	0.268	0.259	25.0	26.8	-0.2	0.0
48.264	24.580	22.857	0.255	0.246	26.9	29.9	-1.3	0.0
53.090	24.824	23.079		0.251		36.0		0.0
58.399	25.068	23.361						
64.239	25.329	23.578						
70.663	25.571	23.814						
77.729	25.843	24.094						
85.502	26.170	24.305						
94.052	26.372							
103.458	26.647							

Table A24: Surface Photometry of NGC 4478

Seeing σ = 0.6 arcsec (R) and 0.9 arcsec (B)

Semi-Major Axis Length (Arcsec)	Surface Brightness		Elliptici 1-b/a		Position Angle N thru E		Cos(4θ) Component X100	
	B	R	B	R	B	R	B	R
0.547	17.833	15.853						
0.662	17.865	15.908						
0.801	17.912	15.983						
0.969	17.975	16.083						
1.173	18.062	16.210						
1.419	18.178	16.363						
1.717	18.319	16.535						
2.078	18.485	16.717	0.115	0.146	146.4	151.7	0.2	0.3
2.514	18.661	16.900	0.128	0.149	147.0	151.9	0.3	0.1
3.043	18.846	17.084	0.140	0.153	148.9	150.8	0.4	0.2
3.681	19.036	17.272	0.152	0.158	149.7	150.8	0.4	0.2
4.455	19.239	17.472	0.162	0.162	148.7	148.8	0.1	0.0
5.390	19.455	17.680	0.168	0.173	148.1	148.0	-0.2	-0.5
6.522	19.686	17.899	0.177	0.188	147.5	147.5	-0.6	-0.7
7.891	19.938	18.149	0.190	0.197	145.9	146.7	-0.6	-0.8
8.681	20.081	18.286	0.191	0.199	146.0	146.6	-0.7	-0.9
9.549	20.232	18.430	0.191	0.201	145.3	146.4	-1.1	-1.0
10.504	20.389	18.590	0.191	0.197	144.9	145.4	-1.0	-1.0
11.554	20.561	18.756	0.190	0.196	144.7	145.5	-1.0	-1.2
12.709	20.744	18.939	0.187	0.190	144.6	145.1	-0.9	-1.0
13.980	20.942	19.130	0.182	0.188	145.5	145.6	-0.8	-0.9
15.378	21.149	19.331	0.178	0.186	143.2	145.5	-0.7	-0.9
16.916	21.367	19.552	0.175	0.178	141.6	143.1	-0.9	-1.0
18.608	21.606	19.792	0.167	0.169	141.1	141.6	-1.0	-1.0
20.469	21.850	20.035	0.163	0.163	140.7	141.2	-1.2	-1.1
22.515	22.105	20.288	0.158	0.160	139.3	140.0	-1.1	-1.0
24.767	22.363	20.549	0.154	0.155	138.7	138.7	-1.1	-1.3
27.244	22.627	20.811	0.152	0.155	137.9	137.2	-1.0	-1.0
29.968	22.902	21.103	0.150	0.152	137.0	137.5	-0.9	-0.9
32.965	23.165	21.377	0.161	0.161	138.6	138.0	-0.8	-0.9
36.261	23.422	21.640	0.171	0.174	141.2	139.1	-0.4	-0.4
39.887	23.690	21.939	0.170	0.177	141.5	139.9	-0.6	-1.0
43.876	23.977	22.247	0.161	0.172	145.3	141.4	-0.4	-0.8
48.264	24.239	22.551	0.156	0.170	150.0	143.3	-0.4	-0.8
53.090	24.495	22.842		0.165		148.0		-0.8
58.399	24.754	23.165						
64.239	25.019	23.497						
70.663	25.241	23.765						
77.729	25.461	24.046						
85.502	25.634	24.299						
94.052	25.826	24.455						
103.458	25.894	24.507						

Table A25: Surface Photometry of NGC 4486

Seeing σ = 0.7 arcsec (R) and 0.8 arcsec (B)

Semi-Major Axis Length (Arcsec)	Surface Brightness		Ellipticity 1-b/a		Position Angle N thru E		Cos(4θ) Component X100	
	B	R	B	R	B	R	B	R
0.547	17.827	15.953						
0.662	17.859	16.005						
0.801	17.910	16.070						
0.969	17.982	16.147						
1.173	18.076	16.236						
1.419	18.177	16.327						
1.717	18.269	16.412						
2.078	18.338	16.480	0.080	0.028	103.0	81.9	0.9	0.0
2.514	18.397	16.548	0.124	0.015	105.2	112.8	2.3	-1.2
3.043	18.462	16.615	0.132	0.019	102.4	99.8	2.9	-0.3
3.681	18.555	16.694	0.052	0.007	100.0	31.6	0.9	-0.4
4.455	18.652	16.774	0.024	0.030	44.0	11.6	0.9	0.2
5.390	18.759	16.878	0.015	0.031	15.6	11.3	-0.1	0.0
6.522	18.889	17.006	0.023	0.033	18.3	8.5	0.3	0.5
7.891	19.049	17.163	0.020	0.033	12.9	10.7	0.4	0.2
8.681	19.140	17.255	0.022	0.029	7.8	4.1	0.4	-0.1
9.549	19.239	17.352	0.023	0.027	6.2	5.6	0.2	0.2
10.504	19.344	17.455	0.023	0.030	-2.0	-0.1	0.1	0.0
11.554	19.453	17.562	0.029	0.033	-4.0	0.1	-0.1	-0.1
12.709	19.570	17.678	0.029	0.032	-1.3	-0.4	0.1	-0.1
13.980	19.691	17.800	0.031	0.032	-2.9	-3.9	0.1	-0.1
15.378	19.817	17.924	0.031	0.032	-5.3	-7.8	0.0	-0.2
16.916	19.943	18.051	0.035	0.034	-6.7	-8.8	0.0	0.0
18.608	20.076	18.183	0.037	0.035	-11.6	-9.2	0.1	-0.1
20.469	20.213	18.320	0.041	0.038	-12.5	-13.4	0.1	0.0
22.515	20.353	18.461	0.041	0.038	-14.7	-16.5	0.0	-0.1
24.767	20.489	18.602	0.048	0.042	-17.6	-18.5	-0.3	-0.1
27.244	20.636	18.749	0.052	0.047	-16.8	-20.0	-0.1	0.0
29.968	20.786	18.895	0.054	0.050	-17.7	-22.3	0.1	0.1
32.965	20.932	19.044	0.055	0.054	-19.9	-24.3	-0.2	-0.2
36.261	21.086	19.194	0.059	0.059	-20.2	-24.4	0.0	-0.1
39.887	21.230	19.345	0.065	0.063	-19.0	-24.4	-0.1	-0.1
43.876	21.379	19.409	0.073	0.070	-20.5	-26.0	0.0	0.0
48.264	21.534	19.655	0.074	0.071	-19.9	-24.4	0.0	0.2
53.090	21.682	19.801	0.079	0.080	-21.4	-25.6	-0.1	-0.1
58.399	21.840	19.963	0.087	0.083	-22.1	-25.9	0.0	0.0
64.239	21.997	20.119	0.091	0.090	-24.7	-27.7	-0.1	0.0
70.663	22.157	20.277	0.094	0.094	-23.5	-27.2	-0.1	0.0
77.729	22.316	20.440	0.096	0.093	-25.7	-27.4	0.0	0.1
85.502	22.478	20.603	0.105	0.098	-25.8	-29.5	0.2	0.1
94.052		20.768		0.100		-32.8		0.1

Table A26: Surface Photometry of NGC 4489

Seeing σ = 0.65 arcsec (R) and 0.9 arcsec (B)

Semi-Major Axis Length (Arcsec)	Surface Brightness B	Surface Brightness R	Ellipticity 1-b/a B	Ellipticity 1-b/a R	Position Angle N thru E B	Position Angle N thru E R	Cos(4θ) Component X100 B	Cos(4θ) Component X100 R
0.547	18.262	16.338						
0.662	18.303	16.410						
0.801	18.366	16.511						
0.969	18.454	16.645						
1.173	18.577	16.823						
1.419	18.745	17.036						
1.717	18.985	17.313						
2.078	19.261	17.595	0.061	0.089	54.5	52.7	0.4	0.3
2.514	19.556	17.896	0.072	0.102	52.9	53.4	0.5	0.3
3.043	19.871	18.201	0.079	0.110	53.3	53.5	0.5	0.2
3.681	20.180	18.510	0.085	0.098	53.8	53.1	0.2	0.3
4.455	20.471	18.787	0.076	0.091	51.7	54.1	0.1	0.2
5.390	20.740	19.050	0.041	0.051	41.6	45.1	-0.1	-0.5
6.522	20.973	19.274	0.041	0.045	-2.8	-4.2	0.1	0.4
7.891	21.213	19.515	0.073	0.075	-19.9	-19.8	0.0	-0.1
8.681	21.360	19.662	0.079	0.079	-22.8	-25.6	-0.1	0.2
9.549	21.508	19.813	0.086	0.084	-22.7	-27.0	0.3	0.2
10.504	21.665	19.959	0.085	0.085	-25.0	-24.6	-0.2	-0.1
11.554	21.815	20.116	0.092	0.087	-23.3	-22.3	0.2	-0.2
12.709	21.975	20.273	0.088	0.085	-23.0	-24.6	0.1	0.0
13.980	22.123	20.418	0.087	0.085	-20.9	-21.6	0.0	-0.1
15.378	22.267	20.556	0.081	0.083	-21.4	-22.4	-0.4	-0.5
16.916	22.395	20.688	0.086	0.084	-23.5	-20.7	-0.9	-0.6
18.608	22.528	20.815	0.085	0.086	-18.4	-18.9	-0.3	-0.2
20.469	22.652	20.945	0.095	0.087	-17.7	-20.3	0.4	0.2
22.515	22.794	21.082	0.101	0.098	-17.8	-17.9	0.1	0.3
24.767	22.980	21.266	0.088	0.092	-21.0	-22.0	-0.2	0.0
27.244	23.181	21.479	0.085	0.084	-18.4	-21.1	-0.4	-0.2
29.968	23.418	21.697	0.082	0.079	-12.6	-15.6	-1.3	-0.4
32.965	23.652	21.911	0.084	0.086	-14.2	-20.2	-0.5	-0.4
36.261	23.876	22.134	0.094	0.092	-20.0	-22.6	-0.1	-0.2
39.887	24.087	22.352	0.106	0.097	-14.8	-20.0	-0.5	-0.6
43.876	24.362	22.606	0.099	0.092	-18.2	-24.1	-0.3	-0.5
48.264	24.629	22.859	0.104	0.099	-21.2	-28.1	0.2	-0.7
53.090	24.963	23.165	0.095	0.095	-24.0	-27.5	-0.5	-1.1
58.399	25.296	23.470	0.093	0.070	-29.4	-27.7	-0.3	-0.3
64.239	25.646	23.785	0.093	0.092	-35.5	-30.1	-0.3	-0.3
70.663	26.052	24.073	0.060	0.007	-33.8	-20.5	-0.3	-0.3
77.729	26.377	24.348	0.060		-14.8		-0.3	
85.502	26.625	24.551	0.038		-76.3		-0.3	
94.052	26.954	24.568						
103.458	27.106	24.694						
113.803	27.781							

Table A27: Surface Photometry of NGC 4551

Seeing σ = 0.7 arcsec (R) and 0.9 arcsec (B)

Semi-Major Axis Length (Arcsec)	Surface Brightness		Ellipticity 1-b/a		Position Angle N thru E		Cos(4θ) Component X100	
	B	R	B	R	B	R	B	R
0.547	18.400	16.425						
0.662	18.435	16.486						
0.801	18.484	16.565						
0.969	18.553	16.668						
1.173	18.644	16.789						
1.419	18.764	16.943						
1.717	18.912	17.113						
2.078	19.084	17.298	0.190	0.235	71.6	70.1	0.5	0.5
2.514	19.268	17.489	0.207	0.243	70.2	70.5	0.5	0.5
3.043	19.466	17.693	0.219	0.242	69.4	69.9	0.5	0.3
3.681	19.669	17.901	0.230	0.243	69.5	70.0	0.2	0.4
4.455	19.885	18.110	0.235	0.243	68.7	69.6	-0.3	-0.3
5.390	20.108	18.328	0.243	0.252	69.0	68.7	-0.6	-0.5
6.522	20.339	18.558	0.251	0.254	69.4	68.8	-0.9	-0.9
7.891	20.590	18.802	0.260	0.261	69.5	69.1	-1.0	-0.7
8.681	20.727	18.936	0.263	0.264	69.1	69.2	-1.1	-1.0
9.549	20.871	19.078	0.262	0.264	68.9	68.1	-0.9	-1.3
10.504	21.019	19.219	0.265	0.265	69.5	69.0	-1.3	-1.1
11.554	21.171	19.370	0.269	0.270	69.5	69.5	-1.2	-1.0
12.709	21.332	19.519	0.275	0.278	69.7	69.6	-0.7	-0.5
13.980	21.501	19.687	0.280	0.283	69.4	68.9	-0.5	-0.1
15.378	21.680	19.859	0.280	0.280	69.2	69.6	-0.3	-0.4
16.916	21.859	20.036	0.288	0.286	69.5	69.7	-0.5	-0.6
18.608	22.058	20.229	0.290	0.292	69.7	69.5	-0.3	-0.4
20.469	22.256	20.429	0.293	0.291	69.8	69.9	-0.5	-0.2
22.515	22.472	20.627	0.297	0.293	69.9	69.7	0.0	0.0
24.767	22.686	20.848	0.297	0.295	69.8	69.5	-0.3	0.0
27.244	22.910	21.089	0.298	0.297	69.5	69.7	-0.3	0.0
29.968	23.171	21.359	0.289	0.278	69.6	69.4	-0.4	0.0
32.965	23.453	21.648	0.273	0.261	69.9	70.2	-0.5	-0.6
36.261	23.720	21.930	0.264	0.249	70.0	71.9	0.0	0.0
39.887	23.997	22.211	0.253	0.231	70.6	72.1	-0.7	-0.5
43.876	24.307	22.532	0.241	0.225	71.6	72.7	-0.2	-0.3
48.264	24.652	22.888	0.214	0.200	71.0	73.1	-0.2	-0.8
53.090	24.961	23.219	0.209		69.0		0.4	
58.399	25.244	23.482						
64.239	25.492	23.718						
70.663	25.695	23.954						
77.729	25.947	24.174						
85.502	26.124	24.516						
94.052	26.240	24.552						

Table A28: Surface Photometry of NGC 4696

Seeing σ = 0.5 arcsec (R) and 0.7 arcsec (B)

Semi-Major Axis Length (Arcsec)	Surface Brightness		Ellipticity 1-b/a		Position Angle N thru E		Cos(4θ) Component X100	
	B	R	B	R	B	R	B	R
0.547	19.213	17.115						
0.662	19.229	17.134						
0.801	19.251	17.162						
0.969	19.283	17.199						
1.173	19.330	17.247						
1.419	19.392	17.310						
1.717	19.474	17.394						
2.078	19.582	17.512	0.113	0.129	122.3	125.6	-0.4	-0.2
2.514	19.722	17.659	0.111	0.123	115.9	117.5	-0.4	-0.4
3.043	19.896	17.835	0.106	0.116	107.9	109.6	0.3	0.0
3.681	20.092	18.029	0.105	0.114	99.8	103.3	0.9	1.0
4.455	20.296	18.220	0.099	0.111	93.7	99.4	1.3	2.0
5.390	20.465	18.389	0.091	0.115	100.3	102.1	0.5	1.3
6.522	20.597	18.531	0.139	0.154	106.8	104.5	1.8	1.3
7.891	20.729	18.680	0.192	0.190	102.1	102.2	0.5	0.3
8.681	20.805	18.767	0.211	0.189	100.4	101.1	0.4	0.3
9.549	20.886	18.850	0.220	0.191	98.7	100.3	0.8	0.3
10.504	20.971	18.941	0.182	0.156	98.9	100.5	-0.1	0.3
11.554	21.064	19.047	0.144	0.132	97.9	97.8	0.1	0.1
12.709	21.164	19.149	0.133	0.124	94.7	96.3	-0.1	0.3
13.980	21.270	19.246	0.128	0.131	93.9	97.3	0.7	0.1
15.378	21.359	19.338	0.143	0.139	93.0	96.9	0.7	0.2
16.916	21.445	19.431	0.155	0.149	93.7	96.4	0.6	0.1
18.608	21.535	19.524	0.159	0.156	93.5	95.5	0.5	0.4
20.469	21.631	19.622	0.159	0.157	93.6	95.3	0.5	0.1
22.515	21.724	19.728	0.164	0.159	95.7	96.4	0.0	-0.1
24.767	21.827	19.839	0.166	0.161	96.2	96.5	-0.2	0.1
27.244	21.945	19.965	0.164	0.156	96.7	97.1	0.1	0.2
29.968	22.058	20.088	0.173	0.162	97.5	97.8	0.4	0.3
32.965	22.189	20.227	0.170	0.161	97.0	97.7	0.0	0.1
36.261	22.303	20.343	0.180	0.175	97.8	99.1	0.3	0.2
39.887	22.414	20.470	0.192	0.184	97.1	97.8	0.1	0.2
43.876	22.536	20.602	0.194	0.191	97.0	97.2	-0.4	0.2
48.264	22.655	20.733	0.198	0.198	96.7	97.8	0.2	-0.3
53.090	22.777	20.861	0.201	0.207	96.6	98.1	0.5	0.4
58.399	22.900	20.987	0.207	0.217	97.5	98.8	0.2	0.4
64.239	23.013		0.220		96.2		0.5	

Table A29: Surface Photometry of NGC 4697

Seeing σ = 0.65 arcsec (R) and 0.8 arcsec (B)

Semi-Major Axis Length (Arcsec)	Surface Brightness		Ellipticity 1-b/a		Position Angle N thru E		Cos(4θ) Component X100	
	B	R	B	R	B	R	B	R
0.547	17.275	15.226						
0.662	17.309	15.273						
0.801	17.356	15.331						
0.969	17.417	15.410						
1.173	17.495	15.512						
1.419	17.594	15.629						
1.717	17.708	15.756						
2.078	17.823	15.887	0.150	0.225	67.9	68.9	-0.2	0.0
2.514	17.937	16.019	0.197	0.260	66.4	67.4	-0.5	-0.3
3.043	18.049	16.150	0.260	0.313	66.0	66.7	0.1	0.3
3.681	18.171	16.294	0.321	0.360	66.1	66.5	1.2	1.1
4.455	18.324	16.470	0.362	0.390	66.0	66.5	1.8	1.5
5.390	18.516	16.677	0.384	0.402	66.2	66.3	1.6	1.6
6.522	18.729	16.894	0.394	0.411	66.2	66.3	1.5	1.5
7.891	18.956	17.123	0.399	0.413	66.1	66.3	1.5	1.5
8.681	19.070	17.239	0.402	0.413	66.0	66.2	1.8	1.8
9.549	19.188	17.358	0.401	0.413	65.9	66.4	1.7	1.6
10.504	19.309	17.479	0.398	0.411	65.9	66.3	1.6	1.3
11.554	19.435	17.606	0.395	0.406	65.9	66.4	1.4	1.4
12.709	19.561	17.734	0.393	0.402	65.7	66.2	1.6	1.4
13.980	19.688	17.862	0.391	0.399	65.6	66.2	1.5	1.3
15.378	19.819	17.995	0.390	0.395	65.9	66.2	1.5	1.3
16.916	19.951	18.126	0.388	0.394	66.0	66.3	1.5	1.6
18.608	20.080	18.253	0.394	0.399	66.2	66.4	1.7	1.6
20.469	20.205	18.381	0.403	0.406	66.3	66.1	1.9	2.0
22.515	20.320	18.502	0.417	0.417	65.9	66.0	2.4	2.4
24.767	20.444	18.621	0.427	0.430	65.8	66.0	2.3	2.6
27.244	20.574	18.756	0.434	0.433	65.7	65.9	1.9	2.2
29.968	20.682	18.893	0.450	0.438	66.1	66.0	1.9	1.7
32.965	20.813	19.005	0.459	0.451	66.0	66.1	1.8	2.1
36.261	20.952	19.143	0.461	0.455	65.6	66.1	1.8	1.8
39.887	21.103	19.297	0.456	0.450	65.7	66.0	1.2	1.4
43.876	21.261	19.457	0.449	0.442	65.9	66.0	1.3	1.3
48.264	21.433	19.635	0.440	0.432	65.6	66.1	1.0	1.2
53.090	21.634	19.834	0.420	0.412	66.0	66.2	0.9	0.9
58.399	21.857	20.042	0.393	0.394	66.3	66.5	0.7	0.8
64.239	22.067	20.264	0.376	0.376	66.7	66.9	0.4	0.3
70.663	22.277	20.481	0.364	0.360	67.1	67.0	0.3	0.3
77.729	22.490	20.689	0.357	0.350	66.9	67.0	0.5	0.4
85.502	22.694	20.895	0.348	0.346	67.4	67.1	-0.4	-0.2
94.052	22.865	21.113		0.337		66.8		0.3

Table A30: Surface Photometry of NGC 4709

Seeing σ = 0.5 arcsec (R) and 0.7 arcsec (B)

Semi-Major Axis Length (Arcsec)	Surface Brightness		Ellipticity 1-b/a		Position Angle N thru E		Cos(4θ) Component X100	
	B	R	B	R	B	R	B	R
0.547	18.475	16.328						
0.662	18.513	16.378						
0.801	18.566	16.443						
0.969	18.637	16.533						
1.173	18.736	16.651						
1.419	18.870	16.798						
1.717	19.029	16.984						
2.078	19.225	17.182	0.176	0.178	91.6	91.1	0.1	0.2
2.514	19.445	17.409	0.184	0.183	91.1	90.5	0.0	0.2
3.043	19.683	17.656	0.185	0.184	91.3	90.7	0.1	0.3
3.681	19.922	17.900	0.194	0.191	91.1	90.8	-0.1	0.2
4.455	20.169	18.144	0.198	0.198	90.5	91.2	-0.1	0.1
5.390	20.424	18.401	0.194	0.194	91.2	90.8	0.0	0.1
6.522	20.698	18.681	0.184	0.180	90.5	91.0	-0.4	-0.4
7.891	20.994	18.984	0.165	0.163	91.5	90.1	-0.5	-0.3
8.681	21.149	19.136	0.150	0.153	91.7	91.0	-0.5	-0.3
9.549	21.285	19.286	0.151	0.145	91.9	91.8	-0.4	-0.1
10.504	21.427	19.428	0.143	0.142	91.4	91.9	-0.4	-0.4
11.554	21.561	19.572	0.142	0.136	92.4	91.7	-0.4	-0.5
12.709	21.696	19.709	0.141	0.134	94.5	95.0	-0.7	-0.2
13.980	21.827	19.853	0.141	0.132	95.4	94.7	-0.2	-0.2
15.378	21.967	19.992	0.134	0.126	94.9	94.6	-0.5	-0.2
16.916	22.089	20.126	0.138	0.129	95.7	95.7	-0.5	-0.5
18.608	22.206	20.253	0.135	0.124	96.6	95.1	-0.3	-0.3
20.469	22.325	20.382	0.138	0.126	96.0	95.8	-0.5	-0.4
22.515	22.447	20.514	0.132	0.127	99.2	96.2	-0.4	-0.4
24.767	22.577	20.653	0.126	0.115	97.1	98.1	-0.9	-0.8
27.244	22.704	20.789	0.120	0.112	96.3	98.5	-1.4	-1.3
29.968	22.835	20.941	0.109	0.110	98.5	95.8	-1.1	-1.3
32.965	22.960	21.093	0.112	0.106	101.6	98.5	-1.0	-1.5
36.261	23.089	21.250	0.106	0.093	101.9	103.2	-1.2	-1.4
39.887	23.225	21.407	0.108	0.104	102.6	103.1	-2.4	-1.6
43.876	23.363	21.569	0.109	0.108	103.1	107.2	-1.4	-0.9
48.264	23.490		0.123		105.9		-1.3	
53.090	23.620							
58.399	23.761							
64.239	23.890							

Table A31: Surface Photometry of NGC 4767

Seeing σ = 0.55 arcsec (R) and 0.7 arcsec (B)

Semi-Major Axis Length (Arcsec)	Surface Brightness		Ellipticity 1-b/a		Position Angle N thru E		Cos(4θ) Component X100	
	B	R	B	R	B	R	B	R
0.547	17.928	15.784						
0.662	17.976	15.857						
0.801	18.044	15.959						
0.969	18.135	16.089						
1.173	18.252	16.240						
1.419	18.401	16.405						
1.717	18.576	16.593						
2.078	18.769	16.787	0.236	0.252	125.0	128.3	0.3	0.3
2.514	18.978	16.996	0.259	0.279	126.9	128.7	0.2	0.3
3.043	19.208	17.231	0.281	0.296	128.0	128.9	0.2	0.2
3.681	19.448	17.472	0.301	0.315	128.0	129.1	0.5	0.2
4.455	19.706	17.726	0.314	0.327	128.2	128.5	0.5	0.2
5.390	19.977	18.008	0.321	0.325	128.5	128.4	0.0	-0.2
6.522	20.256	18.284	0.322	0.326	128.5	128.5	0.3	-0.3
7.891	20.514	18.542	0.336	0.337	128.7	129.4	0.4	0.4
8.681	20.645	18.664	0.338	0.344	129.3	129.4	0.7	0.4
9.549	20.767	18.793	0.347	0.347	129.6	129.5	0.7	0.4
10.504	20.902	18.929	0.346	0.345	129.6	129.5	0.0	0.2
11.554	21.040	19.063	0.350	0.350	129.7	129.2	-0.6	-0.5
12.709	21.174	19.198	0.363	0.359	129.3	129.4	-1.3	-1.2
13.980	21.291	19.318	0.386	0.381	129.4	129.6	-1.1	-1.4
15.378	21.399	19.421	0.414	0.412	129.8	129.7	-0.2	-0.3
16.916	21.521	19.543	0.439	0.437	130.1	129.8	0.7	0.7
18.608	21.696	19.722	0.448	0.441	130.1	130.2	0.8	0.7
20.469	21.890	19.914	0.446	0.440	130.1	130.2	1.2	0.9
22.515	22.076	20.113	0.441	0.432	129.7	129.6	0.6	0.6
24.767	22.247	20.279	0.441	0.435	129.4	129.4	1.1	0.8
27.244	22.412	20.454	0.449	0.440	129.3	129.3	-0.1	0.1
29.968	22.598	20.637	0.456	0.448	129.0	129.0	-0.8	-0.3
32.965	22.786	20.848	0.464	0.446	128.9	129.4	-0.3	0.0
36.261	22.988	21.059	0.458	0.437	129.7	129.5	0.4	0.4
39.887	23.136	21.229	0.468	0.445	130.2	129.9	-0.4	-0.3
43.876	23.304	21.410	0.477	0.453	130.8	130.4	-1.1	-1.2
48.264	23.481	21.552	0.495	0.475	129.6	130.2	0.0	-0.4
53.090	23.704	21.745	0.499	0.480	129.5	130.2	0.2	0.0
58.399	23.943	21.975	0.485	0.477	128.8	129.7	0.0	0.7
64.239	24.156	22.142	0.494	0.492	128.8	129.6	0.0	0.8
70.663	24.354	22.322	0.501		128.4		-0.9	
77.729	24.498	22.498						
85.502	24.706	22.683						
94.052	24.848	22.810						
103.458	24.990							

Table A32: Surface Photometry of NGC 4976

Seeing σ = 0.75 arcsec (R) and 0.9 arcsec (B)

Semi-Major Axis Length (Arcsec)	Surface Brightness		Ellipticity 1-b/a		Position Angle N thru E		Cos(4θ) Component X100	
	B	R	B	R	B	R	B	R
0.547	16.889	14.782						
0.662	16.924	14.838						
0.801	16.977	14.915						
0.969	17.050	15.031						
1.173	17.164	15.196						
1.419	17.328	15.405						
1.717	17.548	15.642						
2.078	17.812	15.892	0.080	0.127	140.1	154.1	0.2	0.3
2.514	18.086	16.146	0.098	0.148	149.1	155.9	0.5	0.4
3.043	18.360	16.412	0.125	0.165	153.3	156.2	0.4	0.5
3.681	18.631	16.690	0.156	0.181	155.7	157.8	0.5	0.5
4.455	18.903	16.949	0.182	0.205	156.6	158.2	0.5	0.7
5.390	19.143	17.184	0.222	0.237	157.8	158.8	0.8	1.0
6.522	19.376	17.412	0.249	0.259	159.0	158.9	0.8	0.7
7.891	19.623	17.660	0.261	0.265	159.2	159.4	0.9	0.7
8.681	19.757	17.788	0.260	0.264	159.8	159.3	0.6	0.3
9.549	19.896	17.930	0.257	0.257	159.7	159.9	0.5	0.4
10.504	20.042	18.076	0.253	0.253	160.2	160.2	0.3	0.5
11.554	20.192	18.227	0.251	0.248	160.0	160.1	0.4	0.4
12.709	20.347	18.378	0.250	0.248	160.1	160.5	0.6	0.6
13.980	20.502	18.530	0.251	0.247	160.4	161.1	0.6	0.5
15.378	20.652	18.676	0.251	0.248	161.2	161.1	0.4	0.5
16.916	20.795	18.820	0.255	0.253	160.9	160.8	0.2	0.5
18.608	20.939	18.963	0.263	0.262	159.9	160.1	0.1	0.2
20.469	21.082	19.102	0.270	0.265	160.1	160.1	0.3	0.2
22.515	21.219	19.234	0.275	0.272	160.7	160.7	0.2	0.3
24.767	21.347	19.366	0.286	0.280	160.4	161.3	0.2	0.1
27.244	21.476	19.491	0.296	0.293	160.7	161.5	0.3	0.3
29.968	21.602	19.612	0.308	0.304	160.2	161.0	0.5	0.4
32.965	21.721	19.732	0.327	0.323	160.3	161.0	0.1	0.2
36.261	21.842	19.854	0.342	0.337	160.6	160.8	0.2	0.2
39.887	21.972	19.979	0.352	0.350	160.7	161.0	-0.1	0.4
43.876	22.108	20.123	0.355	0.351	160.5	160.6	-0.6	-0.1
48.264	22.272	20.284	0.350	0.349	160.1	161.0	-0.8	-0.3
53.090	22.461	20.460	0.343	0.344	160.5	160.2	-0.9	-0.4
58.399	22.665	20.642	0.339	0.345	160.5	160.4	-0.4	-0.5
64.239	22.864	20.822	0.344	0.354	161.1	160.2	-0.4	-0.2
70.663	23.050	20.989	0.361	0.368	161.0	160.7	-0.4	0.3
77.729	23.246	21.180	0.368	0.380	161.7	160.4	0.0	0.5

Table A33: Surface Photometry of NGC 5638

Seeing σ = 0.7 arcsec (R) and 0.9 arcsec (B)

Semi-Major Axis Length (Arcsec)	Surface Brightness		Ellipticity 1-b/a		Position Angle N thru E		Cos(4θ) Component X100	
	B	R	B	R	B	R	B	R
0.547	18.219	16.238						
0.662	18.248	16.287						
0.801	18.292	16.356						
0.969	18.356	16.446						
1.173	18.444	16.560						
1.419	18.554	16.701						
1.717	18.692	16.860						
2.078	18.857	17.036	0.049	0.041	123.4	136.5	0.0	0.1
2.514	19.046	17.226	0.047	0.043	126.9	137.0	0.1	-0.1
3.043	19.252	17.433	0.045	0.044	130.5	137.7	0.1	0.0
3.681	19.473	17.658	0.047	0.046	136.1	139.3	-0.1	0.0
4.455	19.714	17.900	0.048	0.047	135.3	139.4	0.1	0.1
5.390	19.967	18.156	0.051	0.047	139.1	141.1	0.0	0.1
6.522	20.241	18.425	0.049	0.048	138.9	142.3	0.2	0.1
7.891	20.532	18.712	0.050	0.053	140.2	141.3	0.3	0.1
8.681	20.679	18.860	0.056	0.055	140.4	142.2	0.1	0.2
9.549	20.826	19.005	0.056	0.057	142.8	142.1	0.1	-0.1
10.504	20.971	19.145	0.059	0.064	142.4	142.7	0.0	0.1
11.554	21.106	19.281	0.070	0.070	143.4	143.4	0.0	0.2
12.709	21.238	19.414	0.077	0.077	144.5	143.8	0.2	0.1
13.980	21.375	19.550	0.082	0.082	145.4	143.3	0.2	0.2
15.378	21.518	19.692	0.089	0.089	144.9	144.1	0.1	0.1
16.916	21.664	19.838	0.095	0.098	144.3	144.2	0.2	-0.1
18.608	21.822	19.997	0.101	0.098	144.1	143.5	0.0	-0.2
20.469	21.987	20.165	0.103	0.103	144.6	144.6	0.1	-0.1
22.515	22.167	20.344	0.107	0.103	145.6	145.2	0.1	0.0
24.767	22.352	20.533	0.107	0.107	146.7	146.0	0.0	0.0
27.244	22.544	20.728	0.107	0.108	147.3	146.9	0.0	-0.1
29.968	22.736	20.919	0.112	0.112	149.3	148.8	0.3	0.2
32.965	22.928	21.115	0.117	0.114	151.3	150.7	0.6	0.1
36.261	23.116	21.308	0.118	0.118	150.9	151.7	0.0	0.1
39.887	23.320	21.507	0.120	0.124	152.7	152.1	0.1	-0.1
43.876	23.528	21.726	0.119	0.123	151.4	152.3	0.0	0.0
48.264	23.753	21.948	0.122	0.127	156.4	154.7	0.1	0.3
53.090	23.997	22.210	0.119	0.122	160.9	159.8	-0.2	-0.1
58.399	24.223	22.473	0.133	0.120	164.0	164.2	0.0	-0.1
64.239	24.476	22.733	0.130	0.119	165.0	167.8	0.2	0.0
70.663	24.710	22.967	0.118	0.128	168.2	168.9	0.0	0.4
77.729	24.960	23.195						

1987MNRAS.226..747J

Table A34: Surface Photometry of NGC 5813

Seeing σ = 0.6 arcsec (R) and 0.85 arcsec (B)

Semi-Major Axis Length (Arcsec)	Surface Brightness		Ellipticity 1-b/a		Position Angle N thru E		Cos(4θ) Component X100	
	B	R	B	R	B	R	B	R
0.547	17.904	15.848						
0.662	17.938	15.893						
0.801	17.985	15.954						
0.969	18.049	16.040						
1.173	18.138	16.153						
1.419	18.258	16.296						
1.717	18.413	16.471						
2.078	18.602	16.672	0.063	0.065	137.6	141.3	0.0	0.1
2.514	18.817	16.897	0.072	0.073	141.5	143.9	0.2	0.2
3.043	19.058	17.144	0.079	0.079	145.4	146.6	0.2	0.2
3.681	19.314	17.408	0.094	0.090	149.2	148.0	0.3	0.3
4.455	19.593	17.693	0.099	0.090	149.9	149.0	0.2	0.2
5.390	19.886	17.984	0.093	0.087	147.0	147.0	0.4	0.2
6.522	20.179	18.271	0.086	0.084	142.2	143.0	0.9	0.4
7.891	20.466	18.555	0.086	0.080	139.6	141.1	0.7	0.4
8.681	20.597	18.691	0.093	0.086	138.6	140.9	0.5	0.3
9.549	20.735	18.822	0.095	0.087	139.7	139.4	0.4	0.0
10.504	20.861	18.948	0.099	0.092	138.3	138.0	0.2	0.2
11.554	20.983	19.070	0.111	0.101	137.9	138.2	0.3	0.3
12.709	21.110	19.194	0.117	0.107	136.8	137.4	0.3	0.1
13.980	21.234	19.309	0.125	0.120	135.6	135.5	0.3	0.2
15.378	21.356	19.434	0.133	0.124	135.8	137.0	0.3	0.3
16.916	21.479	19.558	0.141	0.130	135.9	136.9	0.0	0.2
18.608	21.611	19.683	0.147	0.140	135.8	137.0	-0.1	0.1
20.469	21.732	19.809	0.160	0.150	135.2	136.2	-0.1	0.3
22.515	21.856	19.931	0.173	0.165	136.1	136.0	0.0	0.2
24.767	21.980	20.054	0.186	0.179	136.2	136.6	0.2	0.3
27.244	22.104	20.174	0.199	0.193	136.3	136.5	0.4	0.4
29.968	22.218	20.290	0.219	0.209	136.4	136.1	0.5	0.4
32.965	22.331	20.405	0.232	0.222	134.0	134.9	-0.1	0.4
36.261	22.446	20.523	0.242	0.235	133.7	134.2	-0.3	-0.1
39.887	22.576	20.649	0.248	0.245	134.3	134.2	-0.3	-0.1
43.876	22.708	20.792	0.252	0.246	134.6	134.2	-0.7	-0.4
48.264	22.861	20.941	0.249	0.248	133.8	133.7	-0.4	-0.5
53.090	23.018	21.095	0.252	0.252	133.7	133.1	-0.2	-0.4
58.399	23.205	21.271	0.249	0.250	134.3	134.2	-0.1	-0.3
64.239	23.369	21.426	0.265	0.264	134.7	134.5	0.2	-0.1
70.663	23.553	21.597	0.269	0.269	134.6	134.1	0.2	0.4
77.729	23.730	21.774	0.276	0.268	132.9	132.9	0.2	-0.6
85.502	23.919	21.954		0.280		133.1		-0.3
94.052	24.128	22.155						
103.458	24.329	22.346						
113.803	24.489							

Table A35: Surface Photometry of NGC 5831

Seeing σ = 0.7 arcsec (R) and 0.85 arcsec (B)

Semi-Major Axis Length (Arcsec)	Surface Brightness		Ellipticity 1-b/a		Position Angle N thru E		Cos(4θ) Component X100	
	B	R	B	R	B	R	B	R
0.547	17.965	15.923						
0.662	18.004	15.989						
0.801	18.061	16.078						
0.969	18.139	16.195						
1.173	18.245	16.347						
1.419	18.387	16.525						
1.717	18.565	16.725						
2.078	18.771	16.936	0.195	0.196	112.8	115.2	0.1	0.3
2.514	18.994	17.163	0.218	0.223	113.7	115.3	0.4	0.5
3.043	19.237	17.401	0.237	0.247	114.5	115.7	0.3	0.5
3.681	19.491	17.657	0.255	0.264	114.9	115.9	0.3	0.3
4.455	19.756	17.923	0.271	0.276	115.5	116.0	0.2	0.3
5.390	20.021	18.190	0.286	0.289	115.7	116.5	0.5	0.5
6.522	20.284	18.454	0.296	0.297	116.2	116.5	0.7	0.5
7.891	20.555	18.723	0.293	0.296	116.7	116.4	0.4	0.3
8.681	20.701	18.865	0.284	0.288	116.6	116.5	0.5	0.3
9.549	20.845	19.012	0.274	0.277	116.6	116.7	0.4	0.3
10.504	21.008	19.170	0.254	0.258	117.5	117.3	0.4	0.4
11.554	21.169	19.341	0.237	0.230	118.1	118.1	0.9	0.6
12.709	21.349	19.514	0.206	0.203	119.8	119.4	0.9	0.9
13.980	21.532	19.695	0.177	0.177	120.9	121.4	0.8	0.9
15.378	21.723	19.888	0.157	0.155	123.4	123.3	0.9	0.9
16.916	21.915	20.078	0.147	0.142	124.6	124.7	1.0	1.2
18.608	22.101	20.267	0.137	0.129	127.1	127.8	1.6	1.5
20.469	22.295	20.460	0.126	0.111	129.1	130.7	0.9	0.9
22.515	22.501	20.645	0.100	0.103	135.1	135.6	0.2	0.1
24.767	22.669	20.826	0.100	0.089	137.5	137.3	-0.3	-0.1
27.244	22.857	21.010	0.090	0.083	141.7	140.1	-0.5	0.0
29.968	23.064	21.208	0.079	0.082	141.0	139.5	-0.2	0.0
32.965	23.238	21.386	0.088	0.093	137.4	135.2	-0.4	0.0
36.261	23.428	21.572	0.107	0.104	135.7	135.3	-0.1	-0.2
39.887	23.616	21.756	0.110	0.118	138.0	139.1	-0.5	-0.4
43.876	23.789	21.940	0.130	0.128	140.8	138.8	-0.5	-0.6
48.264	23.983	22.138	0.128	0.134	141.8	139.8	-0.2	-0.2
53.090	24.202	22.348	0.113	0.134	142.8	140.3	0.4	0.4
58.399	24.423	22.581	0.105	0.129	139.1	135.8	-0.1	0.4
64.239	24.673	22.862		0.093		141.3		-0.2
70.663	24.918	23.114						
77.729	25.173	23.384						
85.502	25.454	23.665						
94.052	25.536	23.758						

Table A36: Surface Photometry of NGC 5845

Seeing σ = 0.9 arcsec (R) and 0.65 arcsec (B)

Semi-Major Axis Length (Arcsec)	Surface Brightness B	Surface Brightness R	Ellipticity 1-b/a B	Ellipticity 1-b/a R	Position Angle N thru E B	Position Angle N thru E R	Cos(4θ) Component X100 B	Cos(4θ) Component X100 R
0.547	17.333	15.292						
0.662	17.370	15.339						
0.801	17.424	15.406						
0.969	17.501	15.508						
1.173	17.607	15.652						
1.419	17.753	15.837						
1.717	17.946	16.066						
2.078	18.194	16.343	0.206	0.236	138.2	142.1	0.3	0.8
2.514	18.494	16.657	0.212	0.236	139.3	142.3	0.1	0.5
3.043	18.839	17.003	0.214	0.235	140.4	142.4	0.1	0.0
3.681	19.210	17.369	0.219	0.234	141.6	143.0	-0.3	-0.4
4.455	19.610	17.763	0.224	0.234	142.7	143.8	-0.4	-0.7
5.390	20.046	18.194	0.233	0.239	143.7	144.1	-0.4	-0.5
6.522	20.514	18.659	0.253	0.256	143.8	144.6	0.1	0.0
7.891	20.992	19.122	0.285	0.290	143.9	144.2	0.6	0.5
8.681	21.239	19.352	0.302	0.310	143.4	143.8	0.9	0.9
9.549	21.457	19.581	0.329	0.328	143.0	143.1	1.3	1.4
10.504	21.698	19.799	0.348	0.351	142.5	142.6	1.6	1.7
11.554	21.944	20.034	0.364	0.366	142.0	141.8	1.5	1.7
12.709	22.224	20.297	0.372	0.370	141.6	141.6	1.2	1.3
13.980	22.465	20.541	0.386	0.377	141.0	141.1	0.6	0.8
15.378	22.736	20.817	0.384	0.370	139.9	140.8	0.6	0.2
16.916	23.031	21.097	0.372	0.358	139.1	139.5	-0.4	0.5
18.608	23.356	21.400	0.362	0.334	139.1	138.5	0.0	-0.2
20.469	23.731	21.740	0.326	0.295	13[illegible].4	138.3	-2.3	0.1
22.515	24.025	22.023	0.311	0.281	136.4	138.7	-1.1	-0.1
24.767	24.344	22.298	0.286	0.252	138.6	137.1	0.6	-0.1
27.244	24.657	22.586	0.255	0.243	139.6	136.5	0.6	0.4
29.968	24.926	22.863	0.238	0.222	139.6	134.1	-2.2	-0.4
32.965	25.222	23.147		0.193		131.2		0.1
36.261	25.485	23.425						
39.887	25.603	23.561						
43.876	25.728	23.732						
48.264	25.888	23.927						
53.090	26.022	24.058						
58.399	26.144	24.256						
64.239	26.331	24.416						
70.663	26.445	24.564						
77.729	26.585	24.677						
85.502	26.693	24.712						
94.052	26.710	24.715						
103.458	26.610	25.188						
113.803	26.252							

Table A37: Surface Photometry of NGC 5898

Seeing σ = 0.5 arcsec (R) and 0.6 arcsec (B)

Semi-Major Axis Length (Arcsec)	Surface Brightness		Ellipticity 1-b/a		Position Angle N thru E		Cos(4θ) Component X100	
	B	R	B	R	B	R	B	R
0.547	17.921	15.813						
0.662	17.970	15.875						
0.801	18.037	15.957						
0.969	18.127	16.063						
1.173	18.242	16.198						
1.419	18.394	16.355						
1.717	18.566	16.542						
2.078	18.773	16.746	0.105	0.128	182.9	182.7	-0.2	-0.1
2.514	18.989	16.969	0.110	0.129	182.3	182.6	0.0	0.1
3.043	19.229	17.210	0.104	0.124	181.4	181.9	0.2	0.1
3.681	19.484	17.479	0.096	0.108	180.0	180.6	0.2	0.2
4.455	19.759	17.762	0.087	0.094	180.9	180.4	0.1	0.1
5.390	20.069	18.076	0.066	0.066	178.7	178.1	0.0	0.3
6.522	20.416	18.415	0.029	0.033	162.9	171.8	0.7	0.5
7.891	20.763	18.750	0.017	0.023	136.8	130.1	-0.4	-0.6
8.681	20.933	18.907	0.020	0.031	116.6	112.9	-1.1	-0.7
9.549	21.092	19.056	0.030	0.042	107.2	105.5	-0.4	0.1
10.504	21.232	19.197	0.044	0.054	102.3	103.5	0.4	0.3
11.554	21.381	19.341	0.055	0.058	104.4	106.5	0.2	-0.1
12.709	21.541	19.499	0.058	0.058	106.1	107.0	-0.2	-0.2
13.980	21.700	19.646	0.057	0.069	115.4	108.5	-0.7	-0.3
15.378	21.834	19.795	0.067	0.070	110.9	108.5	-0.4	-0.8
16.916	21.988	19.974	0.067	0.054	102.2	103.8	-0.3	-0.6
18.608	22.181	20.154	0.047	0.045	99.1	100.3	-0.2	-0.2
20.469	22.357	20.356	0.046	0.029	86.8	77.3	0.9	1.3
22.515	22.536	20.532	0.040	0.034	65.5	65.9	0.9	1.2
24.767	22.710	20.708	0.050	0.042	59.8	59.7	0.9	1.0
27.244	22.877	20.886	0.068	0.053	57.5	54.6	1.0	0.5
29.968	23.037	21.034	0.087	0.080	56.6	56.1	0.7	1.5
32.965	23.193	21.199	0.104	0.084	54.5	54.1	0.5	0.4
36.261	23.365	21.361	0.104	0.087	50.3	53.5	0.1	0.8
39.887	23.530	21.543	0.101	0.081	44.8	52.3	-1.6	0.6
43.876	23.719	21.710	0.085	0.087	41.9	43.9	-0.5	0.1
48.264	23.879	21.866		0.111		42.9		1.5
53.090	24.053	22.024		0.122		40.7		1.5
58.399	24.220	22.206						
64.239	24.421	22.406						
70.663	24.688	22.614						
77.729	24.949	22.857						
85.502	25.168							

Table A38: Surface Photometry of NGC 5903

Seeing σ = 0.6 arcsec (R) and 0.8 arcsec (B)

Semi-Major Axis Length (Arcsec)	Surface Brightness		Ellipticity 1-b/a		Position Angle N thru E		Cos(4θ) Component X100	
	B	R	B	R	B	R	B	R
0.547	18.529	16.416						
0.662	18.551	16.447						
0.801	18.584	16.487						
0.969	18.632	16.548						
1.173	18.698	16.627						
1.419	18.786	16.730						
1.717	18.899	16.865						
2.078	19.045	17.024	0.140	0.155	162.0	161.1	0.1	-0.1
2.514	19.227	17.210	0.151	0.175	162.5	162.4	-0.2	-0.2
3.043	19.437	17.433	0.164	0.192	163.5	162.6	-0.3	-0.3
3.681	19.672	17.679	0.182	0.202	164.5	163.3	-0.6	-0.7
4.455	19.919	17.933	0.199	0.215	165.0	164.3	-0.9	-1.0
5.390	20.172	18.180	0.215	0.233	166.2	164.7	-0.8	-1.0
6.522	20.426	18.432	0.231	0.245	165.8	165.1	-1.2	-1.1
7.891	20.689	18.700	0.233	0.242	164.7	165.1	-1.8	-1.5
8.681	20.841	18.844	0.223	0.234	163.7	164.7	-1.6	-1.3
9.549	20.991	18.998	0.220	0.224	163.6	164.7	-0.9	-1.0
10.504	21.138	19.146	0.216	0.219	163.3	164.7	-1.0	-0.8
11.554	21.287	19.295	0.212	0.215	163.9	165.7	-1.0	-0.9
12.709	21.429	19.441	0.212	0.211	165.4	166.7	-0.9	-0.9
13.980	21.588	19.603	0.205	0.199	165.1	166.0	-0.7	-0.7
15.378	21.746	19.760	0.193	0.190	165.0	165.3	-0.5	-0.6
16.916	21.895	19.905	0.193	0.190	165.0	165.8	-0.8	-0.5
18.608	22.038	20.049	0.197	0.191	164.9	165.9	-0.7	-0.3
20.469	22.180	20.194	0.200	0.193	166.0	166.2	-0.4	-0.3
22.515	22.313	20.328	0.211	0.200	166.7	167.2	-0.1	-0.2
24.767	22.456	20.461	0.203	0.206	166.9	167.1	-0.3	-0.4
27.244	22.586	20.598	0.217	0.208	167.2	167.4	-0.7	-0.5
29.968	22.731	20.738	0.216	0.214	166.0	166.3	-0.7	-0.7
32.965	22.880	20.891	0.210	0.214	166.5	166.8	-0.8	-0.6
36.261	23.045	21.056	0.210	0.214	166.0	166.3	-0.3	0.1
39.887	23.235	21.237	0.202	0.211	166.7	165.6	-0.4	-0.5
43.876	23.415	21.430	0.206	0.211	166.5	165.4	-0.6	-0.3
48.264	23.607	21.634	0.206	0.204	164.7	164.6	-0.8	-0.4
53.090	23.808	21.810	0.211	0.218	166.7	163.2	0.2	-0.5
58.399	23.994	21.988		0.228		161.6		-0.8
64.239	24.191	22.158		0.250		159.7		-0.9
70.663	24.379	22.325		0.259		158.9		-0.5
77.729	24.582	22.509						
85.502	24.725	22.719						
94.052	24.904							

Table A39: Surface Photometry of NGC 6868

Seeing σ = 0.6 arcsec (R) and 0.7 arcsec (B)

Semi-Major Axis Length (Arcsec)	Surface Brightness		Ellipticity 1-b/a		Position Angle N thru E		Cos(4θ) Component X100	
	B	R	B	R	B	R	B	R
0.547	18.119	16.007						
0.662	18.134	16.027						
0.801	18.154	16.054						
0.969	18.183	16.091						
1.173	18.219	16.140						
1.419	18.267	16.210						
1.717	18.335	16.308						
2.078	18.434	16.437	0.156	0.117	103.8	93.1	-0.3	0.5
2.514	18.576	16.597	0.138	0.125	97.1	86.4	0.2	0.6
3.043	18.752	16.788	0.136	0.130	89.1	81.0	0.7	0.3
3.681	18.962	17.003	0.135	0.140	81.9	77.0	0.5	0.0
4.455	19.199	17.250	0.144	0.146	78.4	76.1	0.1	-0.2
5.390	19.461	17.515	0.153	0.155	78.9	76.7	-0.1	-0.3
6.522	19.739	17.789	0.164	0.166	79.5	77.9	-0.2	-0.2
7.891	20.036	18.082	0.164	0.165	78.7	77.4	-0.5	-0.5
8.681	20.194	18.237	0.162	0.164	78.9	77.3	-0.7	-0.5
9.549	20.358	18.392	0.157	0.161	78.0	76.8	-0.4	-0.2
10.504	20.529	18.555	0.152	0.157	78.2	77.0	0.0	-0.1
11.554	20.693	18.714	0.153	0.157	77.6	76.6	0.4	0.2
12.709	20.851	18.875	0.158	0.160	75.5	76.3	0.8	0.4
13.980	21.006	19.030	0.167	0.166	76.3	76.1	1.0	0.7
15.378	21.158	19.188	0.178	0.171	75.9	76.5	0.9	0.6
16.916	21.320	19.338	0.182	0.180	75.5	76.1	0.6	0.6
18.608	21.478	19.484	0.183	0.188	75.3	76.2	0.6	0.6
20.469	21.604	19.630	0.201	0.193	77.4	77.2	0.8	0.7
22.515	21.754	19.782	0.204	0.194	77.2	77.2	0.7	0.8
24.767	21.918	19.939	0.202	0.195	78.0	77.3	0.9	0.9
27.244	22.095	20.108	0.195	0.191	77.3	76.8	0.7	0.7
29.968	22.275	20.283	0.189	0.186	78.1	77.5	0.6	0.9
32.965	22.474	20.464	0.178	0.183	77.5	77.6	0.5	0.6
36.261	22.639	20.643	0.185	0.182	76.1	77.1	0.9	1.0
39.887	22.820	20.822	0.191	0.185	76.5	77.3	1.1	1.4
43.876	23.003	20.988	0.190	0.188	75.9	77.1	1.2	1.5
48.264	23.190	21.167	0.189	0.182	75.4	76.5	1.6	1.4
53.090	23.399	21.340	0.171	0.181	77.1	77.2	0.9	0.9
58.399	23.579	21.495	0.181	0.192	75.2	77.1	1.0	1.0
64.239	23.762	21.641		0.207		76.6		0.7
70.663	23.939	21.771		0.224		76.2		0.6
77.729	24.106	21.894		0.245		77.0		1.0

1987MNRAS.226..747J

Table A40: Surface Photometry of NGC 6876

Seeing σ = 0.4 arcsec (R) and 0.6 arcsec (B)

Semi-Major Axis Length (Arcsec)	Surface Brightness		Ellipticity 1-b/a		Position Angle N thru E		Cos(4θ) Component X100	
	B	R	B	R	B	R	B	R
0.547	18.658	16.658						
0.662	18.693	16.700						
0.801	18.744	16.762						
0.969	18.812	16.852						
1.173	18.905	16.961						
1.419	19.026	17.090						
1.717	19.167	17.222						
2.078	19.320	17.342	0.212	0.271	78.8	80.6	0.7	0.7
2.514	19.477	17.443	0.238	0.335	78.0	78.5	0.6	1.0
3.043	19.629	17.597	0.260	0.335	76.6	75.2	0.8	1.0
3.681	19.783	17.861	0.272	0.284	75.1	75.2	0.8	1.0
4.455	19.925	18.603	0.288	0.292	74.7	74.7	1.0	1.0
5.390	20.067	18.142	0.299	0.302	74.4	74.8	0.6	0.9
6.522	20.204	18.280	0.314	0.307	74.4	74.3	0.6	0.6
7.891	20.351	18.419	0.321	0.319	75.3	75.1	0.6	0.7
8.681	20.431	18.500	0.324	0.318	75.1	75.4	0.0	0.3
9.549	20.524	18.594	0.320	0.311	75.2	75.5	0.0	0.1
10.504	20.624	18.692	0.317	0.307	75.4	75.3	-0.2	0.1
11.554	20.746	18.810	0.302	0.295	75.4	75.5	-0.1	-0.1
12.709	20.875	18.938	0.287	0.281	75.6	76.0	0.1	0.2
13.980	21.020	19.075	0.271	0.268	75.8	75.6	0.3	0.1
15.378	21.179	19.233	0.253	0.247	75.7	75.9	0.3	0.4
16.916	21.359	19.406	0.228	0.225	75.9	76.1	0.6	0.7
18.608	21.538	19.585	0.213	0.203	76.6	76.9	0.8	1.0
20.469	21.723	19 758	0.195	0.189	77.2	77.9	1.1	1.2
22.515	21.890	19.923	0.190	0.180	78.1	78.7	1.1	1.2
24.767	22.057	20.081	0.182	0.174	79.1	79.7	1.0	1.1
27.244	22.231	20.251	0.168	0.155	79.6	80.3	0.7	1.0
29.968	22.421	20.428	0.144	0.136	79.9	80.9	0.5	0.7
32.965	22.625	20.612	0.112	0.113	82.3	83.2	0.5	0.6
36.261	22.819	20.797	0.090	0.081	88.4	91.2	0.7	1.0
39.887	22.994	20.954	0.079	0.076	94.3	96.8	0.8	0.9
43.876	23.162	21.100	0.072	0.078	105.3	104.6	0.3	0.3
48.264	23.326	21.261	0.076	0.069	111.7	112.8	0.1	-0.4
53.090	23.492	21.394	0.081	0.079	113.3	114.4	0.1	-0.3
58.399	23.657	21.536	0.086	0.080	119.5	125.5	-0.5	-0.3
64.239	23.807	21.645	0.097	0.112	122.6	125.9	-0.9	-0.8
70.663	23.966		0.115		128.8		-2.3	
77.729	24.148							
85.502	24.312							

Table A41: Surface Photometry of NGC 6909

Seeing σ = 0.5 arcsec (R) and 0.65 arcsec (B)

Semi-Major Axis Length (Arcsec)	Surface Brightness		Ellipticity 1-b/a		Position Angle N thru E		Cos(4θ) Component X100	
	B	R	B	R	B	R	B	R
0.547	17.910	16.088						
0.662	17.989	16.184						
0.801	18.096	16.308						
0.969	18.235	16.464						
1.173	18.419	16.669						
1.419	18.641	16.911						
1.717	18.894	17.175						
2.078	19.164	17.451	0.180	0.180	66.0	65.6	0.6	0.9
2.514	19.435	17.722	0.182	0.182	65.8	65.9	0.8	0.8
3.043	19.674	17.963	0.201	0.201	66.4	65.9	1.0	0.7
3.681	19.900	18.188	0.226	0.222	66.6	66.9	0.4	0.4
4.455	20.104	18.391	0.257	0.253	68.0	67.8	0.1	0.3
5.390	20.299	18.582	0.292	0.291	68.6	68.8	0.0	0.0
6.522	20.481	18.772	0.338	0.331	69.4	68.9	0.2	0.2
7.891	20.680	18.967	0.372	0.364	69.2	69.0	0.1	0.0
8.681	20.779	19.064	0.389	0.382	68.8	68.9	0.6	0.1
9.549	20.876	19.168	0.408	0.399	69.3	69.2	-0.1	-0.2
10.504	20.988	19.277	0.421	0.414	69.2	69.0	-0.1	-0.2
11.554	21.097	19.386	0.435	0.428	69.2	68.6	-0.4	-0.1
12.709	21.215	19.499	0.447	0.440	69.2	68.9	-0.6	-0.6
13.980	21.339	19.629	0.455	0.447	69.0	69.0	-0.6	-0.9
15.378	21.497	19.779	0.454	0.447	68.9	68.9	-1.5	-1.1
16.916	21.653	19.949	0.455	0.443	68.8	68.9	-1.7	-1.5
18.608	21.831	20.119	0.453	0.444	68.8	69.0	-1.2	-1.3
20.469	22.013	20.300	0.458	0.442	69.0	69.1	-1.6	-0.7
22.515	22.208	20.488	0.455	0.443	68.6	68.9	-1.1	-0.9
24.767	22.415	20.694	0.453	0.442	68.9	68.8	-1.3	-0.7
27.244	22.629	20.907	0.455	0.440	68.5	68.6	-1.4	-0.8
29.968	22.843	21.120	0.456	0.441	68.9	68.8	-2.1	-1.1
32.965	23.063	21.324	0.460	0.444	68.9	68.2	-1.5	-1.1
36.261	23.257	21.525	0.471	0.454	69.2	68.4	-0.8	-1.0
39.887	23.451	21.695	0.482	0.469	68.9	68.6	-1.0	0.4
43.876	23.660	21.882		0.481		67.9		0.0
48.264	23.873	22.071		0.489		67.3		-0.5
53.090	24.027	22.236		0.507		68.1		-0.6
58.399	24.214	22.484						
64.239								
70.663	24.618							
77.729	24.785	23.013						
85.502	24.921							
94.052	25.243							

Table A42: Surface Photometry of NGC 7029

Seeing σ = 0.45 arcsec (R) and 0.65 arcsec (B)

Semi-Major Axis Length (Arcsec)	Surface Brightness		Ellipticity 1-b/a		Position Angle N thru E		Cos(4θ) Component X100	
	B	R	B	R	B	R	B	R
0.547	17.400	15.347						
0.662	17.460	15.435						
0.801	17.539	15.562						
0.969	17.648	15.720						
1.173	17.792	15.916						
1.419	17.980	16.150						
1.717	18.214	16.408						
2.078	18.478	16.689	0.234	0.291	65.1	64.2	0.7	1.3
2.514	18.756	16.983	0.246	0.286	65.1	64.5	0.8	1.4
3.043	19.044	17.281	0.249	0.276	64.8	65.0	0.6	1.0
3.681	19.341	17.575	0.250	0.269	65.4	65.3	0.7	0.8
4.455	19.618	17.853	0.261	0.273	66.0	65.5	0.8	0.8
5.390	19.888	18.116	0.279	0.288	65.4	65.5	0.9	1.0
6.522	20.137	18.371	0.303	0.310	66.1	66.1	1.7	1.6
7.891	20.405	18.624	0.323	0.334	66.8	66.7	2.5	2.5
8.681	20.539	18.754	0.332	0.345	66.3	66.5	3.1	3.1
9.549	20.688	18.891	0.335	0.351	67.2	66.2	3.8	3.7
10.504	20.819	19.028	0.345	0.361	66.6	66.2	4.4	4.2
11.554	20.959	19.163	0.359	0.371	66.3	66.0	4.3	4.2
12.709	21.090	19.305	0.372	0.372	66.5	65.8	3.9	3.9
13.980	21.233	19.442	0.379	0.379	65.8	65.6	3.8	3.7
15.378	21.382	19.595	0.379	0.376	65.6	65.8	3.0	3.3
16.916	21.556	19.771	0.376	0.369	67.0	66.8	2.8	2.6
18.608	21.712	19.939	0.378	0.363	67.1	67.3	1.9	1.9
20.469	21.920	20.120	0.355	0.353	66.3	66.9	1.7	1.6
22.515	22.094	20.316	0.358	0.347	67.3	66.8	1.1	0.9
24.767	22.308	20.513	0.352	0.347	66.8	66.4	0.3	0.7
27.244	22.500	20.706	0.356	0.349	66.2	66.5	0.6	0.1
29.968	22.679	20.886	0.365	0.354	66.6	66.9	-0.4	-0.4
32.965	22.858	21.055	0.377	0.366	67.1	67.1	-1.4	-0.9
36.261	23.042	21.236	0.379	0.374	68.0	67.8	-1.4	-1.2
39.887	23.235	21.433	0.387	0.373	67.4	68.1	-2.5	-2.2
43.876	23.453	21.647	0.391	0.380	67.9	67.8	-3.3	-1.2
48.264	23.687	21.843		0.390		68.7		-1.5
53.090	23.930	22.069		0.391		69.3		-2.6
58.399	24.170	22.308						
64.239	24.413	22.550						
70.663	24.666	22.821						
77.729	24.889	23.054						
85.502	25.118	23.319						
94.052	25.294	23.554						
103.458	25.578							

Table A43: Surface Photometry of NGC 7144

Seeing σ = 0.55 arcsec (R) and 0.8 arcsec (B)

Semi-Major Axis Length (Arcsec)	Surface Brightness		Ellipticity 1-b/a		Position Angle N thru E		Cos(4θ) Component X100	
	B	R	B	R	B	R	B	R
0.547	17.717	15.669						
0.662	17.771	15.769						
0.801	17.841	15.899						
0.969	17.945	16.060						
1.173	18.089	16.253						
1.419	18.265	16.471						
1.717	18.477	16.697						
2.078	18.697	16.926	0.051	0.031	69.9	42.9	-0.1	-0.1
2.514	18.927	17.147	0.037	0.026	66.7	43.7	-0.2	-0.2
3.043	19.148	17.363	0.031	0.019	59.5	40.4	-0.1	-0.1
3.681	19.377	17.581	0.020	0.021	52.6	40.2	0.1	-0.2
4.455	19.620	17.824	0.019	0.018	56.9	37.7	-0.1	-0.1
5.390	19.886	18.093	0.020	0.021	57.5	38.2	-0.2	0.0
6.522	20.154	18.361	0.022	0.023	45.7	39.8	-0.2	-0.4
7.891	20.426	18.622	0.023	0.025	42.5	37.4	0.0	-0.1
8.681	20.563	18.754	0.023	0.031	44.7	38.4	-0.3	-0.3
9.549	20.708	18.902	0.022	0.025	36.5	34.8	0.2	-0.1
10.504	20.858	19.051	0.022	0.022	38.5	38.7	-0.3	-0.1
11.554	21.011	19.203	0.024	0.025	36.3	33.2	-0.1	0.0
12.709	21.174	19.362	0.024	0.026	35.3	33.4	0.2	-0.2
13.980	21.342	19.528	0.023	0.028	31.5	29.7	-0.1	0.0
15.378	21.515	19.696	0.029	0.033	27.6	27.3	0.1	0.0
16.916	21.680	19.869	0.032	0.036	27.3	21.7	0.1	0.0
18.608	21.838	20.023	0.032	0.036	27.2	25.3	0.0	-0.2
20.469	21.975	20.162	0.038	0.042	23.3	21.5	0.0	0.1
22.515	22.111	20.302	0.034	0.040	24.9	19.8	0.1	0.3
24.767	22.248	20.438	0.032	0.040	20.5	17.1	0.2	0.4
27.244	22.385	20.582	0.040	0.041	7.0	12.9	0.4	0.4
29.968	22.532	20.728	0.036	0.046	8.5	12.2	0.1	0.1
32.965	22.684	20.890	0.037	0.038	9.4	8.7	0.2	0.4
36.261	22.849	21.057	0.026	0.034	1.8	4.5	0.2	0.3
39.887	23.017	21.225	0.027	0.034	11.5	1.4	-0.6	0.1
43.876	23.199	21.416	0.023	0.029	1.8	-3.8	-0.6	-0.1
48.264	23.402	21.625	0.027	0.025	179.8	-4.3	-0.3	0.3
53.090	23.619	21.843	0.023	0.026	185.7	-2.9	-0.9	-0.4
58.399	23.818	22.065		0.007		-20.2		-0.2
64.239	24.030	22.250		0.023		101.4		0.1
70.663	24.215	22.431		0.044		84.1		0.1
77.729	24.398	22.615		0.069		79.2		0.1
85.502	24.559	22.759		0.096		83.6		0.1
94.052	24.764							

Table A44: Surface Photometry of NGC 7145

Seeing σ = 0.5 arcsec (R) and 0.75 arcsec (B)

Semi-Major Axis Length (Arcsec)	Surface Brightness		Ellipticity 1-b/a		Position Angle N thru E		Cos(4θ) Component X100	
	B	R	B	R	B	R	B	R
0.547	17.950	16.045						
0.662	18.001	16.119						
0.801	18.068	16.218						
0.969	18.160	16.348						
1.173	18.282	16.502						
1.419	18.443	16.692						
1.717	18.644	16.902						
2.078	18.871	17.130	0.020	0.011	74.0	165.9	-0.1	0.1
2.514	19.112	17.367	0.007	0.012	101.4	155.0	-0.1	0.0
3.043	19.348	17.603	0.012	0.021	129.6	151.0	0.1	0.1
3.681	19.582	17.832	0.020	0.031	134.1	145.6	0.2	0.2
4.455	19.809	18.063	0.027	0.027	136.8	144.4	0.3	0.1
5.390	20.058	18.306	0.025	0.030	132.6	142.1	0.3	0.4
6.522	20.341	18.595	0.030	0.025	132.2	139.8	0.7	0.4
7.891	20.643	18.896	0.038	0.035	128.4	124.6	0.4	0.3
8.681	20.790	19.045	0.046	0.041	124.8	126.0	0.1	0.2
9.549	20.942	19.189	0.051	0.047	124.9	127.5	0.2	0.2
10.504	21.096	19.346	0.050	0.048	120.0	123.6	0.3	0.4
11.554	21.248	19.499	0.056	0.049	120.8	119.4	0.3	0.3
12.709	21.408	19.649	0.053	0.054	116.8	119.9	0.3	0.3
13.980	21.557	19.807	0.060	0.053	118.3	119.0	0.2	0.0
15.378	21.700	19.940	0.066	0.069	116.0	116.2	0.1	0.1
16.916	21.830	20.075	0.078	0.070	117.4	118.8	0.0	0.1
18.608	21.977	20.212	0.068	0.064	119.1	117.0	0.1	0.1
20.469	22.111	20.358	0.067	0.065	122.9	121.9	0.0	0.1
22.515	22.279	20.521	0.051	0.049	130.4	126.7	-0.1	-0.1
24.767	22.436	20.682	0.046	0.045	118.0	124.6	0.5	0.2
27.244	22.621	20.856	0.035	0.044	130.3	132.8	0.2	0.3
29.968	22.808	21.030	0.021	0.046	139.5	140.6	0.1	0.4
32.965	22.988	21.211	0.027	0.044	142.8	139.1	-0.1	0.2
36.261	23.175	21.399	0.032	0.054	150.8	149.5	-0.5	-0.1
39.887	23.357	21.581	0.035	0.055	159.9	154.3	-0.9	-0.1
43.876	23.547	21.773	0.035	0.062	164.2	162.2	-0.8	-0.7
48.264	23.749	21.953	0.034	0.075	169.2	154.4	-1.5	-1.3
53.090	23.960	22.141	0.023	0.050	156.9	157.3	-2.1	-1.2
58.399	24.148	22.325	0.033		155.3		-0.4	
64.239	24.320	22.492						
70.663	24.497	22.638						
77.729	24.695	22.809						
85.502	24.870	23.018						

Table A45: Surface Photometry of IC 2597

Seeing σ = 0.65 arcsec (R) and 0.8 arcsec (B)

Semi-Major Axis Length (Arcsec)	Surface Brightness		Ellipticity 1-b/a		Position Angle N thru E		Cos(4θ) Component X100	
	B	R	B	R	B	R	B	R
0.547	18.449	16.420						
0.662	18.477	16.452						
0.801	18.516	16.497						
0.969	18.567	16.561						
1.173	18.638	16.648						
1.419	18.736	16.760						
1.717	18.862	16.902						
2.078	19.025	17.074	0.164	0.178	12.4	10.7	-0.1	0.1
2.514	19.215	17.276	0.179	0.193	12.0	10.0	0.0	-0.1
3.043	19.435	17.500	0.193	0.206	11.5	10.0	-0.1	-0.1
3.681	19.677	17.747	0.209	0.218	10.9	10.3	-0.1	-0.1
4.455	19.941	18.008	0.221	0.231	10.6	9.9	0.0	-0.1
5.390	20.222	18.293	0.231	0.235	10.4	9.9	-0.1	-0.1
6.522	20.533	18.601	0.231	0.233	10.2	10.2	-0.1	-0.1
7.891	20.855	18.921	0.231	0.230	9.8	9.7	-0.1	-0.2
8.681	21.013	19.081	0.235	0.234	9.6	9.7	0.1	0.1
9.549	21.169	19.239	0.239	0.235	9.4	9.6	-0.2	0.2
10.504	21.324	19.386	0.245	0.244	9.9	9.9	0.2	0.1
11.554	21.470	19.526	0.255	0.254	9.8	10.0	0.2	0.3
12.709	21.613	19.670	0.262	0.259	9.9	10.0	0.4	0.3
13.980	21.755	19.815	0.268	0.262	9.2	9.3	0.5	0.4
15.378	21.911	19.963	0.267	0.262	9.4	9.5	0.4	0.3
16.916	22.057	20.117	0.272	0.262	9.3	9.3	0.3	0.3
18.608	22.212	20.267	0.277	0.269	8.9	9.3	0.3	0.1
20.469	22.379	20.428	0.270	0.267	9.3	8.9	0.0	0.2
22.515	22.535	20.585	0.271	0.270	9.5	9.1	0.1	0.1
24.767	22.705	20.746	0.271	0.268	9.7	8.9	0.1	0.2
27.244	22.852	20.893	0.285	0.276	8.7	8.2	-0.2	0.1
29.968	23.012	21.054	0.286	0.283	8.7	7.0	0.0	0.1
32.965	23.158	21.217	0.295	0.285	8.3	7.5	0.2	0.1
36.261	23.298	21.359	0.312	0.298	7.9	7.0	0.4	0.6
39.887	23.450	21.517	0.319	0.301	8.1	6.9	-0.2	0.5
43.876	23.611	21.669	0.317	0.305	8.6	7.6	-0.5	0.3
48.264	23.767	21.823	0.323	0.311	8.7	8.2	0.3	0.1
53.090	23.937	21.973	0.324	0.314	9.0	7.5	0.4	0.2
58.399	24.125	22.150	0.314	0.311	8.8	7.3	0.5	0.3
64.239	24.313	22.324	0.305	0.304	7.1	7.7	0.2	0.5
70.663	24.502	22.496	0.299		6.8		-0.2	
77.729	24.683	22.682						
85.502	24.861	22.836						
94.052	25.000	22.968						
103.458	25.171	23.116						

Table A46: Surface Photometry of IC 4296

Seeing σ = 0.8 arcsec (R) and 1.1 arcsec (B)

Semi-Major Axis Length (Arcsec)	Surface Brightness		Ellipticity 1-b/a		Position Angle N thru E		Cos(4θ) Component X100	
	B	R	B	R	B	R	B	R
0.547	18.116	16.007						
0.662	18.131	16.029						
0.801	18.155	16.062						
0.969	18.188	16.108						
1.173	18.234	16.172						
1.419	18.300	16.261						
1.717	18.392	16.382						
2.078	18.518	16.543	0.063	0.066	67.9	58.6	0.0	0.1
2.514	18.685	16.743	0.067	0.070	68.0	60.0	0.0	0.1
3.043	18.892	16.971	0.072	0.076	66.0	59.7	-0.1	-0.1
3.681	19.137	17.222	0.076	0.082	65.4	59.6	0.2	0.2
4.455	19.400	17.486	0.080	0.082	63.0	60.1	0.0	0.1
5.390	19.678	17.760	0.083	0.085	61.6	59.5	0.1	0.1
6.522	19.969	18.049	0.086	0.084	61.0	59.1	0.1	0.1
7.891	20.268	18.338	0.091	0.093	59.6	59.5	0.0	0.1
8.681	20.416	18.487	0.095	0.092	60.7	59.9	0.1	0.3
9.549	20.567	18.634	0.097	0.095	60.0	59.7	0.2	0.0
10.504	20.720	18.784	0.098	0.095	61.3	60.9	0.3	0.2
11.554	20.872	18.933	0.098	0.097	60.7	60.7	0.4	0.3
12.709	21.025	19.084	0.096	0.094	60.6	60.0	0.2	0.4
13.980	21.167	19.222	0.102	0.099	60.0	60.0	0.2	0.2
15.378	21.302	19.357	0.110	0.108	59.8	58.6	0.1	0.0
16.916	21.445	19.496	0.108	0.107	58.4	57.9	0.0	-0.1
18.608	21.585	19.640	0.108	0.102	57.9	57.4	-0.2	-0.3
20.469	21.731	19.784	0.108	0.099	57.5	56.8	-0.2	-0.3
22.515	21.873	19.933	0.105	0.094	58.1	57.0	-0.4	-0.3
24.767	22.023	20.081	0.103	0.094	57.3	54.5	-0.5	-0.7
27.244	22.180	20.231	0.098	0.093	57.1	58.9	-0.8	-0.3
29.968	22.338	20.392	0.096	0.087	60.9	60.4	-0.7	-0.6
32.965	22.505	20.553	0.086	0.085	64.2	64.4	-0.5	-0.4
36.261	22.669	20.717	0.087	0.086	63.3	65.6	-0.4	-0.4
39.887	22.835	20.889	0.088	0.087	65.5	65.8	-0.4	-0.1
43.876	23.011	21.058	0.087	0.087	63.8	62.9	0.0	-0.1
48.264	23.193	21.238	0.082	0.083	59.7	59.5	0.1	-0.2
53.090	23.376	21.411	0.081	0.086	56.5	57.0	0.7	0.2
58.399	23.564	21.586	0.071	0.086	53.1	54.7	1.0	0.4
64.239	23.732	21.739	0.078		58.7		0.3	
70.663	23.907	21.914	0.059	0.080	53.2	64.5	-0.2	0.4
77.729	24.069	22.073		0.075		53.1		-0.9
85.502	24.221	22.224						

Table A47: Surface Photometry of IC 4329

Seeing σ = 0.85 arcsec (R) and 1.05 arcsec (B)

Semi-Major Axis Length (Arcsec)	Surface Brightness B	Surface Brightness R	Ellipticity 1-b/a B	Ellipticity 1-b/a R	Position Angle N thru E B	Position Angle N thru E R	Cos(4θ) Component X100 B	Cos(4θ) Component X100 R
0.547	18.643	16.595						
0.662	18.664	16.626						
0.801	18.695	16.670						
0.969	18.741	16.728						
1.173	18.809	16.811						
1.419	18.904	16.925						
1.717	19.035	17.077						
2.078	19.212	17.272	0.064	0.073	74.8	68.2	0.0	0.2
2.514	19.438	17.509	0.069	0.077	72.1	68.7	0.1	0.1
3.043	19.693	17.772	0.081	0.082	71.2	69.1	0.2	0.2
3.681	19.975	18.048	0.088	0.092	69.9	68.5	0.3	0.4
4.455	20.263	18.329	0.100	0.102	69.0	69.3	0.5	0.6
5.390	20.544	18.605	0.119	0.119	68.0	68.4	0.8	0.4
6.522	20.817	18.873	0.136	0.136	67.9	66.8	0.6	0.7
7.891	21.068	19.118	0.165	0.165	68.3	67.2	0.9	0.8
8.681	21.186	19.231	0.179	0.182	67.5	66.9	1.0	0.8
9.549	21.291	19.340	0.202	0.199	67.6	67.1	0.9	0.8
10.504	21.402	19.451	0.214	0.213	67.7	67.6	1.1	0.9
11.554	21.514	19.559	0.229	0.228	67.4	67.4	1.0	0.8
12.709	21.629	19.668	0.242	0.243	66.9	67.0	0.9	1.0
13.980	21.728	19.767	0.265	0.266	66.7	66.7	1.0	1.3
15.378	21.838	19.885	0.281	0.275	67.1	66.5	1.0	1.0
16.916	21.950	19.989	0.296	0.291	66.9	67.0	1.4	0.9
18.608	22.054	20.097	0.310	0.306	66.9	66.4	1.1	0.8
20.469	22.167	20.207	0.324	0.319	66.6	66.6	0.8	0.7
22.515	22.283	20.321	0.335	0.331	66.6	66.7	0.8	0.7
24.767	22.393	20.435	0.347	0.341	66.9	66.8	0.7	0.4
27.244	22.518	20.555	0.351	0.347	66.8	67.0	0.5	0.5
29.968	22.640	20.693	0.359	0.348	66.8	67.0	-0.4	-0.3
32.965	22.763	20.810	0.373	0.365	66.7	67.0	-0.6	-0.1
36.261	22.890	20.930	0.386	0.379	66.5	67.1	0.0	-0.2
39.887	23.000	21.046	0.404	0.394	67.6	67.8	0.0	-0.1
43.876	23.109	21.154	0.422	0.412	68.0	68.4	-0.4	-0.3
48.264	23.223	21.273	0.437	0.426	68.1	68.6	-0.7	-0.7
53.090	23.336	21.386	0.446	0.440	68.0	68.5	-1.0	-0.6
58.399	23.443	21.493	0.460	0.455	67.9	68.5	-1.8	-2.0
64.239	23.561	21.608		0.471		68.5		-1.5
70.663	23.693	21.752						
77.729	23.861	21.930						
85.502	24.062							
94.052	24.282							

Table A48: Surface Photometry of IC 4889

Seeing σ = 0.6 arcsec (R) and 0.75 arcsec (B)

Semi-Major Axis Length (Arcsec)	Surface Brightness		Ellipticity 1-b/a		Position Angle N thru E		Cos(4θ) Component X100	
	B	R	B	R	B	R	B	R
0.547	17.656	15.631						
0.662	17.695	15.680						
0.801	17.747	15.751						
0.969	17.816	15.842						
1.173	17.909	15.959						
1.419	18.028	16.105						
1.717	18.175	16.275						
2.078	18.354	16.477	0.197	0.221	180.9	179.3	0.6	0.6
2.514	18.560	16.702	0.211	0.231	180.6	179.2	0.4	0.7
3.043	18.782	16.938	0.229	0.246	180.0	178.8	0.8	0.6
3.681	19.021	17.184	0.246	0.261	179.3	178.7	1.0	0.9
4.455	19.266	17.434	0.269	0.278	179.1	178.6	1.0	0.9
5.390	19.525	17.691	0.283	0.292	178.8	178.1	0.9	1.0
6.522	19.799	17.961	0.292	0.300	178.2	177.8	0.6	0.8
7.891	20.080	18.238	0.308	0.312	178.1	177.6	0.7	0.9
8.681	20.233	18.382	0.310	0.317	178.4	177.9	0.7	1.1
9.549	20.371	18.521	0.321	0.322	178.3	177.5	0.9	0.9
10.504	20.508	18.666	0.329	0.325	177.6	177.4	1.2	1.2
11.554	20.658	18.812	0.328	0.326	177.4	177.5	1.6	1.4
12.709	20.807	18.961	0.330	0.324	177.0	177.1	1.5	1.1
13.980	20.955	19.115	0.333	0.326	177.5	177.8	1.2	1.3
15.378	21.104	19.269	0.338	0.325	178.3	178.9	1.1	1.6
16.916	21.255	19.413	0.341	0.332	178.5	179.3	1.3	1.3
18.608	21.402	19.566	0.350	0.339	179.0	179.7	0.8	1.1
20.469	21.568	19.722	0.353	0.346	180.1	180.4	0.1	0.4
22.515	21.738	19.883	0.360	0.354	181.4	181.4	0.2	0.3
24.767	21.894	20.051	0.376	0.362	182.3	182.1	0.2	-0.1
27.244	22.058	20.221	0.387	0.368	182.6	182.6	-0.1	-0.2
29.968	22.250	20.402	0.380	0.369	182.9	182.6	0.0	-0.1
32.965	22.465	20.605	0.382	0.370	182.2	182.5	-0.3	0.1
36.261	22.685	20.834	0.374	0.365	182.3	182.7	0.3	0.2
39.887	22.919	21.065	0.367	0.362	182.9	182.7	-0.1	-0.1
43.876	23.176	21.321	0.351	0.339	182.5	181.6	-0.3	0.0
48.264	23.437	21.581	0.326	0.321	181.3	180.4	0.2	-0.1
53.090	23.692	21.864	0.296	0.289	177.7	175.9	0.2	-0.7
58.399	23.936	22.090	0.286		171.2		-0.4	
64.239	24.184	22.322						
70.663	24.415	22.534						
77.729	24.668	22.777						
85.502	24.911	22.964						
94.052	25.149	23.174						
103.458	25.399							

Table A49: Surface Photometry of A1515-23

Seeing σ = 0.5 arcsec (R) and 0.7 arcsec (B)

Semi-Major Axis Length (Arcsec)	Surface Brightness		Ellipticity 1-b/a		Position Angle N thru E		Cos(4θ) Component X100	
	B	R	B	R	B	R	B	R
0.547	18.463	16.223						
0.662	18.508	16.299						
0.801	18.574	16.402						
0.969	18.661	16.533						
1.173	18.780	16.691						
1.419	18.935	16.875						
1.717	19.124	17.088						
2.078	19.346	17.321	0.360	0.419	117.7	118.3	1.1	1.6
2.514	19.596	17.584	0.392	0.450	117.6	118.0	1.6	2.3
3.043	19.873	17.867	0.424	0.481	117.8	118.1	2.2	2.6
3.681	20.177	18.181	0.454	0.504	117.9	118.3	2.3	2.8
4.455	20.495	18.509	0.483	0.525	118.1	118.2	2.6	2.9
5.390	20.831	18.853	0.507	0.542	118.1	118.2	2.6	3.2
6.522	21.185	19.226	0.524	0.548	118.0	118.4	2.8	2.9
7.891	21.551	19.586	0.537	0.558	118.1	118.3	2.6	2.6
8.681	21.740	19.785	0.541	0.557	118.1	118.5	2.2	2.4
9.549	21.949	19.992	0.542	0.554	118.2	118.5	1.8	2.0
10.504	22.171	20.212	0.539	0.547	118.5	118.6	2.0	1.5
11.554	22.380	20.433	0.537	0.542	118.7	118.6	1.6	1.7
12.709	22.631	20.671	0.525	0.529	118.3	118.8	1.4	1.9
13.980	22.840	20.875	0.529	0.528	118.3	118.6	1.1	1.3
15.378	23.052	21.092	0.528	0.526	118.3	118.3	1.1	1.3
16.916	23.282	21.323	0.521	0.524	119.2	118.6	1.0	2.1
18.608	23.496	21.521	0.529	0.529	119.2	118.6	0.6	1.9
20.469	23.728	21.801	0.527	0.519	119.5	118.5	0.4	1.2
22.515	23.973	22.056	0.531	0.509	119.5	119.1	0.4	1.4
24.767	24.268	22.373	0.504	0.477	119.5	121.5	1.4	1.4
27.244	24.515	22.568		0.491		119.7		2.5
29.968	24.814	22.798						
32.965	25.058	23.100						
36.261	25.335	23.327						
39.887	25.570	23.664						
43.876	25.855	23.964						
48.264	26.096	24.321						
53.090	26.326	24.589						
58.399	26.529	24.840						
64.239	26.771	25.195						
70.663	26.862	25.493						
77.729	27.082	25.679						
85.502	27.443	25.816						
94.052	27.023	25.924						